Persoonia 49, 2022: 1–57
www.ingentaconnect.com/content/nhn/pimj

RESEARCH ARTICLE

ISSN (Online) 1878-9080
https://doi.org/10.3767/persoonia.2022.49.01

Extensive morphological and behavioural diversity among fourteen new and seven described species in *Phytophthora* Clade 10 and its evolutionary implications

T. Jung[1,2], I. Milenković[1,3], T. Corcobado[1], T. Májek[1], J. Janoušek[1], T. Kudláček[1], M. Tomšovský[1], Z.Á. Nagy[1], A. Durán[3,4], M. Tarigan[4], E. Sanfuentes von Stowasser[5], R. Singh[6], M. Ferreira[6], J.F. Webber[7], B. Scanu[8], N.M. Chi[9], P.Q. Thu[9], M. Junaid[10], A. Rosmana[10], B. Baharuddin[10], T. Kuswinanti[10], N. Nasri[11], K. Kageyama[12], A. Hieno[12], H. Masuya[13], S. Uematsu[14], J. Oliva[15], M. Redondo[16], C. Maia[17], I. Matsiakh[18], V. Kramarets[18], R. O'Hanlon[19], Ž. Tomić[20], C.M. Brasier[7], M. Horta Jung[1,2]

Key words

allopatric
biogeography
evolution
Gondwana
Laurasia
oomycete
phylogeny
radiation
sympatric

Abstract During extensive surveys of global *Phytophthora* diversity 14 new species detected in natural ecosystems in Chile, Indonesia, USA (Louisiana), Sweden, Ukraine and Vietnam were assigned to *Phytophthora* major Clade 10 based on a multigene phylogeny of nine nuclear and three mitochondrial gene regions. Clade 10 now comprises three subclades. Subclades 10a and 10b contain species with nonpapillate sporangia, a range of breeding systems and a mainly soil- and waterborne lifestyle. These include the previously described *P. afrocarpa*, *P. gallica* and *P. intercalaris* and eight of the new species: *P. ludoviciana*, *P. procera*, *P. pseudogallica*, *P. scandinavica*, *P. subarctica*, *P. tenuimura*, *P. tonkinensis* and *P. ukrainensis*. In contrast, all species in Subclade 10c have papillate sporangia and are self-fertile (or homothallic) with an aerial lifestyle including the known *P. boehmeriae*, *P. gondwanensis*, *P. kernoviae* and *P. morindae* and the new species *P. celebensis*, *P. chilensis*, *P. javanensis*, *P. multiglobulosa*, *P. pseudochilensis* and *P. pseudokernoviae*. All new *Phytophthora* species differed from each other and from related species by their unique combinations of morphological characters, breeding systems, cardinal temperatures and growth rates. The biogeography and evolutionary history of Clade 10 are discussed. We propose that the three subclades originated via the early divergence of pre-Gondwanan ancestors > 175 Mya into water- and soilborne and aerially dispersed lineages and subsequently underwent multiple allopatric and sympatric radiations during their global spread.

Citation: Jung T, Milenković I, Corcobado T, et al. 2022. Extensive morphological and behavioural diversity among fourteen new and seven described species in Phytophthora Clade 10 and its evolutionary implications. Persoonia 49: 1–57. https://doi.org/10.3767/persoonia.2022.49.01.
Effectively published online: 13 August 2022 [Received: 28 April 2022; Accepted: 13 June 2022].

INTRODUCTION

The oomycete genus *Phytophthora* currently includes six obligate biotrophic unculturable species and 192 hemibiotrophic or necrotrophic culturable species (Chen et al. 2022). Most are soil-, water- or aerially dispersed plant pathogens, some causing severe diseases on host species in horticultural, forestry and natural ecosystems (Erwin & Ribeiro 1996, Yang et al. 2017, Jung et al. 2018b, Chen et al. 2022). Recent phylogenetic and phylogenomic studies have demonstrated that the

[1] Mendel University in Brno, Faculty of Forestry and Wood Technology, Department of Forest Protection and Wildlife Management, Phytophthora Research Centre, 613 00 Brno, Czech Republic; corresponding author e-mail: thomas.jung@mendelu.cz and dr.t.jung@gmail.com.
[2] Phytophthora Research and Consultancy, 83131 Nussdorf, Germany.
[3] University of Belgrade, Faculty of Forestry, 11030 Belgrade, Serbia.
[4] Research and Development, Asia Pacific Resources International Limited (APRIL), 28300 Pangkalan Kerinci, Riau, Indonesia.
[5] Laboratorio de Patología Forestal, Facultad Ciencias Forestales y Centro de Biotecnología, Universidad de Concepción, 4030000 Concepción, Chile.
[6] Plant Diagnostic Center, Department of Plant Pathology and Crop Physiology, Louisiana State University Agricultural Center, Baton Rouge, Louisiana, USA.
[7] Forest Research, Alice Holt Lodge, Farnham, Surrey GU10 4LH, UK.
[8] Department of Agricultural Sciences, University of Sassari, Viale Italia 39A, 07100 Sassari, Italy.
[9] Forest Protection Research Centre, Vietnamese Academy of Forest Sciences, 10000 Hanoi, Vietnam.
[10] Department of Plant Pest and Disease, Faculty of Agriculture, Hasanuddin University, Makassar, 90245, South Sulawesi, Indonesia.
[11] Department of Forest Conservation, Faculty of Forestry, Hasanuddin University, Makassar, 90245, South Sulawesi, Indonesia.
[12] River Basin Research Center, Gifu University, Gifu, 501-1193, Japan.
[13] Forestry and Forest Products Research Institute (FFPRI), Tsukuba, Ibaraki, 305-8687, Japan.
[14] Laboratory of Molecular and Cellular Biology, Dept. of Bioregulation and Bio-interaction, Tokyo University of Agriculture and Technology, Fuchu, Tokyo, 183-8509, Japan.
[15] Department of Crop and Forest Sciences, University of Lleida, Lleida 25198, Spain.
[16] Department of Forest Mycology and Plant Pathology, Swedish University of Agricultural Sciences, 750 07 Uppsala, Sweden.
[17] Centre of Marine Sciences (CCMAR), University of Algarve, 8005-139 Faro, Portugal.
[18] Ukrainian National Forestry University, Pryrodna st.19, 79057, Lviv, Ukraine.
[19] Department of Agriculture, Food and the Marine, Dublin 2, D02 WK12, Ireland.
[20] Center for Plant Protection, Croatian Agency for Agriculture and Food, 10000 Zagreb, Croatia.

c. 800 species of obligate biotrophic downy mildews reside as two distinct phylogenetic clades within the paraphyletic genus *Phytophthora*, suggesting their evolution from hemibiotrophic *Phytophthora* ancestors (Thines & Choi 2016, Jung et al. 2017d, McCarthy & Fitzpatrick 2017, Bourret et al. 2018, Fletcher et al. 2018, 2019, Scanu et al. 2021). *Phytophthora* currently resolves into 12 major phylogenetic clades with numerous subclades (Yang et al. 2017, Jung et al. 2017d, Chen et al. 2022). Recently Bourret et al. (2018) proposed additional Clades, 13 and 14, to accommodate the undescribed *Phytophthora* taxon mugwort and the obligate biotrophic *P. cyperi* which is more likely to be a downy mildew, and two further Clades, 15 and 16, comprising the 20 described genera of downy mildews. The evolutionary history of *Phytophthora* is characterised by an early divergence, most likely 175–210 million years ago (Mya) (Jung et al. 2017d), resulting in a main cluster comprising extant *Phytophthora* Clades 1–8, 11–13 and the downy mildew Clades 14–16, and a basal cluster containing extant *Phytophthora* Clades 9 and 10 (Yang et al. 2017, Jung et al. 2017d, Bourret et al. 2018, Scanu et al. 2021, Chen et al. 2022).

In the first ITS-based phylogeny of the genus *Phytophthora* Clade 10 included only a single species, *P. boehmeriae*, described in 1927 from Taiwan (Tucker 1931, Erwin & Ribeiro 1996, Cooke et al. 2000). However, another six Clade 10 species have been described since 2005 including, in chronological order, *P. kernoviae*, *P. gallica*, *P. morindae*, *P. gondwanensis*, *P. intercalaris* and *P. afrocarpa* (Brasier et al. 2005, Jung & Nechwatal 2008, Nelson & Abad 2010, Crous et al. 2015, Yang et al. 2016, Bose et al. 2021). *Phytophthora boehmeriae*, *P. kernoviae* and *P. morindae* are aerially dispersed pathogens producing caducous papillate sporangia in dense sympodia and infecting above-ground plant tissues. *Phytophthora boehmeriae* is noted for causing leaf blight of the herbaceous ramie (*Boehmeria nivea*) and boll rot of cotton (*Gossypium* spp.) in China and Taiwan and leaf blight of sweet pepper (*Capsicum annuum*) in India (Tucker 1931, Erwin & Ribeiro 1996, Chowdappa et al. 2014, Thorpe et al. 2021); *P. kernoviae* for causing aerial bleeding stem lesions on *Fagus sylvatica* trees and leaf and shoot blight of *Rhododendron* spp. and *Drimys winteri* in the UK and Ireland (Brasier et al. 2005, O' Hanlon et al. 2016); and *P. morindae* for leaf blight and fruit rot of *Morinda citrifolia* var. *citrifolia* in Hawaii (Nelson & Abad 2010). *Phytophthora gondwanensis* has been recovered from soil samples around various host plants across Australia and exotic *Eucalyptus smithii* and *Acacia mearnsii* plantations in South Africa and Brazil, respectively, and is also a pathogen of *Zanthoxylum piperitum* in China and *Ficus* sp. in Papua New Guinea (Dos Santos et al. 2006, Crous et al. 2015, Burgess et al. 2021). Its caducous sporangia (Crous et al. 2015) indicate an aerial lifestyle. Another airborne taxon closely related to *P. boehmeriae*, *Phytophthora* taxon boehmeriae-like, was first isolated in 1939 causing brown rot of *Citrus sinensis* fruits in Argentina (Frezzi 1941, 1950, Erwin & Ribeiro 1996, Yang et al. 2017).

In contrast, the previously described Clade 10 species *P. gallica*, *P. intercalaris* and *P. afrocarpa* produce persistent nonpapillate sporangia with mainly internal proliferation (Jung & Nechwatal 2008, Yang et al. 2016, Bose et al. 2021). *Phytophthora gallica* and *P. intercalaris* were exclusively recovered from waterbodies or riparian forests in Europe and the USA (Jung & Nechwatal 2008, Jones et al. 2014, Sims et al. 2015, Yang et al. 2016, Redondo et al. 2018a, b) suggesting a lifestyle as litter decomposers and opportunistic root pathogens of riparian plants similar to primarily aquatic *Phytophthora* species from Clades 6 and 9 (Brasier et al. 2003, Jung et al. 2011, Yang et al. 2014). *Phytophthora afrocarpa* is currently known only from rhizosphere soil of the coniferous tree *Afrocarpus falcatus* in a temperate mountain forest in South Africa (Bose et al. 2021).

For *Phytophthora* taxon canthium, an undescribed Clade 10 taxon from temperate forest soil in South Africa related to *P. boehmeriae*, *P. morindae* and *P. kernoviae*, no information on hosts or morphology is available (Oh et al. 2013). While *P. kernoviae* is damaging as an invasive pathogen in Europe it is relatively benign in natural forests of Valdivia (Chile) and New Zealand suggesting long-term coevolution and, hence, a Southern Hemisphere origin (Gardner et al. 2015, Sanfuentes et al. 2016, Jung et al. 2018a). In 2014, two new Clade 10 taxa closely related to *P. kernoviae*, *P. chilensis* nom. prov. and *P. pseudokernoviae* nom. prov. (Jung et al. 2018a), and a third new Clade 10 taxon were isolated alongside *P. kernoviae* from forest streams and necrotic leaves of *D. winteri* in the Valdivian rainforests. In 2017, two new *Phytophthora* taxa related to *P. gallica*, informally designated as *P.* taxon gallica-like 1 and 2, were detected in a stream running through an evergreen cloud forest in the North of Vietnam (Jung et al. 2020). Recent surveys in Indonesia, USA (Louisiana), Sweden and Ukraine also produced *Phytophthora* isolates which, based on ITS sequence analysis, constituted another three unknown Clade 10 taxa, bringing the total number of new undescribed taxa in Clade 10 to fourteen.

In this study, morphological and physiological characteristics and DNA sequence data from nine nuclear and three mitochondrial gene regions were used to characterise the 14 new *Phytophthora* species from Clade 10; compare them morphologically and behaviourally to the known species in Clade 10 and describe them as *P. celebensis*, *P. chilensis*, *P. javanensis*, *P. ludoviciana*, *P. multiglobulosa*, *P. procera*, *P. pseudochilensis*, *P. pseudogallica*, *P. pseudokernoviae*, *P. scadinavica*, *P. subarctica*, *P. tenuimura*, *P. tonkinensis* and *P. ukrainensis* spp. nov.; and consider the implications of their morphological and behavioural properties and distribution for the evolution of the Clade.

TERMINOLOGY

Definitions of homothallism, heterothallism and sterility

Homothallism and heterothallism are somewhat archaic, quasi-morphological terms used more to describe whether gametangia are formed in single or paired *Phytophthora* cultures rather than the process this represents. Because of their common historical usage in species descriptions we have also used the terms here, but we prefer a more Darwinian definition reflecting the underlying breeding system or breeding strategy. By *homothallic* we mean self-fertility in single culture; but this process does not preclude outbreeding in nature as a result of the fusion of antheridia and oogonia of different genotypes. By *heterothallic* we mean that two mating or compatibility types (A1 and A2) are required to initiate gametogenesis between otherwise largely self-incompatible individuals; but while this process promotes outcrossing, once initiated it can also lead to a significant frequency of self-fertilisation (selfing). By *sterility* we mean an isolate's lack of the intrinsic ability to form gametangia whether in single culture or in pairings with A1 or A2 isolates; but this does not exclude the possibility that it may act as a 'silent' A1 or A2, inducing gametangial formation by selfing in an A2 or an A1 isolate of another species (cf. *P. gonopodyides*, Brasier et al. 2003).

Use of the terms Phytophthora taxon x and Phytophthora sp. x

The informal term '*Phytophthora* taxon x' (cf. Brasier et al. 2003) was developed to cover situations where it was clear that a novel entity of some taxonomic level had been identified, but formal description was likely to be delayed pending further analysis to determine the level of taxonomic distinction (e.g., species, subspecies, variety etc; cf. Brasier & Rayner 1987)

Table 1 Details of isolates from *Phytophthora* major Clades 7, 9 and 10 included in the phylogenetic, morphological and growth-temperature studies. GenBank accession numbers for sequences obtained in the present study are printed in *italics*.

***Phytophthora* species**	**Isolate numbers** [a]		**Origin**		**GenBank accession numbers**					
	International collections	**Local collections**	**Host**	**Location; year; collector; reference**	**28S LSU ITS**	***βtub hsp90***	***tigA rpl10***	***tef-1α enl***	***ras-ypt1 cox1***	***nadh1 rps10***
P. afrocarpa	CBS 147467[ET]	CMW54630[b]	*Afrocarpus falcatus*	South Africa; 2017; K. Sawada; J.M. Hulbert; Bose et al. 2021	n.a. MT762306	MT762324 MT762333	n.a. n.a.	n.a. n.a.	n.a. MT762315	n.a. n.a.
	CBS 147590	CMW54631[b]	*A. falcatus*	South Africa; 2017; K. Sawada; J.M. Hulbert; Bose et al. 2021	n.a. MT762307	MT762325 MT762334	n.a. n.a.	n.a. n.a.	n.a. MT762316	n.a. n.a.
P. boehmeriae	CBS 291.29, IMI180614, ATCC 60238, WPC P6950[ET]	45F9[b]	*Boehmeria nivea*	Taiwan; 1927; K. Sawada; Tucker 1931	HQ665190 HQ643149	EU080162 EU080165	EU080167 EU080161	EU080163 EU080164	MH974993 HQ261251-KT183047	DQ361200 JF770876
	WPC P3963	CPHST BL79[b]	*Gossypium hirsutum*	China; 1989; C.-Y. Shen; n.a.	JAAVTJ010000283 [e] JAAVTJ010000075 [e]	JAAVTJ010000250 [e] JAAVTJ010000384 [e]	JAAVTJ010000206 [e] JAAVTJ010000040 [e]	JAAVTJ010000055 [e] JAAVTJ010000045 [e]	JAAVTJ010000326 [e] JAAVTJ010000225 [e]	JAAVTJ010000225 [e] JAAVTJ010000225 [e]
		SCRP23[b]	*G. hirsutum*	China; 1998; Y. Wang; n.a.	JAGDFL010000638 [e] JAGDFL010000638 [e]	JAGDFL010000070 [e] JAGDFL010000190 [e]	JAGDFL010000109 [e] JAGDFL010000393 [e]	JAGDFL010000202 [e] JAGDFL010000600 [e]	JAGDFL010000236 [e] JAGDFL010000296 [e]	JAGDFL010000296 [e] JAGDFL010000296 [e]
	WPC P7460[b]		*Capsicum annuum*	India, Madhya Pradesh; 1989; N.D. Sharma; n.a.	n.a. FJ801971	n.a. n.a.	n.a. n.a.	n.a. n.a.	n.a. n.a.	n.a. n.a.
		OCPC4[b]	*C. annuum*; fruit rot	India, Bangalore Rural; 2011; S. Madhura; Chowdappa et al. 2014	n.a. KC677806	n.a. n.a.	n.a. n.a.	n.a. n.a.	n.a. n.a.	n.a. n.a.
P. celebensis	CBS 148800[ET]	SL092[bcd]	Fallen bamboo leaf, forest stream R09	Indonesia, Sulawesi; 2019; T. Jung, M. Junaid, N. Nasri; this study	*ON000626* *ON000720*	*OM975899* *OM976416*	*OM974594* *OM974453*	*OM984880* *OM976512*	*ON024938* *ON013786*	*OM976896* *OM976654*
		SL091[bcd]	Fallen bamboo leaf, forest stream R09	Indonesia, Sulawesi; 2019; T. Jung, M. Junaid, N. Nasri; this study	*ON000622* *ON000716*	*OM975895* *OM976412*	*OM974590* *OM974449*	*OM984876* *OM976508*	*ON024934* *ON013782*	*OM976892* *OM976650*
		SL540[bcd]	Fallen bamboo leaf, forest stream R09	Indonesia, Sulawesi; 2019; T. Jung, M. Junaid, N. Nasri; this study	*ON000623* *ON000717*	*OM975896* *OM976413*	*OM974591* *OM974450*	*OM984877* *OM976509*	*ON024935* *ON013783*	*OM976893* *OM976651*
		SL541[bcd]	Fallen bamboo leaf, forest stream R09	Indonesia, Sulawesi; 2019; T. Jung, M. Junaid, N. Nasri; this study	*ON000624* *ON000718*	*OM975897* *OM976414*	*OM974592* *OM974451*	*OM984878* *OM976510*	*ON024936* *ON013784*	*OM976894* *OM976652*
		SL542[bcd]	Fallen bamboo leaf, forest stream R09	Indonesia, Sulawesi; 2019; T. Jung, M. Junaid, N. Nasri; this study	*ON000625* *ON000719*	*OM975898* *OM976415*	*OM974593* *OM974452*	*OM984879* *OM976511*	*ON024937* *ON013785*	*OM976895* *OM976653*
P. chilensis	CBS 148797, NRRL 64353[ET]	CL165[bcd]	Baiting stream R04, Valdivian rainforest	Chile; 2014; T. Jung, A. Durán, E. Sanfuentes; Jung et al. 2018b	*ON000632* *ON000726*	*OM975905* *OM976422*	*OM974600* *OM974459*	*OM984886* *OM976518*	*ON024944* *ON013792*	*OM976902* *OM976660*
		CL166[bcd]	Baiting stream R04, Valdivian rainforest	Chile; 2014; T. Jung, A. Durán, E. Sanfuentes; Jung et al. 2018b	*ON000627* *ON000721*	*OM975900* *OM976417*	*OM974595* *OM974454*	*OM984881* *OM976513*	*ON024939* *ON013787*	*OM976897* *OM976655*
		CL169[bcd]	Baiting stream R04, Valdivian rainforest	Chile; 2014; T. Jung, A. Durán, E. Sanfuentes; Jung et al. 2018b	*ON000628* *ON000722*	*OM975901* *OM976418*	*OM974596* *OM974455*	*OM984882* *OM976514*	*ON024940* *ON013788*	*OM976898* *OM976656*
		CL170[bcd]	Baiting stream R04, Valdivian rainforest	Chile; 2014; T. Jung, A. Durán, E. Sanfuentes; Jung et al. 2018b	*ON000629* *ON000723*	*OM975902* *OM976419*	*OM974597* *OM974456*	*OM984883* *OM976515*	*ON024941* *ON013789*	*OM976899* *OM976657*
		CL171[bcd]	Baiting stream R05, Valdivian rainforest	Chile; 2014; T. Jung, A. Durán, E. Sanfuentes; Jung et al. 2018b	*ON000630* *ON000724*	*OM975903* *OM976420*	*OM974598* *OM974457*	*OM984884* *OM976516*	*ON024942* *ON013790*	*OM976900* *OM976658*

Table 1 (cont.)

Phytophthora species	Isolate numbers [a]		Origin		GenBank accession numbers					
	International collections	Local collections	Host	Location; year; collector; reference	28S LSU ITS	*βtub hsp90*	*tigA rpl10*	*tef-1α enl*	*ras-ypt1 cox1*	*nadh1 rps10*
		CL172[bcd]	Baiting stream R05, Valdivian rainforest	Chile; 2014; T. Jung, A. Durán, E. Sanfuentes; Jung et al. 2018b	*ON000631 ON000725*	*OM975904 OM976421*	*OM974599 OM974458*	*OM984885 OM976517*	*ON024943 ON013791*	*OM976901 OM976659*
P. cinnamomi		TW012[c]	*Cinnamomum micranthum*	Taiwan; 2013; T. Jung; Jung et al. 2017b	*ON000634 ON000728*	*OM975907 OM976424*	n.a. *OM974461*	*OM984888 OM976519*	n.a. *ON013794*	*OM976904 OM976662*
		TJ1123, MP74[c]	n.a.	Australia (WA); n.a.; CALM[e]; Hüberli 1995	*ON000633 ON000727*	*OM975906 OM976423*	*OM974601 OM974460*	*OM984887 n.a.*	n.a. *ON013793*	*OM976903 OM976661*
P. constricta	CBS 125801	VHS 16130, TJ306, 55C3[b]	Kwongan heathland	Australia, WA; 2006; VHS; Rea et al. 2011	*ON000635 ON000729*	*OM975908 OM976425*	*OM974602 OM974462*	*OM984889 OM976520*	*ON024945 ON013795*	*OM976905 OM976663*
P. fallax	CBS 119109, ICMP 15575[ET]	46J2, WPC P10722, CPHST BL63, NZFS 310L[b]	*Eucalyptus salignae*, leaf necrosis	New Zealand, Rotoehu Forst; 1992; C. Barr; Dick et al. 2006	KX252573 MG865489	KX252569 KX252572	KX252574 KX252568	KX252570 KX252571	MH443229 MH136885-KC733451	KX252570 JQ439192
	ICMP 17563	NZFS 310K[b]	*Eucalyptus delagatensis*	New Zealand, Owaka Valley; 1997; R.E. Beever; Winkworth et al. 2020	n.a.	n.a.	n.a.	n.a.	n.a. MN883608 [f]	MN883608 [f] MN883608 [f]
P. gallica	CBS 111474[ET]	GAL1[b]	*Quercus robur*, riparian forest	France; 1998; T. Jung; Jung & Nechwatal 2008	KX252594 KF317090	KX252590 KX252593	KX252595 KX252589	KX252591 KX252592	MH443236 MH136893-KF317112	n.a. n.a.
	NRRL 66988	SFB267[bcd]	Stream baiting, mountain forest	Serbia; 2017; I. Milenković; this study	*ON000637 ON000731*	*OM975910 OM976427*	*OM974604 OM974464*	*OM984891 OM976522*	*ON024947 ON013797*	*OM976907 OM976665*
		MO130[bcd]	Stream baiting, broadleaved forest	Czech Republic; 2019; H. Czech Republic; 2019; Ďatková; Ďatková 2020	*ON000636 ON000730*	*OM975909 OM976426*	*OM974603 OM974463*	*OM984890 OM976521*	*ON024946 ON013796*	*OM976906 OM976664*
		TJ582 = 20. VRBJOH 7/15[bcd]	*Alnus glutinosa*, swamp forest	Croatia; 2014; Z. Tomić; this study	*ON000639 ON000733*	*OM975912 OM976429*	*OM974606 OM974466*	*OM984893 OM976524*	*ON024949 ON013799*	*OM976909 OM976667*
		SW423[b]	Stream baiting, *Pinus silvestris* forest	Sweden, SW Sweden; 2017; I. Milenković, T. Corcobado; this study	*ON000638 ON000732*	*OM975911 OM976428*	*OM974605 OM974465*	*OM984892 OM976523*	*ON024948 ON013798*	*OM976908 OM976666*
		UA399[b]	*A. glutinosa*, soil	Ukraine, Transcarpathia region; 2019; I. Milenković, T. Corcobado; this study	*ON000640 ON000734*	*OM975913 OM976430*	*OM974607 OM974467*	*n.a. OM976525*	*ON024950 ON013800*	*OM976910 OM976668*
		33-4-R.1[b]	*Alnus rhombifolia* rhizosphere	Oregon, USA; 2010; L.L. Sims; Sims et al. 2015	n.a. KJ666760	n.a. n.a.	n.a. n.a.	n.a. n.a.	n.a. n.a.	n.a. n.a.
		76-P1[b]	Baiting of a waterbody	New York State, USA; 2010 or 2011; L.A. Jones; Jones et al. 2014	n.a. KJ865228	n.a. n.a.	n.a. n.a.	n.a. n.a.	n.a. n.a.	n.a. n.a.
P. gondwanensis	CBS 139336[ET]	CMW42633, W1858[b]	Gondwana rainforest soil	Australia, NSW; 2014; K. Scarlett; Crous et al. 2015	n.a. KP070695	KP070605 OL466916	n.a. OK533441	OK267378 n.a.	n.a. OK185360	n.a. n.a.
	NRRL 64120	JP1308[bcd]	Fallen leaf, forest stream R37	Japan, Amami Island; 2018; T. Jung, K. Kageyama, H. Masuya; this study	*ON000641 ON000735*	*OM975914 OM976431*	*OM974608 OM974468*	*OM984894 OM976526*	*ON024951 ON013801*	*OM976911 OM976669*
		JP2350[bcd]	Fallen leaf, forest stream R37	Japan, Amami Island; 2018; T. Jung, K. Kageyama, H. Masuya; this study	*ON000642 ON000736*	*OM975915 OM976432*	*OM974609 OM974469*	*OM984895 OM976527*	*ON024952 ON013802*	*OM976912 OM976670*
		JP2351[bcd]	Fallen leaf, forest stream R37	Japan, Amami Island; 2018; T. Jung, K. Kageyama, H. Masuya; this study	*ON000643 ON000737*	*OM975916 OM976433*	*OM974610 OM974470*	*OM984896 OM976528*	*ON024953 ON013803*	*OM976913 OM976671*
		JP2352[bcd]	Fallen leaf, forest stream R37	Japan, Amami Island; 2018; T. Jung, K. Kageyama, H. Masuya; this study	*ON000644 ON000738*	*OM975917 OM976434*	*OM974611 OM974471*	*OM984897 OM976529*	*ON024954 ON013804*	*OM976914 OM976672*

Table 1 (cont.)

Phytophthora species	Isolate numbers [a]		Origin		GenBank accession numbers					
	International collections	Local collections	Host	Location; year; collector; reference	28S LSU ITS	*βtub* *hsp90*	*tigA* *rpl10*	*tef-1α* *enl*	*ras-ypt1* *cox1*	*nadh1* *rps10*
		JP2353[bcd]	Fallen leaf, forest stream R37	Japan, Amami Island; 2018; T. Jung, K. Kageyama, H. Masuya; this study	*ON000645* *ON000739*	*OM975918* *OM976435*	*OM974612* *OM974472*	*OM984898* *OM976530*	*ON024955* *ON013805*	*OM976915* *OM976673*
	ATTC 46717 WPC P1257 [bg]		*Ficus* sp., soil	Papua New Guinea; before 1994; n.a.	n.a. FJ801722	n.a. n.a.	n.a. n.a.	n.a. n.a.	n.a. HQ261253	n.a. n.a.
		ALT-18[bg]	*Acacia mearnsii*, plantation	Brazil, Rio Grande do Sul; 2005; A.F. Dos Santos; Dos Santos et al. 2006	n.a. KX396302	KX396337 n.a.	n.a. n.a.	KX396325 n.a.	n.a. KX396277	n.a. n.a.
	CBS 100410	VHS 3488[bg]	*Persoonia longifolia*, soil	Australia, WA; n.a.; F. Tay; n.a.	n.a. KJ755133	n.a. n.a.	n.a. n.a.	n.a. n.a.	n.a. n.a.	n.a. n.a.
		CMW19441[bg]	*Eucalyptus smithii*, plantation	South Africa, KwaZulu-Natal; before 2007; B. Maseko; Maseko et al. 2007	n.a. DQ988207	DQ988246 n.a.	n.a. n.a.	n.a. n.a.	n.a. n.a.	n.a. n.a.
	ATCC MYA-3893, IMI 403470	22G7, S833, p43[bg]	n.a.	n.a.; n.a.; Schmitthenner? Yang et al. 2017	KX252608 KT183035	KX252604 KX252607	KX252609 KX252603	KX252605 KX252606	n.a. KT183046	n.a. n.a.
P. intercalaris	CBS 140632[ET]	45B7[b]	Stream water	USA, Virginia; 2007; X. Yang; Yang et al. 2016	KX252615 KT163268	KT163336 KX252614	KX252616 KX252610	KX252612 KX252613	n.a. OK185358-KT163315	n.a. n.a.
	CBS 140631	49A7[b]		Yang et al. 2016	KX252629 KT163273	KX252625 KX252628	KX252630 KX252624	KX252626 KX252627	n.a. KT163320	n.a. n.a.
	NRRL 64027	TJ567[bcd]	Ornamental nursery plant of *Aronia* sp.	Croatia; 2014; Z. Tomić; this study	*ON000646* *ON000740*	*OM975919* *OM976436*	*OM974613* *OM974473*	*OM984899* *OM976531*	*ON024956* *ON013806*	*OM976916* *OM976674*
P. javanensis	CBS 149203, NRRL 64129[ET]	JV025a[bcd]	Fallen leaf, forest stream R01	Indonesia, Java; 2019; T. Jung, M. Junaid, N. Nasri; this study	*ON000656* *ON000750*	*OM975929* *OM976446*	*OM974623* *OM974483*	*OM984909* *OM976541*	*ON024966* *ON013816*	*OM976926* *OM976684*
		JV025b[bcd]	Fallen leaf, forest stream R01	Indonesia, Java; 2019; T. Jung, M. Junaid, N. Nasri; this study	*ON000647* *ON000741*	*OM975920* *OM976437*	*OM974614* *OM974474*	*OM984900* *OM976532*	*ON024957* *ON013807*	*OM976917* *OM976675*
		JV191[bcd]	Fallen leaf, forest stream R01	Indonesia, Java; 2019; T. Jung, M. Junaid, N. Nasri; this study	*ON000648* *ON000742*	*OM975921* *OM976438*	*OM974615* *OM974475*	*OM984901* *OM976533*	*ON024958* *ON013808*	*OM976918* *OM976676*
		JV192[bcd]	Fallen leaf, forest stream R01	Indonesia, Java; 2019; T. Jung, M. Junaid, N. Nasri; this study	*ON000649* *ON000743*	*OM975922* *OM976439*	*OM974616* *OM974476*	*OM984902* *OM976534*	*ON024959* *ON013809*	*OM976919* *OM976677*
		JV193[bcd]	Fallen leaf, forest stream R01	Indonesia, Java; 2019; T. Jung, M. Junaid, N. Nasri; this study	*ON000650* *ON000744*	*OM975923* *OM976440*	*OM974617* *OM974477*	*OM984903* *OM976535*	*ON024960* *ON013810*	*OM976920* *OM976678*
		SL081[bcd]	Fallen leaf, forest stream R07	Indonesia, Sulawesi; 2019; T. Jung, M. Junaid, N. Nasri; this study	*ON000651* *ON000745*	*OM975924* *OM976441*	*OM974618* *OM974478*	*OM984904* *OM976536*	*ON024961* *ON013811*	*OM976921* *OM976679*
		SL084[bcd]	Fallen leaf, forest stream R07	Indonesia, Sulawesi; 2019; T. Jung, M. Junaid, N. Nasri; this study	*ON000652* *ON000746*	*OM975925* *OM976442*	*OM974619* *OM974479*	*OM984905* *OM976537*	*ON024962* *ON013812*	*OM976922* *OM976680*
		SL0537[bcd]	Fallen leaf, forest stream R07	Indonesia, Sulawesi; 2019; T. Jung, M. Junaid, N. Nasri; this study	*ON000653* *ON000747*	*OM975926* *OM976443*	*OM974620* *OM974480*	*OM984906* *OM976538*	*ON024963* *ON013813*	*OM976923* *OM976681*
		SL0538[bcd]	Fallen leaf, forest stream R07	Indonesia, Sulawesi; 2019; T. Jung, M. Junaid, N. Nasri; this study	*ON000654* *ON000748*	*OM975927* *OM976444*	*OM974621* *OM974481*	*OM984907* *OM976539*	*ON024964* *ON013814*	*OM976924* *OM976682*
		SL0539[bcd]	Fallen leaf, forest stream R07	Indonesia, Sulawesi; 2019; T. Jung, M. Junaid, N. Nasri; this study	*ON000655* *ON000749*	*OM975928* *OM976445*	*OM974622* *OM974482*	*OM984908* *OM976540*	*ON024965* *ON013815*	*OM976925* *OM976683*

Table 1 (cont.)

Phytophthora species	Isolate numbers [a]		Origin		GenBank accession numbers					
	International collections	Local collections	Host	Location; year; collector; reference	28S LSU ITS	*βtub hsp90*	*tigA rpl10*	*tef-1α enl*	*ras-ypt1 cox1*	*nadh1 rps10*
P. kernoviae	IMI 393170, WPC P19827[ET]	CPHST BL 91, P1571[b]	*Fagus sylvatica*, bark canker	UK, Cornwall; 2004; C.M. Brasier; Brasier et al. 2005	VKKV0100 0063 [e] VKKV0100 0063 [e]	VKKV0100 0263 [e] VKKV0100 0311 [e]	VKKV0100 0441 [e] VKKV0100 0402 [e]	VKKV0100 0415-0416[e] VKKV0100 0008 [e]	VKKV01000 091 [e] VKKV01000 418 [e]	VKKV01000 418 [e] VKKV01000 418 [e]
		00238/432[b]	*Rhododendron ponticum*	UK, Scotland; 2010; A. Schlenzig; Sambles et al. 2015	AOFI02000 967 [e] AOFI02000 967 [e]	AOFI02000 572 [e] AOFI02000 890 [e]	AOFI03000 088 [e] AOFI02000 251 [e]	AOFI02000 453 [e] AOFI02000 244 [e]	AOFI030000 34 [e] AOFI020003 41 [e]	AOFI020003 41 [e] AOFI020003 41 [e]
		00629/1[b]	*R. ponticum*	UK, Scotland; 2011; A. Schlenzig; Sambles et al. 2015	AOFJ02000 931 [e] AOFJ02000 931 [e]	AOFJ02000 547 [e] AOFJ02000 791 [e]	AOFJ02000 111 [e] AOFJ02000 243 [e]	AOFJ02001 008 [e] AOFJ02000 237 [e]	AOFJ02000 030 [e] AOFJ02000 333 [e]	AOFJ02000 333 [e] AOFJ02000 333 [e]
		00844/4[b]	*R. ponticum*	UK, Scotland; 2011; A. Schlenzig; Sambles et al. 2015	AOFK0200 0947 [e] AOFK0200 0947 [e]	AOFK0200 0552 [e] AOFK0200 0796 [e]	AOFK0200 0104 [e] AOFK0200 0229 [e]	AOFK0200 0492 [e] AOFK0200 0248 [e]	AOFK02000 030 [e] AOFK02000 336 [e]	AOFK02000 336 [e] AOFK02000 336 [e]
	NRRL 64156	CL155[bcd]	Baiting stream R01, Valdivian rainforest	Chile; 2014; T. Jung, A. Durán, E. Sanfuentes; Jung et al. 2018b	*ON000657 ON000751*	*OM975930 OM976447*	*OM974624 OM974484*	*OM984910 OM976542*	*ON024967 ON013817*	*OM976927 OM976685*
		CL167[bcd]	Baiting stream R04, Valdivian rainforest	Chile; 2014; T. Jung, A. Durán, E. Sanfuentes; Jung et al. 2018b	*ON000658 ON000752*	*OM975931 OM976448*	*OM974625 OM974485*	*OM984911 OM976543*	*ON024968 ON013818*	*OM976928 OM976686*
		CL213[bcd]	Baiting stream R09, Valdivian rainforest	Chile; 2014; T. Jung, A. Durán, E. Sanfuentes; Jung et al. 2018b	*ON000659 ON000753*	*OM975932 OM976449*	*OM974626 OM974486*	*OM984912 OM976544*	*ON024969 ON013819*	*OM976929 OM976687*
		CL233[bcd]	Baiting stream R13, Valdivian rainforest	Chile; 2014; T. Jung, A. Durán, E. Sanfuentes; Jung et al. 2018b	*ON000660 ON000754*	*OM975933 OM976450*	*OM974627 OM974487*	*OM984913 OM976545*	*ON024970 ON013820*	*OM976930 OM976688*
		CL234[bcd]	Baiting stream R13, Valdivian rainforest	Chile; 2014; T. Jung, A. Durán, E. Sanfuentes; Jung et al. 2018b	*ON000661 ON000755*	*OM975934 OM976451*	*OM974628 OM974488*	*OM984914 OM976546*	*ON024971 ON013821*	*OM976931 OM976689*
		PR11-532, TJ1605[bcd]	*Rhododendron* sp.	Ireland, Kerry; 2011; R. O'Hanlon; O'Hanlon et al. 2016	*ON000663 ON000757*	*OM975936 OM976453*	*OM974630 OM974490*	*OM984916 OM976548*	*ON024973 ON013823*	*OM976933 OM976691*
		PR12-106, TJ1604[bcd]	*R. ponticum*	Ireland, Cork; 2012; R. O'Hanlon; O'Hanlon et al. 2016	*ON000662 ON000756*	*OM975935 OM976452*	*OM974629 OM974489*	*OM984915 OM976547*	*ON024972 ON013822*	*OM976932 OM976690*
		PR12-513, TJ1607[bcd]	*Rhododendron* sp.	Ireland, Kerry; 2011; R. O'Hanlon; O'Hanlon et al. 2016	*ON000664 ON000758*	*OM975937 OM976454*	*OM974631 OM974491*	*OM984917 OM976549*	*ON024974 ON013824*	*OM976934 OM976692*
		Chile 1[b]	*Drimys winteri* leaf litter, Valdivian rainforest	Chile; 2014; E. Sanfuentes; Studholme et al. 2019	MBAB0100 2152 [e] MBAB0100 2152 [e]	MBAB0100 0005 [e] MBAB0100 0009 [e]	MBAB0100 0353 [e] MBAB0100 1629 [e]	MBAB0100 1709 [e] MBAB0100 1403 [e]	MBAB01001 431 [e] MBAB01000 528 [e]	MBAB01000 528 [e] MBAB01000 528 [e]
		Chile 2[b]	*D. winteri* leaf litter, Valdivian rainforest	Chile; 2012; E. Sanfuentes; Studholme et al. 2019	n.a. n.a.	MAYM0200 2138 [e] MAYM0200 1247 [e]	MAYM0200 1352 [e] MAYM0200 1485 [e]	MAYM0200 2226 [e] MAYM0200 0769 [e]	MAYM0200 0340 [e] MAYM0200 0148 [e]	MAYM0200 2296 [e] MAYM0200 1662 [e]
		Chile 4[b]	*D. winteri* leaf litter, Valdivian rainforest	Chile; 2012; E. Sanfuentes; Studholme et al. 2019	MBDN0200 1104 [e] MBDN0200 1104 [e]	MBDN0200 0444 [e] MBDN0200 0637 [e]	MBDN0200 0007 [e] MBDN0200 0110 [e]	MBDN0200 1933 [e] MBDN0200 0197 [e]	MBDN02000 021 [e] MBDN02000 533 [e]	MBDN02001 413 [e] MBDN02000 817 [e]
		NZFS 2646[b]	*Annona cherimola*	New Zealand, Northland; 2005; n.a.; Studholme et al. 2016	JPWV0200 0770 [e] JPWV0200 0770 [e]	JPWV0200 0072 [e] JPWV0200 0617 [e]	JPWV0200 0085 [e] JPWV0200 0195 [e]	JPWV0200 1728 [e] JPWV0200 0175 [e]	JPWV02000 032 [e] JPWV02000 257 [e]	JPWV02000 257 [e] JPWV02000 257 [e]

Table 1 (cont.)

Phytophthora species	Isolate numbers [a]		Origin		GenBank accession numbers					
	International collections	Local collections	Host	Location; year; collector; reference	28S LSU ITS	*βtub hsp90*	*tigA rpl10*	*tef-1α enl*	*ras-ypt1 cox1*	*nadh1 rps10*
		NZFS 3630[b]	*Pinus radiata*	New Zealand, Tokoroa; 2011; n.a.; Studholme et al. 2016	JPWU02000930 [e] JPWU02000930 [e]	JPWU02000457 [e] JPWU02000634 [e]	JPWU02000080 [e] JPWU02000196 [e]	JPWU02000131 [e] JPWU02000174 [e]	JPWU02000011 [e] JPWU02000272 [e]	JPWU02000272 [e] JPWU02000272 [e]
P. ludoviciana	CBS 149205, NRRL 64143[ET]	LU057[bcd]	Fallen leaf, forest stream R01	USA, Louisiana; 2020; T. Corcobado, T. Májek; this study	*ON000666 ON000760*	*OM975939 OM976456*	*OM974633 OM974493*	*OM984919 OM976551*	*ON024976 ON013826*	*OM976936 OM976694*
		LU038[bcd]	Fallen leaf, forest stream R01	USA, Louisiana; 2020; T. Corcobado, T. Májek; this study	*ON000665 ON000759*	*OM975938 OM976455*	*OM974632 OM974492*	*OM984918 OM976550*	*ON024975 ON013825*	*OM976935 OM976693*
P. morindae	CBS 121982[ET]	62B5[b]	*Morinda citrifolia*; black flag disease	USA, Hawaii; 2005; S.C. Nelson; Nelson & Abad 2010	KX252638 MH620178	KX252634 KX252637	KX252639 KX252633	KX252635 KX252636	MH988446 MH136936-KT183050	n.a. n.a.
P. multiglobulosa	CBS 148799[ET]	SL005[bcd]	Fallen leaf, forest stream R01	Indonesia, Sulawesi; 2019; T. Jung, M. Junaid, N. Nasri; this study	*ON000669 ON000763*	*OM975942 OM976459*	*OM974636 OM974496*	*OM984922 OM976554*	*ON024979 ON013829*	*OM976939 OM976697*
		SL006[bcd]	Fallen leaf, forest stream R01	Indonesia, Sulawesi; 2019; T. Jung, M. Junaid, N. Nasri; this study	*ON000667 ON000761*	*OM975940 OM976457*	*OM974634 OM974494*	*OM984920 OM976552*	*ON024977 ON013827*	*OM976937 OM976695*
		SL007[bcd]	Fallen leaf, forest stream R01	Indonesia, Sulawesi; 2019; T. Jung, M. Junaid, N. Nasri; this study	*ON000668 ON000762*	*OM975941 OM976458*	*OM974635 OM974495*	*OM984921 OM976553*	*ON024978 ON013828*	*OM976938 OM976696*
P. procera	CBS 149226 NRRL 64144[ET]	LU013[bcd]	Fallen leaf, forest stream R01	USA, Louisiana; 2020; T. Corcobado, T. Májek; this study	*ON000673 ON000767*	*OM975946 OM976463*	*OM974640 OM974500*	*OM984926* n.a.	*ON024983 ON013833*	*OM976942 OM976701*
		LU007[bcd]	Fallen leaf, forest stream R01	USA, Louisiana; 2020; T. Corcobado, T. Májek; this study	*ON000670 ON000764*	*OM975943 OM976460*	*OM974637 OM974497*	*OM984923 OM976555*	*ON024980 ON013830*	n.a. *OM976698*
		LU010[bcd]	Fallen leaf, forest stream R01	USA, Louisiana; 2020; T. Corcobado, T. Májek; this study	*ON000671 ON000765*	*OM975944 OM976461*	*OM974638 OM974498*	*OM984924 OM976556*	*ON024981 ON013831*	*OM976940 OM976699*
		LU056[bcd]	Fallen leaf, forest stream R01	USA, Louisiana; 2020; T. Corcobado, T. Májek; this study	*ON000672 ON000766*	*OM975945 OM976462*	*OM974639 OM974499*	*OM984925 OM976557*	*ON024982 ON013832*	*OM976941 OM976700*
P. pseudochilensis	CBS 148798, NRRL 64352[ET]	CL168[bcd]	Baiting stream R04, Valdivian rainforest	Chile; 2014; T. Jung, A. Durán, E. Sanfuentes; Jung et al. 2018b	*ON000679 ON000773*	*OM975952 OM976469*	*OM974646 OM974506*	*OM984932 OM976563*	*ON024989 ON013839*	*OM976948 OM976707*
		CL335[bcd]	Baiting stream R04, Valdivian rainforest	Chile; 2014; T. Jung, A. Durán, E. Sanfuentes; Jung et al. 2018b	*ON000674 ON000768*	*OM975947 OM976464*	*OM974641 OM974501*	*OM984927 OM976558*	*ON024984 ON013834*	*OM976943 OM976702*
		CL336[bcd]	Baiting stream R04, Valdivian rainforest	Chile; 2014; T. Jung, A. Durán, E. Sanfuentes; Jung et al. 2018b	*ON000675 ON000769*	*OM975948 OM976465*	*OM974642 OM974502*	*OM984928 OM976559*	*ON024985 ON013835*	*OM976944 OM976703*
		CL337[bcd]	Baiting stream R04, Valdivian rainforest	Chile; 2014; T. Jung, A. Durán, E. Sanfuentes; Jung et al. 2018b	*ON000676 ON000770*	*OM975949 OM976466*	*OM974643 OM974503*	*OM984929 OM976560*	*ON024986 ON013836*	*OM976945 OM976704*
		CL338[bcd]	Baiting stream R04, Valdivian rainforest	Chile; 2014; T. Jung, A. Durán, E. Sanfuentes; Jung et al. 2018b	*ON000677 ON000771*	*OM975950 OM976467*	*OM974644 OM974504*	*OM984930 OM976561*	*ON024987 ON013837*	*OM976946 OM976705*
		CL339[bcd]	Baiting stream R04, Valdivian rainforest	Chile; 2014; T. Jung, A. Durán, E. Sanfuentes; Jung et al. 2018b	*ON000678 ON000772*	*OM975951 OM976468*	*OM974645 OM974505*	*OM984931 OM976562*	*ON024988 ON013838*	*OM976947 OM976706*
P. pseudogallica	CBS 149206, NRRL 64136[ET]	VN861[bcd]	Fallen leaf, stream R02, cloud forest	Vietnam; 2017; T. Jung, N.M. Chi; Jung et al. 2020	*ON000680 ON000774*	*OM975953 OM976470*	*OM974647 OM974507*	*OM984933 OM976564*	*ON024990 ON013840*	*OM976949 OM976708*
		VN910[bcd]	Fallen leaf, stream R02, cloud forest	Vietnam; 2017; T. Jung, N.M. Chi; Jung et al. 2020	*ON000681 ON000775*	*OM975954 OM976471*	*OM974648 OM974508*	*OM984934 OM976565*	*ON024991 ON013841*	*OM976950 OM976709*
		VN920[bcd]	Fallen leaf, stream R02, cloud forest	Vietnam; 2017; T. Jung, N.M. Chi; Jung et al. 2020	*ON000682 ON000776*	*OM975955 OM976472*	*OM974649 OM974509*	*OM984935 OM976566*	*ON024992 ON013842*	*OM976951 OM976710*
		VN922[bcd]	Fallen leaf, stream R02, cloud forest	Vietnam; 2017; T. Jung, N.M. Chi; Jung et al. 2020	*ON000683 ON000777*	*OM975956 OM976473*	*OM974650 OM974510*	*OM984936 OM976567*	*ON024993 ON013843*	*OM976952 OM976711*

Table 1 (cont.)

Phytophthora species	Isolate numbers [a]		Origin		GenBank accession numbers					
	International collections	Local collections	Host	Location; year; collector; reference	28S LSU ITS	*βtub hsp90*	*tigA rpl10*	*tef-1α enl*	*ras-ypt1 cox1*	*nadh1 rps10*
P. pseudokernoviae	CBS 148796, NRRL 64351[ET]	CL012[bcd]	Fallen *D. winteri* leaf, Valdivian rainforest	Chile; 2014; T. Jung, A. Durán, E. Sanfuentes; Jung et al. 2018b	*ON000686 ON000780*	*OM975959 OM976476*	*OM974653 OM974513*	*OM984939 OM976570*	*ON024996 ON013846*	*OM976955 OM976714*
		CL013[bcd]	Fallen *D. winteri* leaf, Valdivian rainforest	Chile; 2014; T. Jung, A. Durán, E. Sanfuentes; Jung et al. 2018b	*ON000684 ON000778*	*OM975957 OM976474*	*OM974651 OM974511*	*OM984937 OM976568*	*ON024994 ON013844*	*OM976953 OM976712*
		CL156[bcd]	Leaf of *D. winteri* seedling, Valdivian rainforest	Chile; 2014; T. Jung, A. Durán, E. Sanfuentes; Jung et al. 2018b	*ON000685 ON000779*	*OM975958 OM976475*	*OM974652 OM974512*	*OM984938 OM976569*	*ON024995 ON013845*	*OM976954 OM976713*
		Chile 6[bh]	*D. winteri* leaf litter, Valdivian rainforest	Chile; 2014; E. Sanfuentes; Studholme et al. 2019	MBDO02000514 [e] MBDO02000514 [e]	MBDO02000455 [e] MBDO02000600 [e]	MBDO02000053 [e] MBDO02000109 [e]	MBDO02001754 [e] MBDO02000427 [e]	MBDO02000016 [e] MBDO02000562 [e]	MBDO02000923 [e] MBDO02000811 [e]
		Chile 7[bh]	*D. winteri* leaf litter, Valdivian rainforest	Chile; 2014; E. Sanfuentes; Studholme et al. 2019	MBAD02001209 [e] MBAD02001209 [e]	MBAD02002676 [e] MBAD02000923 [e]	MBAD02000192 [e] MBAD02001760 [e]	MBAD02000493 [e] MBAD02000835 [e]	MBAD02000695 [e] MBAD02000110 [e]	n.a. n.a.
P. scandinavica	CBS 149204, NRRL 66990[ET]	SW325[bcd]	Riverbank soil in boreal forest	Sweden, Kiruna; 2017; I. Milenković, T. Corcobado; this study	*ON000692 ON000786*	*OM975965 OM976482*	*OM974659 OM974519*	*OM984945 OM976576*	*ON025002 ON013852*	*OM976961 OM976720*
		SW314[bcd]	Riverbank soil in boreal forest	Sweden, Kiruna; 2017; I. Milenković, T. Corcobado; this study	*ON000687 ON000781*	*OM975960 OM976477*	*OM974654 OM974514*	*OM984940 OM976571*	*ON024997 ON013847*	*OM976956 OM976715*
		SW315[bcd]	Riverbank soil in boreal forest	Sweden, Kiruna; 2017; I. Milenković, T. Corcobado; this study	*ON000688 ON000782*	*OM975961 OM976478*	*OM974655 OM974515*	*OM984941 OM976572*	*ON024998 ON013848*	*OM976957 OM976716*
		SW316[bcd]	Riverbank soil in boreal forest	Sweden, Kiruna; 2017; I. Milenković, T. Corcobado; this study	*ON000689 ON000783*	*OM975962 OM976479*	*OM974656 OM974516*	*OM984942 OM976573*	*ON024999 ON013849*	*OM976958 OM976717*
		SW326[bcd]	Riverbank soil in boreal forest	Sweden, Kiruna; 2017; I. Milenković, T. Corcobado; this study	*ON000690 ON000784*	*OM975963 OM976480*	*OM974657 OM974517*	*OM984943 OM976574*	*ON025000 ON013850*	*OM976959 OM976718*
		SW327[bcd]	Riverbank soil in boreal forest	Sweden, Kiruna; 2017; I. Milenković, T. Corcobado; this study	*ON000691 ON000785*	*OM975964 OM976481*	*OM974658 OM974518*	*OM984944 OM976575*	*ON025001 ON013851*	*OM976960 OM976719*
P. subarctica	CBS 148850, NRRL 64339[ET]	SW176[bcd]	Baiting stream R09, boreal forest	Sweden, Kiruna; 2017; I. Milenković, T. Corcobado; this study	*ON000696 ON000790*	*OM975969 OM976486*	*OM974663 OM974523*	*OM984949 OM976580*	*ON025006 ON013856*	*OM976965 OM976724*
		SW639[bcd]	Baiting stream R09, boreal forest	Sweden, Kiruna; 2017; I. Milenković, T. Corcobado; this study	*ON000693 ON000787*	*OM975966 OM976483*	*OM974660 OM974520*	*OM984946 OM976577*	*ON025003 ON013853*	*OM976962 OM976721*
		SW640[bcd]	Baiting stream R09, boreal forest	Sweden, Kiruna; 2017; I. Milenković, T. Corcobado; this study	*ON000694 ON000788*	*OM975967 OM976484*	*OM974661 OM974521*	*OM984947 OM976578*	*ON025004 ON013854*	*OM976963 OM976722*
P. subarctica		SW641[bcd]	Baiting stream R09, boreal forest	Sweden, Kiruna; 2017; I. Milenković, T. Corcobado; this study	*ON000695 ON000789*	*OM975968 OM976485*	*OM974662 OM974522*	*OM984948 OM976579*	*ON025005 ON013855*	*OM976964 OM976723*
P. tenuimura	CBS 149227 NRRL 64142[ET]	LU052[bcd]	Fallen leaf, forest stream R01	USA, Louisiana; 2020; T. Corcobado, T. Májek; this study	*ON000704 ON000798*	*OM975977 OM976494*	*OM974671 OM974531*	*OM984957 OM976588*	*ON025014 ON013864*	*OM976973 OM976732*

Table 1 (cont.)

Phytophthora species	Isolate numbers [a]		Origin		GenBank accession numbers					
	International collections	Local collections	Host	Location; year; collector; reference	28S LSU ITS	*βtub hsp90*	*tigA rpl10*	*tef-1α enl*	*ras-ypt1 cox1*	*nadh1 rps10*
		LU050[bcd]	Fallen leaf, forest stream R01	USA, Louisiana; 2020; T. Corcobado, T. Májek; this study	*ON000697 ON000791*	*OM975970 OM976487*	*OM974664 OM974524*	*OM984950 OM976581*	*ON025007 ON013857*	*OM976966 OM976725*
		LU051[bcd]	Fallen leaf, forest stream R01	USA, Louisiana; 2020; T. Corcobado, T. Májek; this study	*ON000698 ON000792*	*OM975971 OM976488*	*OM974665 OM974525*	*OM984951 OM976582*	*ON025008 ON013858*	*OM976967 OM976726*
		LU062[bcd]	Fallen leaf, forest stream R01	USA, Louisiana; 2020; T. Corcobado, T. Májek; this study	*ON000699 ON000793*	*OM975972 OM976489*	*OM974666 OM974526*	*OM984952 OM976583*	*ON025009 ON013859*	*OM976968 OM976727*
		LU065[bcd]	Fallen leaf, forest stream R01	USA, Louisiana; 2020; T. Corcobado, T. Májek; this study	*ON000700 ON000794*	*OM975973 OM976490*	*OM974667 OM974527*	*OM984953 OM976584*	*ON025010 ON013860*	*OM976969 OM976728*
		LU066[bcd]	Fallen leaf, forest stream R01	USA, Louisiana; 2020; T. Corcobado, T. Májek; this study	*ON000701 ON000795*	*OM975974 OM976491*	*OM974668 OM974528*	*OM984954 OM976585*	*ON025011 ON013861*	*OM976970 OM976729*
		LU073[bcd]	Fallen leaf, forest stream R01	USA, Louisiana; 2020; T. Corcobado, T. Májek; this study	*ON000702 ON000796*	*OM975975 OM976492*	*OM974669 OM974529*	*OM984955 OM976586*	*ON025012 ON013862*	*OM976971 OM976730*
		LU074[bcd]	Fallen leaf, forest stream R01	USA, Louisiana; 2020; T. Corcobado, T. Májek; this study	*ON000703 ON000797*	*OM975976 OM976493*	*OM974670 OM974530*	*OM984956 OM976587*	*ON025013 ON013863*	*OM976972 OM976731*
P. tonkinensis	CBS 148852, NRRL 64356[ET]	VN859[bcd]	Fallen leaf, stream R02, cloud forest	Vietnam; 2017; T. Jung, N.M. Chi; Jung et al. 2020	*ON000705 ON000799*	*OM975978 OM976495*	*OM974672 OM974532*	*OM984958 OM976589*	*ON025015 ON013865*	*OM976974 OM976733*
		VN1106[bcd]	Fallen leaf, stream R02, cloud forest	Vietnam; 2017; T. Jung, N.M. Chi; Jung et al. 2020	*ON000706 ON000800*	*OM975979 OM976496*	*OM974673 OM974533*	*OM984959 OM976590*	*ON025016 ON013866*	*OM976975 OM976734*
		VN1107[bcd]	Fallen leaf, stream R02, cloud forest	Vietnam; 2017; T. Jung, N.M. Chi; Jung et al. 2020	*ON000707 ON000801*	*OM975980 OM976497*	*OM974674 OM974534*	*OM984960 OM976591*	*ON025017 ON013867*	*OM976976 OM976735*
		VN1108[bcd]	Fallen leaf, stream R02, cloud forest	Vietnam; 2017; T. Jung, N.M. Chi; Jung et al. 2020	*ON000708 ON000802*	*OM975981 OM976498*	*OM974675 OM974535*	*OM984961 OM976592*	*ON025018 ON013868*	*OM976977 OM976736*
		VN1109[bcd]	Fallen leaf, stream R02, cloud forest	Vietnam; 2017; T. Jung, N.M. Chi; Jung et al. 2020	*ON000709 ON000803*	*OM975982 OM976499*	*OM974676 OM974536*	*OM984962 OM976593*	*ON025019 ON013869*	*OM976978 OM976737*
P. ukrainensis	CBS 148851, NRRL 64255[ET]	UA373[bcd]	Fallen *Quercus* leaf, Vereshchytsia River	Ukraine; 2019; I. Milenković, T. Corcobado, I. Matsiakh; this study	*ON000711 ON000805*	*OM975984 OM976501*	*OM974678 OM974538*	*OM984964 OM976595*	*ON025021 ON013871*	*OM976980 OM976739*
		UA376[b]	Fallen *Quercus* leaf, Vereshchytsia River	Ukraine; 2019; I. Milenković, T. Corcobado; this study	*ON000712 ON000806*	*OM975985 OM976502*	*OM974679 OM974539*	n.a. *OM976596*	*ON025022 ON013872*	*OM976981 OM976740*
		UA430[bcd]	Fallen *Quercus* leaf, Vereshchytsia River	Ukraine; 2019; I. Milenković, T. Corcobado, I. Matsiakh; this study	*ON000713 ON000807*	*OM975986 OM976503*	*OM974680 OM974540*	*OM984965 OM976597*	*ON025023 ON013873*	*OM976982 OM976741*
		UA431[bcd]	Fallen *Quercus* leaf, Vereshchytsia River	Ukraine; 2019; I. Milenković, T. Corcobado, I. Matsiakh; this study	*ON000714 ON000808*	*OM975987 OM976504*	*OM974681 OM974541*	*OM984966 OM976598*	*ON025024 ON013874*	*OM976983 OM976742*
		UA432[bcd]	Fallen *Quercus* leaf, Vereshchytsia River	Ukraine; 2019; I. Milenković, T. Corcobado, I. Matsiakh; this study	*ON000715 ON000809*	*OM975988 OM976505*	*OM974682 OM974542*	*OM984967 OM976599*	*ON025025 ON013875*	*OM976984 OM976743*
		SW154[bcd]	Baiting stream R08, boreal forest	Sweden, Kiruna; 2017; I. Milenković, T. Corcobado; this study	*ON000710 ON000804*	*OM975983 OM976500*	*OM974677 OM974537*	*OM984963 OM976594*	*ON025020 ON013870*	*OM976979 OM976738*
P. taxon boehmeriae-like	CBS 357.52, IMI 32199, ATTC 60173, WPC P1378	45F8[bg]	*Citrus sinensis*, fruit brown rot	Argentina, Corrientes; 1939; M.J. Frezzi; Frezzi 1941	KX252645 KF317089	KX252641 KX252644	KX252646 KX252640	KX252642 KX252643	n.a. KF317111-HQ261252	n.a. n.a.
P. taxon boehmeriae-like 2		Psld[bg]	*Zanthoxylum piperitum*	China, Shannxi; ca 2014; W. Jiefei; n.a.	n.a. KJ854387	n.a. n.a.	n.a. n.a.	n.a. n.a.	n.a. n.a.	n.a. n.a.
P. taxon boehmeriae-like 2		Pme002[bi]	*Medicago sativa*	China; n.a.; C.Z. Lan; n.a.	n.a. MG823393	n.a. n.a.	n.a. n.a.	n.a. n.a.	n.a. n.a.	n.a. n.a.

Table 1 (cont.)

Phytophthora species	Isolate numbers [a]		Origin		GenBank accession numbers					
	International collections	Local collections	Host	Location; year; collector; reference	28S LSU ITS	*βtub hsp90*	*tigA rpl10*	*tef-1α enl*	*ras-ypt1 cox1*	*nadh1 rps10*
P. taxon canthium		CMW35236[b]	Forest soil	South Africa, Eastern Cape; ca 2013; E. Oh; Oh et al. 2013	n.a. KC855189	n.a. n.a.	n.a. n.a.	n.a. n.a.	n.a. KC855134	n.a. n.a.
P. taxon gallica-like 3		DGW18203.2[bj]		China, Hebei, Saihanba Forest; n.a.	n.a. OK083779	n.a. n.a.	n.a. n.a.	n.a. n.a.	n.a. n.a.	n.a. n.a.
P. taxon koreanensis		KACC 40173[bg]	*Ailanthus altissima*, leaf blight	Korea, Manchon Mountain; 1993; J.S. Kim; Kim & Kim 2004	n.a. AF228076	n.a. n.a.	n.a. n.a.	n.a. n.a.	n.a. n.a.	n.a. n.a.
P. taxon Maryland 6		808_GUN_1_c[b]	Stream baiting	USA, Maryland; 2009; Y. Balci; n.a.	n.a. KC479202	n.a. n.a.	n.a. n.a.	n.a. n.a.	n.a. n.a.	n.a. n.a.

n.a. = not available.
[a] Abbreviations of isolates and culture collections: ATCC = American Type Culture Collection, Manassas, USA; CBS = Centraalbureau voor Schimmelcultures, Utrecht, Netherlands; CMW = Forestry and Agricultural Biotechnology Institute (FABI), Pretoria, South Africa; CPHST BL = culture collection of IDPhy (https://idtools.org/id/phytophthora/); IMI = CABI Bioscience, UK; NRRL = Agriculture Research Service (ARS) Culture Collection, Peoria, IL, USA; SCRP = The James Hutton Institute, Dundee, UK; VHS = Vegetation Health Service Collection, Department of Environment and Conservation, Perth, Australia; WPC = World Phytophthora Collection, University of California Riverside, USA; other isolate names and numbers are as given by the collectors and on GenBank, respectively. [ET] indicates ex-type strains.
[b] Isolates used in the phylogenetic studies.
[c] Isolates used in the morphological studies.
[d] Isolates used in the temperature-growth studies.
[e] Genome sequence sourced from the GenBank Whole-Genome Shotgun contigs.
[f] Mitochondrial genome sequence.
[g] Originally identified as *P. boehmeriae*.
[h] Originally identified as *P. kernoviae*.
[i] Originally identified as *P. medicaginis*.
[j] Originally identified as *P. gallica*.

and because of the often considerable time required to produce the appropriate publication. This situation has arisen more frequently as more and more novel *Phytophthora* taxa are being discovered. In this regard, we do not concur with the use of the informal terminology '*Phytophthora* sp. x' in the same context. A putative new taxon is not a species (or a 'sp.') until its correct hierarchical taxonomic status has been defined (as far as is reasonable), and its proposed name has been formally designated under the ICNafp (International Code of Nomenclature for algae, fungi, and plants; https://www.iapt-taxon.org) guidelines. On this basis we consider that a casual use of '*Phytophthora* sp. x' in the case of a putative but only partially characterised new taxon is somewhat prejudicial to the final outcome. We have therefore confined ourselves to use the term '*Phytophthora* taxon x' throughout this manuscript.

MATERIAL AND METHODS

Phytophthora isolates

Details of all isolates used in the phylogenetic, morphological and physiological studies are given in Table 1. Sampling and isolation methods from forest soil and river systems were described in Jung et al. (2017a, 2018a, 2020). The isolates of *P. celebensis*, *P. chilensis*, *P. pseudochilensis*, *P. pseudogallica*, *P. javanensis*, *P. ludoviciana*, *P. multiglobulosa*, *P. procera*, *P. subarctica*, *P. tenuimura*, *P. tonkinensis* and *P. ukrainensis* spp. nov. were recovered from forest streams in Valdivian rainforests in Chile, a montane cloud forest in Vietnam, tropical lowland rainforests in Indonesia, a swamp forest in Louisiana, boreal forests in Sweden and a riparian forest in Ukraine (Fig. 1; Table 1), by plating necrotic baiting leaves or naturally fallen floating leaves onto selective PARPNH-agar (Jung et al. 1996, 2020). All isolates of *P. pseudokernoviae* sp. nov. were isolated from necrotic *Drimys winteri* leaves in a Valdivian rainforest (Fig. 1d–e) whereas all isolates of *P. scandinavica* sp. nov. were baited in the lab from riverbank soil collected in the Kiruna area of northern Sweden using young *Fagus sylvatica* leaves as baits (Jung et al. 2019). In addition, for comparative studies isolates of four described Clade 10 species were used which had been obtained between 2014 and 2018: *P. kernoviae* from forest streams in Valdivian rainforests (Jung et al. 2018a) and from *Rhododendron* spp. in Ireland (O'Hanlon et al. 2016); *P. gallica* from forest streams and riparian ecosystems in Croatia, Czech Republic, Serbia, Sweden and Ukraine; *P. intercalaris* from a nursery seedling of *Aronia* in Croatia; and *P. gondwanensis* from a forest stream on Amami Island, Japan (Table 1). For all isolates, single hyphal tip cultures were produced under the stereomicroscope at ×20 from the margins of fresh cultures on V8-juice agar (V8A; 16 g agar, 3 g $CaCO_3$, 100 mL Campbell's V8 juice, 900 mL distilled water; Jung et al. 1999). Stock cultures were maintained on V8A and carrot juice agar (CA; 20 g agar, 3 g $CaCO_3$, 100 mL carrot juice, 900 mL distilled water; Scanu et al. 2014) at 10 °C in the dark. All isolates of the 14 new *Phytophthora* spp. are preserved in the culture collection maintained at Mendel University in Brno. Ex-type cultures were deposited at the Agriculture Research Service (ARS) Culture Collection, Peoria, IL, USA, and/or the CBS Culture Collection (CBS) at the Westerdijk Institute, Utrecht, Netherlands (Table 1). Dried V8A cultures of the 14 ex-type isolates were deposited as holotypes in the herbarium of the Hungarian Natural History Museum, Budapest, Hungary.

DNA isolation, amplification and sequencing

For all *Phytophthora* isolates from Clade 10 obtained in this study and for the ex-type isolate CBS 125801 of *P. constricta* from Clade 9 DNA was extracted from c. 15–100 mg of mycelium scraped from 1–3-wk-old V8A cultures, placed into 2 mL

Fig. 1 Natural habitats of known and new *Phytophthora* species from phylogenetic Clade 10. a. Flooded swamp forest near Archie in Louisiana, USA (*P. ludoviciana*, *P. procera*, *P. tenuimura*); b. river running through a boreal forest near Kiruna in northern Sweden (*P. scandinavica*, *P. ukrainensis*); c–e. Valdivian rainforest in Parque Oncol near Valdivia, Chile (*P. chilensis*, *P. kernoviae*, *P. pseudochilensis*, *P. pseudokernoviae*); d–e. fallen leaves and seedling of *Drimys winteri* with necrotic lesions (arrows) from which *P. pseudokernoviae* was isolated; f. stream running through a montane cloud forest at the Fansipan in northern Vietnam (*P. pseudogallica*, *P. tonkinensis*); g. waterfall in a submontane tropical rainforest in Java, Indonesia (*P. javanensis*); h. tropical hill rainforest in Sulawesi, Indonesia (*P. multiglobulosa*); i. submontane tropical rainforest in Sulawesi, Indonesia (*P. celebensis*).

homogenisation tubes (Lysis Matrix A; MP Biomedicals, Irvine, USA) and disrupted using a Precellys Evolution instrument (Bertin Technologies, Montigny-le-Bretonneux, France) until the mixture was homogenous. DNA was purified using the Monarch Genomic DNA Purification Kit (New England Biolabs, Ipswich, USA) and treated with RNase A following manufacturer's protocol for tissue samples. DNA was eluted with 100 µL of pre-warmed elution buffer and preserved at -80 °C for long-term storage.

Nine nuclear gene regions, i.e., the internal transcribed spacer region (ITS1–5.8S–ITS2) of the ribosomal RNA gene (ITS), the 5' terminal domain of the large subunit (28S-LSU) of the nuclear ribosomal RNA, heat shock protein 90 (*hsp90*), β-tubulin (*βtub*), 60S ribosomal protein L10 (*rpl10*), *TIGA* gene fusion protein (genes encoding triose-phosphate isomerase (TPI) and glyceraldehyde-3-phosphate dehydrogenase (GAPDH) fused and forming a single transcriptional unit: *tigA*), translation elongation factor 1 alpha (*tef-1α*), enolase (*enl*), *Ras*-like GTP-binding protein *YPT1* (*ras-ypt1*), and the three mitochondrial genes cytochrome-c oxidase 1 (*cox1*), subunit 1 of NADH dehydrogenase (*nadh1*) and 40S ribosomal protein S10 (*rps10*) were amplified and sequenced (Table 2). PCR amplifications were performed using a LightCycler 480 II instrument (Roche, Basel, Switzerland) or Eppendorf Mastercycler nexus GSX1 (Eppendorf, Hamburg, Germany). As demonstrated by Yang & Hong (2018), PCR success rate is highly variable for each locus. Therefore, the FM83 primer (*cox1*; Martin & Tooley 2003) and the *tigA* primers (Blair et al. 2008) were re-designed and the new reverse Ypt_820 primer (*ras-ypt1*) was designed in order to obtain a longer fragment of the coding sequence (Table 2).

Table 2 PCR conditions and primers used for amplification and sequencing of *Phytophthora* isolates from Clade 10.

Locus	Primer names	Primer sequences (5'-3')	Orientation	Annealing temperature (°C)	Extension time (s)	Reference for primer sequences
βtub [a,b]	TUBUF2	CGGTAACAACTGGGCCAAGG	Forward	68	12	Kroon et al. (2004)
	TUBUR1	CCTGGTACTGCTGGTACTCAG	Reverse			
	Btub_F1A	GCCAAGTTCTGGGARGTSAT	Forward	66	15	Blair et al. (2008)
	Btub_R1A	CCTGGTACTGCTGGTAYTCMGA	Reverse			
cox1 [d]	OomCoxI-Levup [a]	TCAWCWMGATGGCTTTTTTCAAC	Forward	60	10	Robideau et al. (2011)
	OomCoxI-Levlo [a]	CYTCHGGRTGWCCRAAAAACCAAA	Reverse			
	COXF4N [c]	GTATTTCTTCTTTATTAGGTGC	Forward	50	65	Kroon et al. (2004)
	COXR4N [c]	CGTGAACTAATGTTACATATAC	Reverse			
	OomCoxI-Levup [c]	TCAWCWMGATGGCTTTTTTCAAC	Forward	50	80	Robideau et al. (2011), this study.
	FM83_Oom [c]	CHCCNATAAARAATAACCARAARTG	Reverse			
	FM84 [c]	TTTAATTTTTAGTGCTTTTGC	Forward	50	95	Martin & Tooley (2003), this study.
	FM83_Oom [c]	CHCCNATAAARAATAACCARAARTG	Reverse			
tef-1α [a]	EF1A_FL	GGTCACCTGATCTACAAGTGC	Forward	60	15	Blair et al. (2008)
	EF1A_RL	CCTTCTTGTTCACCGACTTG	Reverse			
enl [e]	Enl_for [d]	CTTTGACTCGCGTGGCAAC	Forward	55–58	90	Blair et al. (2008)
	Enl_FY [d]	CAACCCSACCGTYGAGGT	Forward			
	Enl_rev	CCTCCTCAATACGMAGAAGC	Reverse			
hsp90 [a]	HSP90_F1int	CAAGGTGATCCCGGACAAGGC	Forward	63–66	15	Blair et al. (2008)
	HSP90R1	ACACCCTTGACRAACGACAG	Reverse			
ITS [a]	ITS1	TCCGTAGGTGAACCTGCGG	Forward	63–65	12	White et al. (1990), Cooke et al. (2000)
	ITS4 [f]	TCCTCCGCTTATTGATATGC	Reverse			
	ITS6 [f]	GAAGGTGAAGTCGTAACAAGG	Forward			
LSU [a,g]	CTB6	GCATATCAATAAGCGGAGG	Forward	53	20	Garbelotto et al. (1997), Hopple & Vilgalys (1994)
	LR3 [h]	CCGTGTTTCAAGACGGG	Reverse			
	LR3R [h]	GTCTTGAAACACGGACC	Forward			
	LR7	TACTACCACCAAGATCT	Reverse			
nadh1 [c]	NADHF1	CTGTGGCTTATTTTACTTTAG	Forward	50	65	Kroon et al. (2004)
	NADHR1	CAGCAGTATACAAAAACCAAC	Reverse			
ras-ypt1 [a]	Ypt1F	CGACCATYGGYGTKGACTTT	Forward	60–62	7	Chen & Roxby (1996), this study
	Ypt_820	CCATCATCATGAADGCYTTYTCR	Reverse			
rpl10 [a]	60SL10_for	GCTAAGTGTTACCGTTTCCAG	Forward	62–64	7	Martin & Tooley (2003)
	60SL10_rev	ACTTCTTGGAGCCCAGCAC	Reverse			
rps10 [i]	rps10_DB_FOR	GTTGGTTAGAGYARAAGACT	Forward	48	30	Foster et al. (2022)
	rps10_DB_REV	RTAYACTCTAACCAACTGAGT	Reverse			
tigA [c]	Tig_FY_Oom	TYGTGGGCGGHAAYTGGAA	Forward	60–63	120	This study
	G3PDH_for_Oom [h]	TBGCBATYAAYGGHTTYGG	Forward			
	Tig_rev_Oom [h]	CCRAADCCRTTRATVGCVA	Reverse			
	G3PDH_rev_Oom	DCCCCACTCRTTGTCRTACCAM	Reverse			

[a] PCR protocol 1: 20 µl volume containing 10.4 µl H_2O, 4 µl Q5 Reaction Buffer (5X), 1 µl of each primer (10 µM), 0.4 µl deoxynucleotide (dNTP) mixture (Meridian Bioscience, Memphis, USA) (2.5 mM each), 0.2 µl of Q5 High-Fidelity DNA Polymerase (2 U/µl) (New England Biolabs, Ipswich, USA), and 3 µl of gDNA. Initial denaturation for 30 s at 98 °C; 35 cycles consisting of 5 s at 98 °C, 20 s at optimised annealing temperature for each primer set, optimised length of extension at 72 °C; 2 min at 72 °C for final extension.

[b] Two primer pairs were used separately: TUBUF2/TUBUR1 or Btub_F1A/Btub_R1A.

[c] PCR protocol 2: 20 µl volume containing 10 µl H_2O, 4 µl PrimeSTAR GXL Buffer (5X), 0.8 µl of each primer, 1.6 µl dNTP mixture, 0.4 µl PrimeSTAR GXL DNA Polymerase (1.25 U/µl) (TaKaRa Bio, Kusatsu, Shiga, Japan), and 3 µl of gDNA. Initial denaturation for 5s at 98 °C; 35 cycles consisting of 10 s at 98 °C, 15 s at optimised annealing temperature, optimised length of extension at 68 °C; 5 min at 68 °C for final extension.

[d] COX4FN/COX4RN primers were used to obtain the amplicons for sequencing. For samples that did not amplify with COX4N primers, two sets of alternative primers (OomCoxI-Levup/FM83_Oom; FM84/FM83_Oom) were used.

[e] Two primer combinations were used separately: Enl_for/Enl_rev or Enl_FY/Enl_rev.

[f] Two primer combinations were used separately: ITS1/ITS4 or ITS6/ITS4.

[g] Double concentration of Q5 polymerase.

[h] Primers used exclusively for sequencing.

[i] PCR protocol 3: 20 µl volume containing 6.2 µl H_2O, 10 µl One*Taq* Hot Start Quick-Load 2X Master Mix with Standard Buffer (New England Biolabs, Ipswich, USA) 0.4 µl of each primer, and 3 µl of gDNA. Initial denaturation for 5 s at 98 °C; 35 cycles consisting of 30 s at 98 °C, 30 s at optimised annealing temperature, optimised length of extension at 72 °C; 7 min at 72 °C for final extension.

Global alignments of *cox1*, *tigA* and *ras-ypt1* complete sequences were produced, including both sequences obtained from GenBank and own unpublished sequences, representing all described species and undescribed taxa of *Phytophthora* and *Halophytophthora* (if available) and *Nothophytophthora*, and selected species from other oomycete genera. Each nucleotide of each primer was carefully checked whether it is conserved and, if necessary, replaced by a degenerate nucleotide. All primers were synthesized by Elizabeth Pharmacon spol. s.r.o. (Brno, Czech Republic). Their annealing temperatures were estimated using Tm calculator (http://tmcalculator.neb.com/#!/main) and adjusted empirically, according to observed PCR amplification rates. Table 2 provides a comprehensive overview of the PCR conditions and the primers used.

PCR products were visualised by gel electrophoresis (300 V; 5 min) using 2 % agarose gel stained by DNA Stain G (SERVA, Heidelberg, Germany). All amplicons were purified and sequenced in both directions by Eurofins Genomics GmbH (Cologne and Ebersberg, Germany) using the amplification primers, except for the LSU and *tigA* amplicons which required each two additional primers (Table 2). Electropherograms were quality checked and forward and reverse reads were compiled using Geneious Prime® v. 2022.0.2 (Biomatters Ltd., Auckland, New Zealand). Pronounced double peaks were considered as heterozygous positions and labelled according to the IUPAC (International Union of Pure and Applied Chemistry; https://iupac.org) coding system. All sequences generated in this study were deposited in GenBank and accession numbers are given in Table 1.

Phylogenetic analysis

For phylogenetic analyses, the sequences obtained in this study were complemented with publicly available sequences of isolates from *Phytophthora* Clade10 sourced from the GenBank Nucleotide Collection and GenBank Whole-Genome Shotgun contigs (Table 1). The sequences of all loci used in the analyses were aligned using the MAFFT v. 7 (Katoh & Standley 2013) plugin within the Geneious Prime® software by the E-INS-I strategy (ITS) or the G-INS-I strategy (all other loci). The ITS alignments in this study were manually edited and adjusted.

Since for the informally designated Clade 10 taxa *P.* taxon canthium and *P.* taxon Maryland 6 and several isolates of *P. boehmeriae* and *P. gallica* only sequences from the ITS and partly a few other gene regions were available at GenBank, they could not be included in the multigene phylogenetic analyses of this study. To assess the phylogenetic positions of *P.* taxon canthium and *P.* taxon Maryland 6 within Clade 10 and to confirm the identity of a geographically representative range of isolates designated at GenBank as *P. boehmeriae* and *P. gallica*, respectively, an 892-characters ITS-dataset was analysed. It included 74 isolates of the 14 new *Phytophthora* species, 53 isolates belonging to the seven described species and three informally designated taxa of Clade 10, and two isolates of the Clade 9 species *P. constricta* (CBS 125801) and *P. fallax* (CBS 119109) as outgroup taxa.

The relative phylogenetic positions of the 14 new and eight described or informally designated *Phytophthora* species from Clade 10 were assessed with a 12-partition (LSU, ITS, *βtub*, *hsp90*, *tigA*, *rpl10*, *tef-1α*, *enl*, *ras-ypt1*, *cox1*, *nadh1*, *rps10*) dataset (11 259 characters) which included 88 Clade 10 isolates representative of genetic variation and geographic distribution and *P. constricta* (CBS 125801) and *P. fallax* as outgroup taxa. For *P. fallax*, sequences from two isolates (CBS 119109 and ICMP 17563) were combined since for neither of them all 12 loci were available at GenBank (the two isolates shared an identical *cox1* sequence). For *P.* taxon boehmeriae-like and *P. morindae* *ras-ypt1*, *nadh1* and *rps10* genes were not available. Their 9-gene alignments included in the 12-partition dataset contained 9 650 characters. For *P. afrocarpa* only ITS, *βtub*, *hsp90* and *cox1* sequences (3 141 characters) could be included in the 12-partition dataset. The 90-isolates datasets of the 12 loci were also analysed separately.

For Maximum Likelihood (ML) analyses best-fit substitution models were selected using ModelFinder (Kalyaanamoorthy et al. 2017) based on the corrected Akaike Information Criterion (AICc). The phylogeny was reconstructed with IQ-TREE v. 1.6.12 (Nguyen et al. 2015) using 2 000 standard nonparametric bootstrap replicates. As a summarizing tree the 50 % majority rule consensus tree was built with SumTrees v. 4.4.0 within the Python library DendroPy v. 4.4.0 (Sukumaran & Holder 2010). Edge lengths of the summarizing tree were calculated as mean lengths for the corresponding edges in the input set of trees.

Bayesian Inference (BI) analyses were performed using BEAST 2 (Bouckaert et al. 2014). For all BI analyses Metropolis coupled MCMC (MC3) implemented in the CoupledMCMC package (Müller & Bouckaert 2019) was used with four chains – three heated and one cold. The chain length was always set to 20 000 000, except for the concatenated 12-loci dataset where it was 40 000 000, and every 5 000th state was sampled. Target switch probability was set to the recommended value of 0.234 (Kone & Kofke 2005, Atchadé et al. 2011). Site models for individual partitions were automatically selected by model averaging implemented in the bModelTest package (Bouckaert & Drummond 2017). As a clock model the uncorrelated lognormal relaxed molecular clock model (Drummond et al. 2006) was used in all cases. The unit of branch lengths of the sampled trees was set to be substitutions per site. Parameter estimates were summarized with TreeAnnotator v. 2.6.0 (part of BEAST 2) and mapped onto the 50 % majority-rule consensus tree created by SumTrees v. 4.4.0 (Sukumaran & Holder 2010). The option 'force-rooted' was set for SumTrees telling the program to treat all the trees as rooted. The posterior estimates of the parameters were summarised with Tracer (Rambaut et al. 2018). The quality of the parameter estimates was assessed based on visual analysis of the trace plots and ESS values. The minimum ESS value for the parameter estimates to be considered properly sampled was 200 (standard setting). The likelihood and most of the other parameters of all the final trees were higher than 200. In all BI analyses a 25 % burn-in was used.

Phylogenetic trees were visualised in TreeGraph2 v. 2.15.0-887 beta (Stöver & Müller 2010) and/or MEGA 11 v. 11.0.11 (Tamura et al. 2021) and edited in figure editor programs. All datasets and trees deriving from BI and ML analyses were deposited in the Dryad Digital Repository (https://datadryad.org; https://doi.org/10.5061/dryad.41ns1rngw).

Morphology of asexual and sexual structures

Morphological features of sporangia, oogonia, oospores, antheridia, chlamydospores, hyphal swellings and aggregations of all isolates of the 14 new species and selected isolates of related species from Clade 10 were compared with each other.

To induce the formation of sporangia, two 12–15 mm square discs were cut from the growing edge of a 3–7-d-old V8A colony and flooded in a 90 mm diam Petri dish with non-sterile soil extract (50 g of filtered oak forest soil in 1000 mL of distilled water, filtered after 24 h) just above the surface of the aerial mycelium (Jung et al. 1996). The Petri dishes were incubated at 20 °C and natural daylight near a window and the soil extract changed after c. 6 h. Shape, type of apex, caducity and special features of sporangia and the formation of hyphal swellings and aggregations were recorded after 24–48 h. For each isolate 50

sporangia were measured at ×400 using a compound microscope (Zeiss Imager.Z2), a digital camera (Zeiss Axiocam ICc3) and a biometric software (Zeiss ZEN).

The formation of chlamydospores, gametangia (oogonia and antheridia) and their characteristic features were examined on V8A after 21–30 d growth at 20 °C in the dark. Self-sterile isolates of *P. ludoviciana*, *P. procera*, *P. pseudogallica*, *P. subarctica* and *P. ukrainensis* were paired on V8A with known A1 and A2 mating type tester strains of *P. cinnamomi* (A1: TW12; A2: MP74) and examined after 4 wk incubation at 20 °C in the dark in order to determine their mating type (Jung et al. 2017c). For each isolate of homothallic species each 50 oogonia, oospores and antheridia chosen at random were measured under a compound microscope at ×400 as described before. The oospore wall index was calculated according to Dick (1990). In addition, if present, the diameters of 50 chlamydospores per isolate were measured.

Colony morphology, growth rates and cardinal temperatures

Colony growth patterns of all 14 new Clade 10 species and *P. gallica*, *P. gondwanensis*, *P. intercalaris* and *P. kernoviae* were described from 10–14-d-old cultures grown at 20 °C in the dark on V8A, CA and potato-dextrose agar (PDA; HiMedia, Mumbai, India). Colony morphologies were described according to patterns observed previously (Erwin & Ribeiro 1996, Brasier et al. 2005, Jung & Nechwatal 2008, Jung et al. 2011, 2017b, c, d).

For temperature-growth relationships, representative isolates of all 14 new Clade 10 species, *P. gallica*, *P. gondwanensis*, *P. intercalaris* and *P. kernoviae* (Table 1) were sub-cultured onto V8A in 90 mm Petri dishes and incubated for 24 h at 20 °C to stimulate onset of growth (Jung et al. 2002). Then three replicate plates per isolate were transferred to 10, 15, 20, 25, 27.5, 30, 32.5 and 35 °C. Radial growth was recorded after 7–14 d, before colonies reached the margin of the Petri dishes, along two lines intersecting the centre of the inoculum at right angles and the mean growth rates (mm/d) were calculated. Plates showing no growth at 25, 27.5, 30, 32.5 or 35 °C were returned to 20 °C to determine the lethal temperatures.

RESULTS

Phylogenetic analysis

The relative phylogenetic positions of the designated Clade 10 taxa *P.* taxon canthium and *P.* taxon Maryland 6 and the identity of a geographically representative range of isolates designated at GenBank as *P. boehmeriae* and *P. gallica* was studied using an 892-characters ITS-dataset (129 isolates). The ML bootstrap best tree and the 50 % majority consensus rule tree derived from the BI analysis showed nearly identical topology, and the latter is presented here with both BI Posterior Probability and ML bootstrap values included (Fig. 2; Dryad dataset: https://doi.org/10.5061/dryad.41ns1rngw). In both phylogenetic analyses of the ITS dataset the deeper phylogeny within Clade 10 could not be resolved and was characterised by a strongly supported polytomy of three clusters comprising all soil- and waterborne taxa with nonpapillate persistent sporangia (Subclades 10a and 10b) and one large cluster of airborne species with papillate caducous sporangia (Subclade 10c) (Fig. 2). Isolates 33-4-R.1 from Oregon and 76-P1 from New York State were confirmed to belong to *P. gallica*. However, isolate DGW182032 from north-eastern China, originally assigned to *P. gallica*, resided on a separate branch differing from its nearest relatives *P. gallica* and *P. subarctica* at 7–8 positions, and is, hence, re-designated here as *Phytophthora* taxon gallica-like 3. Differing from the ex-type isolate of *P. intercalaris* from Virginia at 10 positions isolate 808_GUN_1_c of the informally designated *P.* taxon Maryland 6 from a stream in Maryland clustered in the BI analysis with *P. intercalaris* while in the ML analysis it resided with strong support in sister position to the latter (Fig. 2; Dryad dataset: https://doi.org/10.5061/dryad.41ns1rngw). *Phytophthora* taxon canthium from the Cape Province in South Africa clustered together with the airborne *P. morindae* from Hawaii in sister position to a polytomy containing the four airborne species which constitute the *P. kernoviae* complex, i.e., *P. kernoviae*, *P. chilensis*, *P. pseudochilensis* and *P. pseudokernoviae* (Fig. 2), differing from the *P. kernoviae* complex and *P. morindae* at 39–42 and 44 positions, respectively. *Phytophthora boehmeriae* isolates WPC P3963 and SCRP23 from cotton in China and isolates WPC P7460 and OCPC4 from sweet pepper in India were confirmed to belong to *P. boehmeriae*. Conversely, isolates ATTC 46717 from *Ficus* soil in Papua New Guinea, ALT-18 from an *Acacia mearnsii* plantation in Brazil, CBS 100410 from *Persoonia longifolia* in Western Australia, and CMW 19441 from a *Eucalyptus smithii* plantation in South Africa, all originally identified as *P. boehmeriae*, resided within and, hence, were re-designated as *P. gondwanensis*. Isolate KACC 40173 from *Ailanthus altissima* in Korea, originally also identified as *P. boehmeriae*, clustered with *P. boehmeriae* but resided on a considerably longer branch. Differing from *P. boehmeriae* isolates at 11–12 positions isolate KACC 40173 most likely belongs to an undescribed sister species of *P. boehmeriae* which is designated here as *Phytophthora* taxon koreanensis. The unnamed isolate PsId from *Zanthoxylum piperitum* in China and isolate Pme002 from *Medicago sativa* in China, erroneously identified as *P. medicaginis*, clustered in sister position to *P.* taxon boehmeriae-like from orange plantations in Argentina. Differing from the latter at 9 and 14 positions, respectively, isolates PsId and Pme002 most likely constitute an unknown sister species of *P.* taxon boehmeriae-like which is designated here as *Phytophthora* taxon boehmeriae-like 2.

Phytophthora taxon canthium was also included in the BI and ML analyses of a 1 346 characters *cox1* dataset which included 114 isolates of the 14 new and the seven described species from Clade 10, and *P. constricta* and *P. fallax* as outgroup taxa. The overall topology of the *cox1* trees (not shown; Dryad dataset: https://doi.org/10.5061/dryad.41ns1rngw) was similar to the ITS trees. *Phytophthora* taxon canthium formed a polytomy together with two clusters containing all 11 papillate airborne Clade 10 taxa. Across a sequence length of 855 characters *P.* taxon canthium differed from the latter at 29–38 positions (genetic distance = 3.4–4.4 %).

The relative phylogenetic positions of the 14 new Clade 10 species and the phylogenetic structure of Clade 10 were studied using a 12-partition (LSU, ITS, *βtub*, *hsp90*, *tigA*, *rpl10*, *tef-1α*, *enl*, *ras-ypt1*, *cox1*, *nadh1*, *rps10*) dataset of 90 isolates from the 14 new and eight described or informally designated *Phytophthora* taxa from Clade 10 with *P. constricta* and *P. fallax* from Clade 9 as outgroup taxa. In both the BI and ML analyses support for most nodes was strong and equivalent. The ML bootstrap best tree and the fifty percent majority rule consensus tree derived from the BI analysis showed nearly identical topology amongst species with the exception that in the BI analysis the *P. intercalaris* - *P. scandinavica* cluster resided within Subclade 10b whereas in the ML analysis it resided in a sister position to Subclade 10c but with low bootstrap support. The BI tree is presented here with both Bayesian Posterior Probability values and Maximum Likelihood bootstrap values included (Fig. 3; Dryad dataset: https://doi.org/10.5061/dryad.41ns1rngw). Both BI and ML analyses revealed 22 discrete and fully supported lineages within Clade 10 unambiguously corresponding to the seven described species *P. afrocarpa*, *P. boehmeriae*, *P. gallica*, *P. gondwanensis*, *P. intercalaris*, *P. kernoviae* and *P. morindae*;

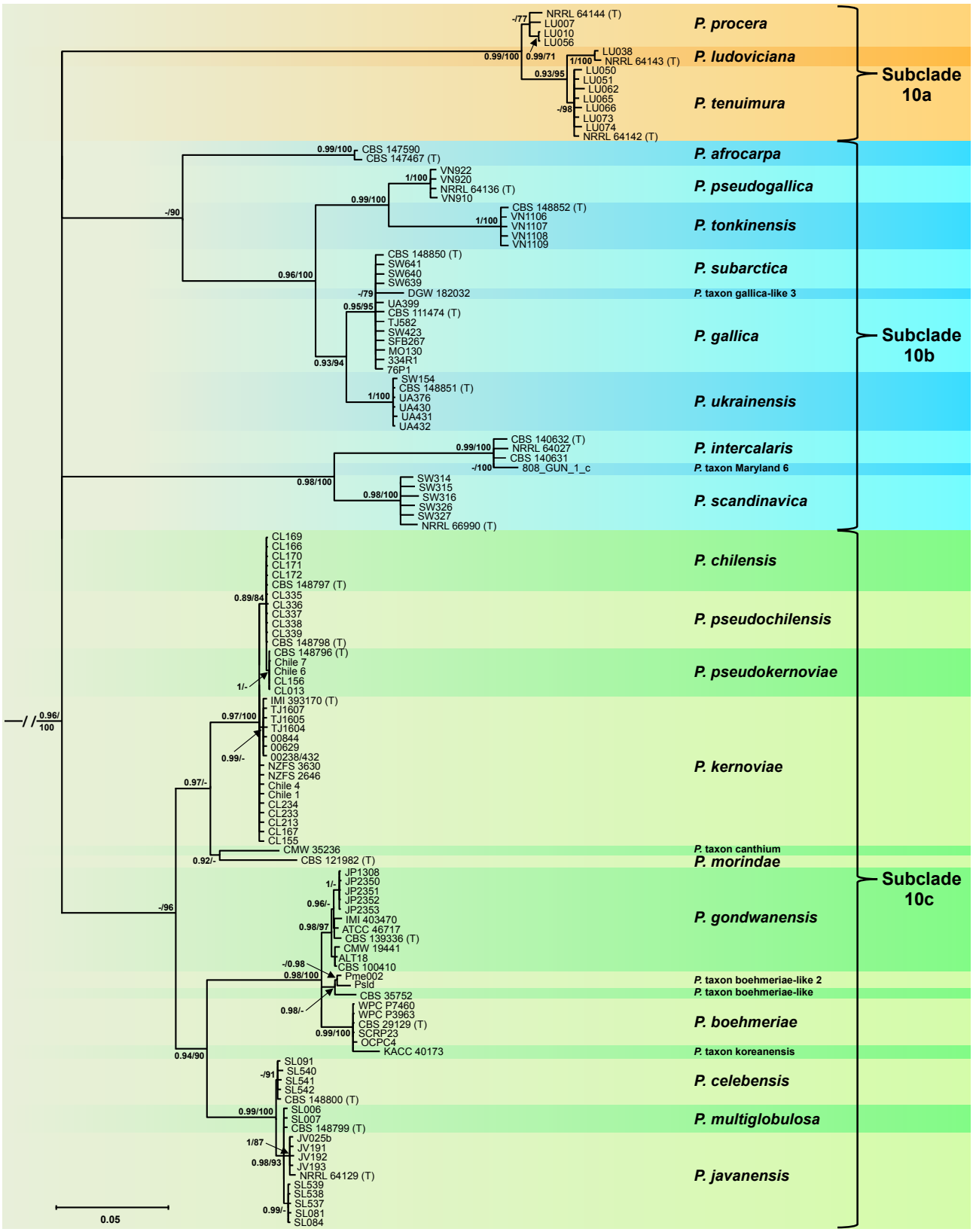

Fig. 2 Fifty percent majority rule consensus phylogram derived from Bayesian inference analysis of an ITS dataset of *Phytophthora* major Clade10. Bayesian posterior probabilities and Maximum Likelihood bootstrap values (in %) are indicated but not shown below 0.80 and 70 %, respectively. *Phytophthora constricta* and *P. fallax* from Clade 9 were used as outgroup taxa (not shown). Subclades are indicated as in the multigene phylogeny in Fig. 3. (T) designates ex-type isolates. — Scale bar indicates 0.05 expected changes per site per branch.

the 14 new species *P. celebensis*, *P. chilensis*, *P. javanensis*, *P. ludoviciana*, *P. multiglobulosa*, *P. procera*, *P. pseudochilensis*, *P. pseudogallica*, *P. pseudokernoviae*, *P. scandinavica*, *P. subarctica*, *P. tenuimura*, *P. tonkinensis* and *P. ukrainensis*; and the informally designated *P.* taxon boehmeriae-like (Fig. 3). The overall structure of Clade 10 was characterised by two Subclades (10a and 10b) which contained the 11 water- or soil-borne species with nonpapillate persistent sporangia, and the large Subclade 10c comprising all 11 airborne taxa with papillate caducous sporangia. Subclades 10a and 10c had strong support values whereas in Subclade 10b the relative phylogenetic positions of the *P. intercalaris-P. scandinavica* cluster and the cluster containing the other six species could not be resolved (Fig. 3). The early diverged Subclade 10a which

included *P. procera* and the sister species *P. ludoviciana* and *P. tenuimura*, all isolated from an inundated swamp forest in Louisiana, resided in a strongly supported basal position to a large cluster containing the other two subclades. Within Subclade 10b the distantly related *P. scandinavica* from riverbank soil in Northern Sweden and *P. intercalaris* from waterbodies in Eastern North America grouped together in sister position to a large cluster containing the other six species. However, due to low support values and inconsistent grouping in the BI and ML analyses the relative phylogenetic positions of the two clusters remained ambiguous (Fig. 3). Although for *P. afrocarpa* only ITS, *βtub*, *hsp90* and *cox1* sequences were available its

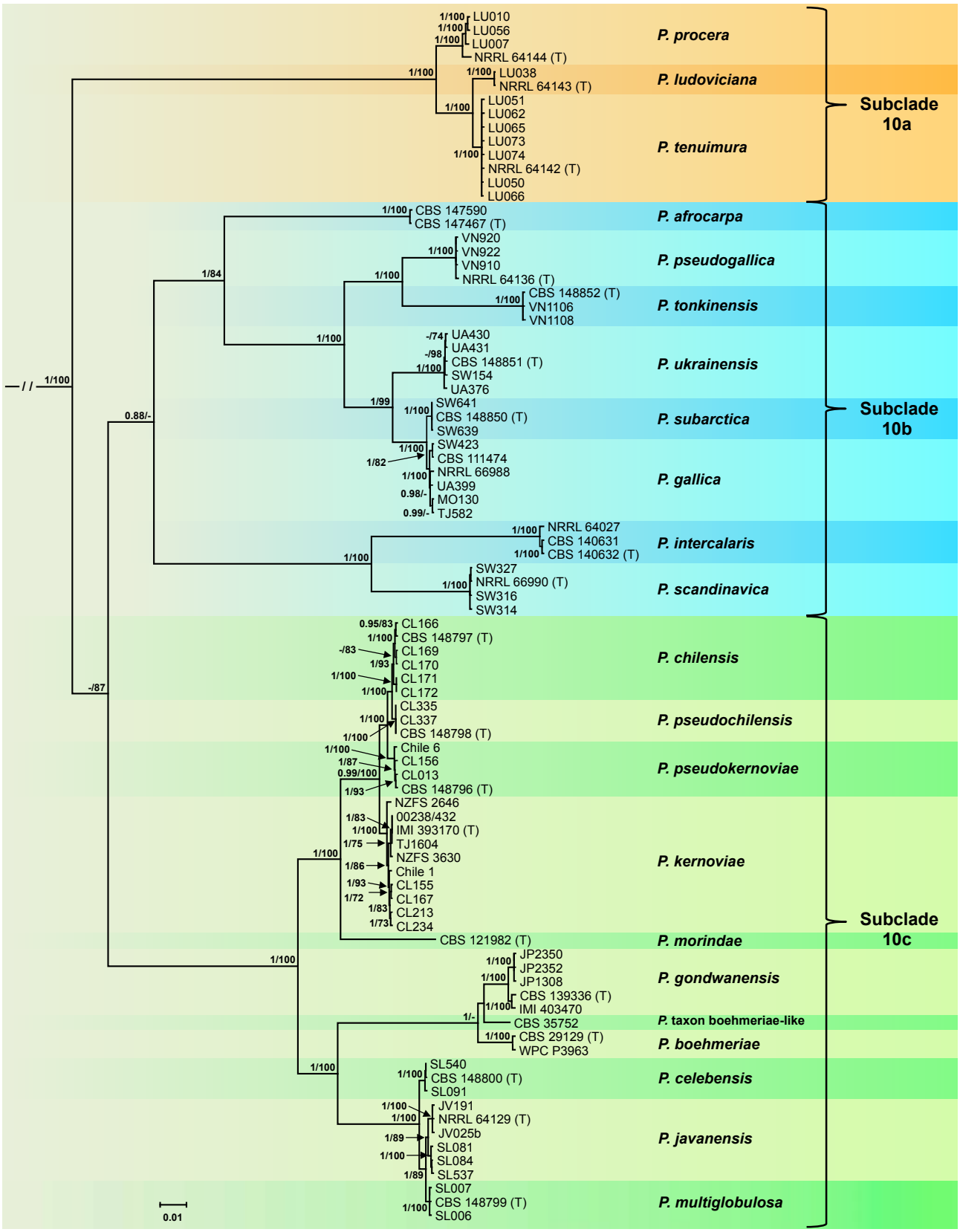

Fig. 3 Fifty percent majority rule consensus phylogram derived from Bayesian inference analysis of a concatenated twelve-locus (LSU, ITS, *βtub*, *hsp90*, *tigA*, *rpl10*, *tef-1α*, *enl*, *ras-ypt1*, *cox1*, *nadh1*, *rps10*) dataset of *Phytophthora* major Clade10. Bayesian posterior probabilities and Maximum Likelihood bootstrap values (in %) are indicated but not shown below 0.80 and 70 %, respectively. *Phytophthora constricta* and *P. fallax* from Clade 9 were used as outgroup taxa (not shown). (T) designates ex-type isolates. — Scale bar indicates 0.01 expected changes per site per branch.

Table 3 Pairwise numbers of different positions along a 11259 character multigene (LSU, ITS, *βtub*, *hsp90*, *tigA*, *rpl10*, *tef-1α*, *enl*, *ras-ypt1*, *cox1*, *nadh1*, *rps10*) sequence alignment among 21 described *Phytophthora* species and *P.* taxon boehmeriae-like from Clade 10.

***Phytophthora* species**	***P. ludoviciana***	***P. tenuimura***	***P. procera***	***P. afrocarpa*** [a]	***P. gallica***	***P. subarctica***	***P. intercalaris***	***P. pseudogallica***	***P. scandinavica***	***P. tonkinensis***	***P. ukrainensis***	***P. boehmeriae***	***P. t. boehmeriae-like*** [c]	***P. morindae*** [c]	***P. gondwanensis***	***P. kernoviae***	***P. chilensis***	***P. pseudochilensis***	***P. pseudokernoviae***	***P. celebensis***	***P. javanensis***	***P. multiglobulosa***
P. ludoviciana	0-3	**155-162**	318-320	322	990-993	996	1087	1039-1042	1077	1065-1066	987-996	1121-1128	827-828	857-858	1129-1130	1144-1156	1153-1156	1163-1164	1148-1155	1153-1154	1135-1143	1126-1127
P. tenuimura		2-27	324-332	320-325	990-1000	999-1004	1091-1097	1046-1052	1077-1081	1063-1072	988-1002	1119-1131	817-822	860-864	1130-1135	1160-1177	1161-1168	1175-1179	1158-1168	1147-1154	1131-1146	1125-1132
P. procera			14-44	305-309	975-982	988-990	1070-1073	1030-1031	1064-1067	1064-1065	972-981	1106-1112	815	855	1098-1099	1141-1150	1142-1146	1156-1157	1141-1146	1119	1104-1111	1095
P. afrocarpa [a]				0	211-216	216	264-268	255	257	279	218	305	297	279	305	278-280	275-276	294	279-280	281	284-285	283 [b]
P. gallica					18/36	**144-148**	816-820	569-577	802-808	655-660	374-391	939-947	697-704	731-737	932-941	976-987	984-991	995-1000	978-988	954-962	932-942	925-933
P. subarctica						0	832	580-581	824	659	387-394	951-955	707	740	947	987-993	994-997	1002	983-988	957	940-941	933
P. intercalaris							0	927-928	488	987	817-825	998-1001	758	757	999	1033-1041	1021-1023	1034	1011-1017	1009	991-998	987
P. pseudogallica								0-1	907-908	438-439	593-598	1028-1035	806-807	806-807	1031-1032	1039-1050	1033-1038	1046-1047	1031-1035	1015-1016	1002-1006	992-993
P. scandinavica									0	943	795-800	944-948	718	722	953	979-987	977-982	992	973-975	957	936-946	937
P. tonkinensis										0	656-660	1067-1074	823	837	1076	1083-1089	1078-1079	1089	1072-1077	1084	1070-1077	1067
P. ukrainensis											0-20	952-963	735-742	744-752	952-959	980-995	972-984	984-990	966-981	952-961	933-949	928-937
P. boehmeriae												12-13	268-273	536-542	311-314	753-769	749-764	757-767	735-750	622-629	599-619	596-607
P. t. boehmeriae-like [c]													0	507	223	545-551	534-535	548	525-531	426	416-420	413
P. morindae [c]														0	529	370-374	356-358	367	344-348	508	496-501	492
P. gondwanensis															0-41	744-751	725-728	737	719-725	606	580-589	580
P. kernoviae																0-24	**198-208**	**210-217**	**180-192**	686-693	677-690	675-680
P. chilensis																	0-19	**45-56**	**76-86**	680-684	676-690	672-676
P. pseudochilensis																		0	**93-97**	691	688-696	682
P. pseudokernoviae																			4-13	672-675	664-679	661-666
P. celebensis																				0	**91-102**	**98**
P. javanensis																					0-32	**36-50**
P. multiglobulosa																						0

[a] For *P. afrocarpa* only four gene regions (ITS, *βtub*, *hsp90*, *cox1*) with a combined alignment length of 3286 bp were available.

[b] The overlap between the *cox1* sequences of *P. afrocarpa* and *P. multiglobulosa* was only 434 bp; the pairwise alignment length was 3125 bp.

[c] For *P.* taxon boehmeriae-like and *P. morindae ras-ypt1*, *nadh1* and *rps10* genes were not available; the 9-gene alignment length was 9650 bp.

Due to the occurrence of intraspecfic variation pairwise differences between species also showed slight variations which is indicated by two numbers separated by a hyphen.

Pairwise numbers of different positions between sister species and among species complexes are shown in **bold** type.

Table 4 Pairwise sequence differences (%) along a 11 259 character multigene (LSU, ITS, *βtub*, *hsp90*, *tigA*, *rpl10*, *tef-1α*, *enl*, *ras-ypt1*, *cox1*, *nadh1*, *rps10*) sequence alignment among 21 described *Phytophthora* species and *P.* taxon boehmeriae-like from Clade 10.

***Phytophthora* species**	***P. ludoviciana***	***P. tenuimura***	***P. procera***	***P. afrocarpa*** [a]	***P. gallica***	***P. subarctica***	***P. intercalaris***	***P. pseudogallica***	***P. scandinavica***	***P. tonkinensis***	***P. ukrainensis***	***P. boehmeriae***	***P.* t. boehmeriae-like** [c]	***P. morindae*** [c]	***P. gondwanensis***	***P. kernoviae***	***P. chilensis***	***P. pseudochilensis***	***P. pseudokernoviae***	***P. celebensis***	***P. javanensis***	***P. multiglobulosa***
P. ludoviciana	0.03	**1.39-1.45**	2.85-2.86	9.8	8.86-8.89	8.92	9.73	9.3-9.33	9.68	9.67-9.68	8.85-8.94	10.03-10.1	8.65-8.66	8.96-8.97	10.11-10.57	10.24-10.37	10.32-10.35	10.41-10.42	10.28-10.34	10.48	10.31-10.38	10.23-10.24
P. tenuimura		0.02-0.24	2.81-2.97	9.74-9.89	8.81-8.9	8.89-8.93	9.71-9.76	9.31-9.36	9.63-9.66	9.6-9.68	8.81-8.94	9.96-10.06	8.48-8.54	8.93-8.97	10.06-10.54	10.34-10.49	10.33-10.39	10.46-10.49	10.3-10.39	10.36-10.42	10.21-10.35	10.16-10.22
P. procera			0.13-0.44	9.28-9.41	8.73-9.94	8.84-8.97	9.58-9.78	9.22-9.43	9.57-9.84	9.66-9.81	8.72-9.0	9.9-9.99	8.48-8.52	8.9-8.94	9.83-10.49	10.23-10.4	10.22-10.32	10.35-10.44	10.21-10.28	10.17-10.24	10.03-10.21	9.95-10.06
P. afrocarpa [a]				0	6.42-6.58	6.58	8.04-8.16	7.76	7.82	8.49	6.64	9.28	9.04	8.49	9.28	8.46-8.52	8.37-8.4	8.95	8.49-8.52	8.55	8.65-8.68	9.06 [b]
P. gallica					0.16-0.31	**1.28-1.31**	7.25-7.28	5.05-5.12	7.15-7.21	5.9-5.95	3.33-3.47	8.31-8.42	7.22-7.3	7.58-7.64	8.28-8.66	8.68-8.83	8.74-8.8	8.84-8.88	8.69-8.78	8.6-8.67	8.4-8.49	8.33-8.41
P. subarctica						0	7.39	5.15-5.16	7.35	5.94	3.44-3.51	8.45-8.48	7.33	7.67	8.41-8.66	8.78-8.89	8.83-8.84	8.9	8.73-8.78	8.63	8.47-8.48	8.41
P. intercalaris							0	8.23-8.24	4.35	8.89	7.27-7.34	8.86-8.89	7.85	7.84	8.87-9.2	9.2-9.29	9.07-9.09	9.18	8.98-9.03	9.09	8.93-9.0	8.89
P. pseudogallica								0-0.01	8.09-8.1	3.95-3.96	5.27-5.32	9.13-9.19	8.35-8.36	8.35-8.36	9.16-9.51	9.25-9.36	9.17-9.22	9.29-9.3	9.16-9.19	9.15-9.16	9.03-9.07	8.94-8.95
P. scandinavica									0	8.53	7.09-7.14	8.42-8.46	6.4	6.44	8.5-8.61	8.76-8.85	8.72-8.76	8.85	8.68-8.7	8.66	8.47-8.56	8.48
P. tonkinensis										0	5.92-5.96	9.61-9.68	8.67	8.82	9.69-9.97	9.76-9.89	9.71-9.72	9.81	9.66-9.7	9.77	9.64-9.71	9.61
P. ukrainensis											0-0.18	8.47-8.56	6.54-6.6	7.73-7.81	8.47-8.76	8.73-8.91	8.65-8.75	8.76-8-81	8.6-8.73	8.6-8.67	8.43-8.56	8.38-8.46
P. boehmeriae												0.11-0.12	2.78-2.83	5.55-5.62	2.72-2.79	6.69-6.88	6.65-6.79	6.72-6.81	6.53-6.66	5.61-5.67	5.4-5.58	5.37-5.47
***P.* t. boehmeriae-like** [c]													0	5.25	2.01-2.31	5.65-5.73	5.53-5.54	5.68	5.44-5.5	4.49	4.4-4.44	4.35
P. morindae [c]														0	5.13-5.48	3.83-3.9	3.69-3.71	3.8	3.56-3.61	5.36	5.25-5.3	5.18
P. gondwanensis															0-0.42	6.61-6.79	6.44-6.48	6.55-6.59	6.37-6.45	5.42-5.46	5.23-5.4	5.23-5.31
P. kernoviae																0.01-0.19	**1.76-1.86**	**1.87-1.94**	**1.6-1.72**	6.18-6.29	6.13-6.29	6.08-6.17
P. chilensis																	0-0.17	**0.4-0.5**	**0.68-0.76**	6.13-6.15	6.09-6.20	6.06-6.09
P. pseudochilensis																		0	**0.83-0.86**	6.23	6.2-6.27	6.15
P. pseudokernoviae																			0.04-0.12	6.06-6.08	5.98-6.12	5.96-6.0
P. celebensis																				0	**0.82-0.92**	**0.88**
P. javanensis																					0-0.28	**0.32-0.45**
P. multiglobulosa																						0

[a] For *P. afrocarpa* only four gene regions (ITS, *βtub*, *hsp90*, *cox1*) with a combined alignment length of 3 286 bp were available.

[b] The overlap between the *cox1* sequences of *P. afrocarpa* and *P. multiglobulosa* was only 434 bp; the pairwise alignment length was 3 125 bp.

[c] For *P.* taxon boehmeriae-like and *P. morindae ras-ypt1*, *nadh1* and *rps10* genes were not available; the 9-gene alignment length was 9 650 bp.

Due to the occurrence of intraspecfic variation pairwise differences between species also showed slight variations which is indicated by two numbers separated by a hyphen.

Pairwise sequence differences between sister species and among species complexes are shown in **bold** type.

Table 5 Numbers of unique polymorphic positions, heterozygous positions and indels along a 11 259 character multigene (LSU, ITS, *βtub*, *hsp90*, *tigA*, *rpl10*, *tef-1α*, *enl*, *ras-ypt1*, *cox1*, *nadh1*, *rps10*) sequence alignment for 21 described *Phytophthora* species and *P.* taxon boehmeriae-like from Clade 10.

	Nonpapillate species										Airborne papillate species											Sister species and species complexes										
	Primarily aquatic									Soil-borne																						
	P. gallica	*P. intercalaris*	*P. ludoviciana*	*P. procera*	*P. pseudogallica*	*P. subarctica*	*P. tenuimura*	*P. tonkinensis*	*P. ukrainensis*	*P. scandinavica*	*P. boehmeriae*	*P. taxon boehmeriae-like*[c]	*P. morindae*[c]	*P. gondwanensis*	*P. kernoviae*	*P. chilensis*	*P. pseudochilensis*	*P. pseudokernoviae*	*P. celebensis*	*P. javanensis*	*P. multiglobulosa*[d]	*P. gallica + P. subarctica*	*P. ludoviciana + P. tenuimura*	*P. ludoviciana, P. procera + P. tenuimura*	*P. chilensis + P. pseudochilensis*	*P. chilensis + P. pseudokernoviae*	*P. pseudochilensis + P. pseudokernoviae*	*P. chilensis, P. pseudochilensis + P. pseudokernoviae*	*P. chilensis, P. pseudochilensis, P. pseudokernoviae + P.*	*P. celebensis + P. javanensis*	*P. celebensis + P. multiglobulosa*	*P. javanensis + P. multiglobulosa*	*P. celebensis + P. javanensis + P. multiglobulosa*
Total no. of unique polymorphic positions present in > 50 % of isolates	33	78	56	73	82	53	46	125	64	100	65	39	77	64	44	11	23	20	28	15	8	50	48	251	10	3	2	16	73	4	0	8	116
No. of unique heterozygous positions present in > 50 % of isolates[a]	11	17	39	8	23	45	11	6	21	1	0	12	0	4	2	3	3	5	4	7	2	10	9	2	0	1	1	0	0	0	0	1	0
No. of unique indel positions present in > 50 % of isolates[a]	0	0	1	1	1	0	1	3	4	8	0	0	1	0	0	0	18[e]	0	0	0	0	16	3	89	0	0	0	1	3	0	0	0	11
Total no. of additional unique polymorphic positions present in individual isolates	27	30	1	18	1	0	19	0	1	0	4	0	0	10	7	0	0	1	0	0	0	n.a.	n.a	n.a.	n.a	n.a	n.a	n.a	n.a.	n.a	n.a	n.a	n.a
No. of additional unique heterozygous positions present in individual isolates[b]	24	29	1	14	1	0	11	0	1	0	0	0	0	4	4	0	0	1	0	0	0	n.a.	n.a	n.a.	n.a	n.a	n.a	n.a	n.a.	n.a	n.a	n.a	n.a
Total no. of heterozygous positions present in > 50 % of isolates	25	18	60	13	32	59	34	9	26	2	0	12	1	5	3	4	5	6	5	8	1	n.a.	n.a	n.a.	n.a	n.a	n.a	n.a	n.a.	n.a	n.a	n.a	n.a
No. of additional heterozygous positions present in individual isolates	30	42	3	19	1	0	18	0	5	0	0	0	0	7	7	0	0	1	0	0	0	n.a	n.a	n.a.	n.a	n.a	n.a	n.a	n.a.	n.a	n.a	n.a	n.a

[a] The no. of unique heterozygous positions and the number of unique indels are included in the total no. of unique polymorphic positions present in the majority of isolates of a species.
[b] The no. of unique heterozygous positions is included in the total no. of unique polymorphic positions present in individual isolates of a species.
[c] For *P.* taxon boehmeriae-like and *P. morindae ras-ypt1*, *nadh1* and *rps10* genes were not available; 9-gene alignment length 9 650 bp.
[d] Due to a shorter length of the *cox1* sequence the length of the 12-gene alignment of *P. multiglobulosa*; was 11 098 bp.
[e] all indels in *hsp90*.
[f] all indels in *ras-ypt1*.
Due to the occurrence of intraspecfic variation some unique polymorphisms were only present in individual isolates of a species.
Nucleotides missing from the terminal part(s) of partial sequences and undetermined bases (N) were not considered as polymorphisms.

phylogenetic position was unambiguously resolved in both BI and ML analyses. *Phytophthora afrocarpa* resided in a distinct well supported basal position of a cluster containing three predominantly aquatic species from Europe, i.e., *P. ukrainensis* and the sister species *P. gallica* and *P. subarctica*, and the two sister species *P. pseudogallica* and *P. tonkinensis* from a mountain stream in Northern Vietnam (Fig. 3). The fully supported Subclade 10c comprised three clusters of airborne species with papillate caducous sporangia. The two sister species *P. javanensis* and *P. multiglobulosa* grouped with *P. celebensis* forming the *P. celebensis* complex. Despite their close relationship the separation of these three species was well supported in both BI and ML analyses (Fig. 3). The *P. celebensis* complex resided in sister position to a cluster containing *P. gondwanensis* from Australia and Japan, *P. boehmeriae* from China and Taiwan and *P.* taxon boehmeriae-like from Argentina. The third cluster of Subclade 10c comprised the four species from the *P. kernoviae* complex, i.e., *P. kernoviae*, *P. pseudokernoviae* and the two sister species *P. chilensis* and *P. pseudochilensis*. The separation of the closely related *P. chilensis*, *P. pseudochilensis* and *P. pseudokernoviae* was strongly supported (Fig. 3). *Phytophthora morindae* from Hawaii resided in sister position to the *P. kernoviae* complex but was quite distinct from all other lineages. Due to low support values (BI 0.58, ML 0.87) the relative phylogenetic positions of Subclades 10b and 10c could not be unambiguously resolved.

Across the 11 259-character multigene alignment the 21 *Phytophthora* species from Clade 10 differed from each other at 36–1179 positions (Table 3) corresponding to sequence differences of 0.32–10.49 % (Table 4). The three species from the early diverged *P. ludoviciana* - *P. procera* - *P. tenuimura* complex (= Subclade 10a) were very distinct differing from all other Clade 10 species at 972–1179 positions (= 8.48–10.57 %). The sister species *P. ludoviciana* with *P. tenuimura*, and *P. gallica* with *P. subarctica* showed differences at 155–162 and 144–148 positions (Table 3), respectively, corresponding to sequence differences of 1.39–1.45 and 1.28–1.31 % (Table 4), respectively. Within the *P. kernoviae*-*P. chilensis*-*P. pseudochilensis*-*P. pseudokernoviae* complex the individual species were discriminated by 45–217 bp (= 0.4–1.94 %) (Table 3, 4). *Phytophthora celebensis*, *P. javanensis* and *P. multiglobulosa* differed from each other at 36–102 positions (0.32–0.92 %) (Table 3, 4). There were in total 2667 polymorphic sites (23.7 %) within Clade 10 of which 770 (28.8 %) were species-specific. With 59.2 and 40.5 %, respectively, the *ras-ypt1* and ITS alignments had the highest proportions of polymorphic sites while the LSU and *rpl10* regions (9.0 and 15.5 % polymorphic sites, respectively) were most conserved. The six known Clade 10 species *P. boehmeriae*, *P. gallica*, *P. gondwanensis*, *P. intercalaris*, *P. kernoviae*, *P. morindae* and *P.* taxon boehmeriae-like had 65, 33, 64, 78, 44, 77 and 39 unique polymorphisms shared by most or all isolates of the respective species (Table 5). In addition, individual isolates of *P. boehmeriae*, *P. gallica*, *P. gondwanensis*, *P. intercalaris* and *P. kernoviae* had another 4, 27, 10, 30 and 7 polymorphisms, respectively (Table 5). The 14 new Clade 10 species *P. celebensis*, *P. chilensis*, *P. javanensis*, *P. ludoviciana*, *P. multiglobulosa*, *P. procera*, *P. pseudochilensis*, *P. pseudogallica*, *P. pseudokernoviae*, *P. scandinavica*, *P. subarctica*, *P. tenuimura*, *P. tonkinensis* and *P. ukrainensis* had 28, 11, 15, 56, 8, 73, 23, 82, 20, 100, 53, 46, 125 and 64 unique polymorphisms, respectively, shared by most or all isolates of the respective species (Table 5). In individual isolates of *P. ludoviciana*, *P. procera*, *P. pseudogallica*, *P. pseudokernoviae*, *P. tenuimura* and *P. ukrainensis* additional 1, 18, 1, 1, 19 and 1 polymorphisms were present (Table 5). In addition, the sister species *P. ludoviciana* with *P. tenuimura*, *P. gallica* with *P. subarctica*, *P. chilensis* with *P. pseudochilensis*, and *P. javanensis* with *P. multiglobulosa* shared 48, 50,10 and 8 unique polymorphisms. Moreover, 251, 73 and 116 unique polymorphisms were shared by the individual species from Subclade 10a, the *P. kernoviae* complex and the *P. celebensis* complex, respectively (Table 5). The LSU, ITS, *hsp90*, *ras-ypt1* and *rps10* alignments contained one or multiple indels of in total 3, 106, 24, 146 and 6 characters, respectively, which were partly shared between related Clade 10 species. Noteworthy, the *ras-ypt1* sequences of *P. ludoviciana*, *P. procera* and *P. tenuimura* shared 89 unique indel positions. The *hsp90* sequence of *P. pseudochilensis* was characterised by a unique 18-character insertion at positions 433–451 (Table 5) while the *hsp90* sequences of the four species from the *P. kernoviae* complex shared a unique 3-character insertion at positions 467–469 (Table 5). Heterozygous positions were present in all nine nuclear gene regions except of LSU, and in all Clade 10 taxa except of *P. boehmeriae*. The frequencies of heterozygous sites varied considerably between and within species and between different lifestyles (Table 5). Across the 11 259 characters alignment the soilborne *P. scandinavica* was heterozygous at only 2 positions. Likewise, including additional heterozygous positions present only in individual isolates, the 11 airborne species had only 0–12 (on average 5.7) heterozygous positions (Table 5). In contrast, the nine primarily aquatic species were heterozygous at 9–70 (on average 43.7) positions (Table 5). With 55, 60, 63 and 59 heterozygous positions, respectively, *P. gallica*, *P. intercalaris*, *P. ludoviciana* and *P. subarctica* might be of hybrid origin. The mitochondrial *cox1*, *nadh1* and *rps10* genes contained no heterozygous sites.

TAXONOMY

Morphological and physiological characters and morphometric data of the 14 new *Phytophthora* species and related species from Clade 10 are given in the comprehensive Tables 6–8.

Phytophthora ludoviciana T. Jung, T. Májek, M. Ferreira & I. Milenković, *sp. nov.* — MycoBank MB 842943; Fig. 4

Etymology. Name refers to the origin of all known isolates (*ludoviciana* Lat. = from Louisiana).

Typus. USA, Louisiana, Archie, isolated from a naturally fallen leaf in a flooded swamp forest. Mar. 2020, *T. Corcobado & T. Májek* (holotype HNHM-MYC-009703, dried culture on V8A, Herbarium of the Hungarian Natural History Museum, Budapest, Hungary; ex-type culture CBS 149205 = NRRL 64143 = LU057). ITS and *cox1* sequences GenBank ON000760 and ON013826, respectively.

Sporangia, hyphae & chlamydospores (Fig. 4a–q) — Sporangia of *P. ludoviciana* were not observed on solid agar but were produced readily in non-sterile soil extract after 2–3 d. Sporangia were non-caducous with a nonpapillate flat apex (Fig. 4a–c, e–j) which was sometimes curved or asymmetric (Fig. 4i–k). Sporangia were borne terminally on unbranched sporangiophores which often widened towards to the sporangial base (Fig. 4e, j–m). Sporangial shapes were ovoid to elongated-ovoid (67 %; Fig. 4a–e), ellipsoid to elongated ellipsoid (11 %; Fig. 4f–g), tubular (20.5 %; Fig. 4h–m) or less frequently obpyriform (1.5 %). Sporangia often had a conspicuous, sometimes sombrero-like basal plug (Fig. 4j–m) and proliferated almost exclusively internal in an extended way (Fig. 4l–m). Internal nested or external proliferation were only rarely observed. Sporangial dimensions averaged 41.6 ± 4.7 × 26.3 ± 2.6 µm with an overall range of 30.5–68.9 × 18.3–30.8 µm and isolate means of 41.2–42.1 × 25.4–27.1 µm. The length/breadth ratio of the sporangia averaged 1.59 ± 0.17 with a range of isolate means of 1.56–1.63. Zoospores were discharged through an exit pore 7.1–16.2 µm wide (av. 10.4 ± 1.9 µm) (Fig. 4d, k–m). They were limoniform to

Table 6 Morphological characters and dimensions (mean ± SD; µm), cardinal temperatures (°C) and temperature-growth relations (mm/d) on V8-juice agar of *Phytophthora* species from Subclades 10a and 10b. Most discriminating characters are highlighted in **bold**. Percentages in brackets are ranges of isolate means. – means character not observed.

	Subclade 10a			Subclade 10b				
	P. ludoviciana	***P. procera***	***P. tenuimura***	***P. afrocarpa***	***P. gallica***	***P. intercalaris***	***P. pseudogallica***	***P. scandinavica***
No. of isolates/source	2[a]	4[a]	7[a]	Bose et al. (2021)	Jung & Nechwatal (2008)	Yang et al. (2016)	4[a]	5[a]
Sporangia	**67 % ovoid-elongated ovoid, 20.5 % tubular, 11 % ellipsoid-elong. ellipsoid** (obpyriform)	**50%** ovoid-**elong. ovoid, 30.7%** ellipsoid-**elong. ellipsoid, 8% tubular,** 8% limoniform (obpyrif.)	55.2% ovoid-elong. ovoid, 40.8 ellipsoid-elong. ellipsoid (tubular, pyriform, obovoid)	ovoid, elongated ovoid, rarely obpyriform	**35 % obpyriform**, 24 % ovoid, **17 % peanut-shaped**, 12 % limoniform	ovoid, ellipsoid, pyriform, obpyriform, limoniform	**94.5 % ovoid to broad-ovoid**, 4.5 % globose to subglobose (obpyriform)	70.8 % ovoid, **29.2 % obpyriform**
apex	nonpapillate	nonpapillate	nonpapillate	nonpapillate	nonpapillate	nonpapillate	nonpapillate	nonpapillate
lxb mean	41.6 ± 4.7 x 26.3 ± 2.6	**60.2±11.3 x 25.2±3.9**	45.7±8.4 x 25.0±2.3	28±1.2 x 18.6±0.7	52.5±11 x 27±5	38.7±5.0 x 27.0±2.9	**25.2±2.7 x 21.3±2.5**	**52.9±6.6 x 37.1±4.2**
range of isolate means	41.2–42.1 x 25.4–27.1	**49.3-70.2 x 21.3-27.7**	40.1-54.5 x 23.6-25.8	n.a.	51-54 x 25-29	n.a.	**24.3-26.7 x 20.1-22.8**	51.0-55.9 x 36.1-38.3
total range	30.5–68.9 x 18.3–30.8	**29.1-92.6 x 12.7-33.5**	30.6-84.9 x 15.6-30.4	13.3–49.5 x 7.4–31.2	30-100 x 19-47.5	25.2-52.5 x 19.2-37.0	**19.4-33.7 x 13.0-29.5**	35.5-72.4 x 28.3-50.8
l/b ratio	1.59 ± 0.17	**2.45 ± 0.61**	1.83 ± 0.34	**1.5 ± 0.01**	2 ± 0.5	1.43	**1.2 ± 0.1**	1.43 ± 0.14
caducity	–	–	–	**–**	–	–	–	–
pedicels	–	–	–	**–**	–	–	–	–
internal proliferation	extended (rarely nested)	nested and extended	nested and extended	**only extended**	nested and extended	nested and extended	nested and extended	nested and extended
exitpores	10.4 ± 1.9	10.3 ± 1.8	9.7 ± 2.0	7.3 ± 0.7	11.5 ± 3	n.a.	8.6 ± 1.5	13.2 ± 2.6
sympodia	very rare, lax	rare, dense or lax	very rare, lax	frequent	-	infrequent, lax	rare, lax	rare, lax
zoospore cysts	9.2 ± 1.0	10.2 ± 1.2	8.9 ± 1.2	5.2-12.6	n.a.	n.a.	11.5 ± 1.7	13.7 ± 1.4
Breeding system	sterile	sterile	**homothallic**	sterile	sterile	**heterothallic** (only A1)	sterile	**homothallic**
Oogonia			**golden-brown with age**			all ornamented		
mean diam	–	–	42.2 ± 6.3	–	–	40.8 ± 6.5	–	40.5 ± 6.4
range of isolate means	–	–	39.9-44.7	–	–	n.a.	–	38.8-42.5
total range	–	–	26.1-60.5	–	–	n.a.	–	19.1-64.4
tapering base	–	–	2.0% (0-4%)	–	–	n.a.	–	5.6% (2-10%)
elongated/excentric/ comma-shaped	–	–	21.5% (12-38%)	–	–	n.a.	–	33.6% (28-40%)
Oospores	–	–		–	–		–	
plerotic oospores	–	–	**98% (96-100%)**	–	–	n.a.	–	**13.2% (6-18%)**
mean diam	–	–	39.7 ± 5.8	–	–	35.8 ± 5.2	–	39.2 ± 6.8
Total range	–	–	24.4-54.2	–	–	n.a.	–	16.8-51.7
wall diam	–	–	**1.3 ± 0.2**	–	–	n.a.	–	**3.1 ± 0.9**
oospore wall index	–	–	**0.20 ± 0.03**	–	–	n.a.	–	**0.45 ± 0.06**
Abortion rate	–	–	11.0% (6-16%)	–	–	**100%**	–	20% (12-24%)
Antheridia	–	–	100% paragynous	–	–	**100% amphigynous**	–	100% paragynous
size	–	–	15.1±3.5 x 9.7±6.0	–	–	20.3 x 15.5	–	15.1±2.9 x 11.7±2.1
Chlamydospores	–	–	–	globose, in clusters; dark-brown when mature	globose, pyriform, club-shaped, irregular	globose	91% globose, 9% sub-globose; **golden-brown; multiple lipid globules**	–
size	–	–	–	26.2 ± 0.46	47.5 ± 7	49.8 ± 7	47.3 ± 11.7	–
Hyphal swellings	limoniform, rare; **undulating hyphae**	limoniform, rare; **undulating hyphae**	–; **undulating hyphae**	globose or subglobose; **some catenulate**	in water; globose or irregular	limoniform or irregular	–	elongated, irregular, limoniform, subglobose
Hyphal aggregations	**+**	**–**	**–**	n.a.	n.a.	n.a.	**+**	**-**
Maximum temperature	**> 32.5 – < 35**	**>32.5-<35**	>30-<32.5	**30**	>30-<32.5	**>32.5-<35**	>25-<27.5	27.5-30 (30-32.5)
Optimum temperature	27.5	25	27.5	25	20	25	20	20
Growth rate at 20 °C	0.95 ± 0.09	0.92 ± 0.11	0.92 ± 0.14	n.a.	1.3 ± 0.22	2.5	1.63 ± 0.18	**4.7 ± 0.06**
Growth rate at 25 °C	1.37 ± 0.07	1.07 ± 0.08	1.07 ± 0.19	n.a.	1.0 ± 0.19	3.1	1.53 ± 0.23	**4.6 ± 0.04**

[a] Numbers of isolates included in the growth tests: *P. ludoviciana* = 2; *P. procera* = 4; *P. tenuimura* = 7; *P. gallica* = 3; *P. intercalaris* = 1; *P. pseudogallica* = 4; *P. scandinavica* = 5.

Table 7 Morphological characters and dimensions (mean ± SD; µm), cardinal temperatures (°C) and temperature-growth relations (mm/d) on V8-juice agar of *Phytophthora* species from Subclades 10b and 10c. Most discriminating characters are highlighted in **bold**. Percentages in brackets are ranges of isolate means; – means character not observed.

	Subclade 10b			Subclade 10c				
	P. subarctica	***P. tonkinensis***	***P. ukrainensis***	***P. boehmeriae***[b]	***P. boehmeriae***[c]	***P.* t. boehmeriae-like**[d]	***P. morindae***	***P. gondwanensis***
No. of isolates/source	4[a]	4[a]	4[a]	Tucker 1931	Chowdappa et al. 2014	Frezzi 1950	Nelson & Abad 2010	5[a]
Sporangia	**72.8 % ovoid-elongated ovoid**, 7.2 % limoniform, **7.2 % ampulliform**, 6.1 % obpyriform (pyrif., ellips.)	**36.4% sub-globose, 35.7% broad-ovoid**, 25.3% ovoid (obpyriform, ellipsoid)	73.6% ovoid, 23.6% obpyriform (ellipsoid, subglobose, ampulliform)	globose, ovoid, ellipsoid, obturbinate	globose, ovoid, ellipsoid, (obturbinate, obpyriform)	globose to subglobose, ovoid	ellipsoid, obpyriform, limoniform, mouse-shaped	59.3% ovoid to broad-ovoid, **36.7 limoniform**, (subglobose, obovoid, obpyriform)
apex	nonpapillate	nonpapillate	nonpapillate	papillate, **few bipapillate**	papillate	papillate	papillate, **few bipapillate**	papillate, **few bipapillate**
lxb mean	53.8 ± 11.5 x 31.6 ± 4.1	**29.0±3.2 x 23.7±3.1**	**35.9±4.7 x 26.2±3.4**	**51.8 x 40.1**	**35.3±4.8 x 20.5±3.4**	42 x 34	42 x 21.8	44.7±3.9 x 28.7±2.9
range of isolate means	43.5–58.2 x 29.2–34.1	**27.8-29.8 x 23.0-24.0**	**34.0-38.1 x 23.5-29.9**	n.a.	32.8-38.8 x 18.2-28.6	n.a.	n.a.	42.9-46.0 x 27.7-30.0
total range	32.7–127.6 x 16.3–39.5	**19.5-37.1 x 14.5-31.6**	26.3-58.2 x 18.7-36.3	28-69 x 20-51	n.a.	18.5-53 x 11.5-46	30-54 x 19.2-24	35.7-62.2 x 21.5-35.7
l/b ratio	1.73 ± 0.46	**1.23 ± 0.15**	1.38 ± 0.19	**1.29**	**1.72** (1.22-1.96)	**1.20**	**1.93**	1.57 ± 0.16
caducity	(+)	–	–	+	+	+	+	+
pedicels	–	–	–	**<5**	**4.1 ± 0.6**	**4.5** (3.5-16)	**26 (8-66)**	**3.5 ± 1.3**
internal proliferation	nested and extended	nested and extended	nested and extended	**–**	–	**–**	**–**	–
exitpores	10.4 ± 1.7	9.8 ± 1.7	8.4 ± 1.5	n.a.	n.a.	n.a.	n.a.	3.3 ± 0.5
sympodia	rare, lax	–	–	frequent	n.a.	**loose, up to 16 sporangia**	**dense, umbellate**	dense, **3-5 sporangia**
zoospore cysts	10.6 ± 0.9	10.4 ± 1.0	10.4 ± 1.1	n.a.	n.a.	11.5-14	n.a.	9.5 ± 0.7
Breeding system	sterile	**homothallic**	sterile	homothallic	homothallic	homothallic	homothallic	homothallic
Oogonia		**golden-brown with age**		globose to subglobose				
mean diam	–	46.2 ± 6.2	–	26.5	22.5 ± 3.9	**31.5**	**30.4**	28.1 ± 3.0
range of isolate means	–	45.1-48.4	–	20.9-31.7	21.9-25.1	n.a.	n.a.	27.2-28.9
total range	–	30.3-59.1	–	n.a.	n.a.	19-38	21.6-39.6	14.1-33.0
tapering base	–	11% (0-22%)	–	n.a.	n.a.	occurring	**frequent**	13.3% (10-16%)
comma-shaped	–	23% (12-40%)	–	n.a.	n.a.	n.a.	n.a.	31.3% (24-38%)
elongated/excentric	–		–	n.a.	n.a.	n.a.	–	22.7% (20-26%)
Oospores	–		–					
plerotic oospores	–	69% (56-84%)	–	predominantly	predominantly	predominantly	100%	75.3% (70-80%)
mean diam	–	42.9 ± 5.5	–	23.3	n.a.	27.5	30.3	23.9 ± 2.6
Total range	–	28.4-56.9	–	15.7-27.6	n.a.	16-34	21-38.9	11.6-28.7
wall diam	–	1.6 ± 0.3	–	≤ 2	n.a.	n.a.	3.2 (2.4-3.6)	**2.0 ± 0.34**
oospore wall index	–	0.24 ± 0.03	–	n.a.	n.a.	n.a.	n.a.	**0.42 ± 0.04**
Abortion rate	–	6.3% (4-8%)	–	n.a.	n.a.	n.a.	n.a.	**44.7% (24-66%)**
Antheridia	–	**98% paragynous**	–	100% amphigynous	100% amphigynous	100% amphigynous	100% amphigynous	100% amphigynous
size	–	14.1±2.2 x 10.8±2.0	–	12-16 x 11-15	12.4±2.1 x 10.0±1.3	16.5x14.5 (12.5-21 x 8-16)	11.2 x 8.5	12.4±2.1 x 10.0±1.3
Chlamydospores	–	–	–	rare; thickwalled (2µm)	+ (27 out of 43 isolates)	+	–	–
size	–	–	–	41.4 (16-51)	–	29.5 (17-42)	–	–
Hyphal swellings	limoniform, rare	**coralloid, irregular hyphae**	ovoid, limoniform; 9.1 ± 1.5; **coralloid hyphae**	–	–	–	–	–
Hyphal aggregations	**–**	**+**	**+**	n.a.	n.a.	n.a.	n.a.	**–**
Maximum temperature	>30-<32.5	**>20-<25**	**>32.5-<35** (30-32.5)	**32.5**	<35	<35	**27**	**>30-<32.5**
Optimum temperature	25	20	**32.5** (30)	**25**	n.a	n.a.	20	**27.5**
Growth rate at 20 °C	1.21 ± 0.14	1.13 ± 0.1	1.48 ± 0.21	**4.4**	n.a.	n.a.	2.9	**3.17 ± 0.3**
Growth rate at 25 °C	1.31 ± 0.16	0	2.15 ± 0.12	**6.6**	**7.6 ± 0.06**	n.a.	n.a.	**5.05 ± 0.21**

[a] Numbers of isolates included in the growth tests: *P. subarctica* = 4; *P. tonkinensis* = 5; *P. ukrainensis* = 4; *P. gondwanensis* = 5.
[b] Morphological studies and temperature-growth test performed on cornmeal agar.
[c] Morphological studies performed on CA; temperature-growth test performed on CA and only at 24 and 35 °C.
[d] Morphological studies performed on PDA; temperature-growth test performed on PDA.

Table 8 Morphological characters and dimensions (mean ± SD; µm), cardinal temperatures (°C) and temperature-growth relations (mm/d) on V8-juice agar of *Phytophthora* species from Subclade 10c. Most discriminating characters are highlighted in **bold**. Percentages in brackets are ranges of isolate means. – indicates character not observed.

	Subclade 10c							
	***P. kernoviae* (Chile)**	***P. kernoviae* (Ireland)**	***P. chilensis***	***P. pseudochilensis***	***P. pseudokernoviae***	***P. celebensis***	***P. javanensis***	***P. multiglobulosa***
No. of isolates/source	5[a]	3[a]	6[a]	6[a]	4[a]	5[a]	10[a]	3[a]
Sporangia	**91.2 % broad-ovoid to elongated-ovoid**, 5.2 % limoniform (subglobose, ellipsoid, mouse-shaped)	**82.7% broad-ovoid to elongated-ovoid**, **13.3% limoniform** (subglobose, mouse-shaped)	**91.6% broad-ovoid to elongated-ovoid**, 3.3% limoniform (obovoid, obpyriform, ellipsoid)	74% ovoid to elongated ovoid, **9.5% obpyriform**, 8% limoniform-elongated limoniform (ellipsoid, obovoid)	**88% ovoid**, **12% limoniform**	52.8% ovoid to broad-ovoid, 41.6 limoniform, (ellipsoid, subglobose, pyriform)	53.6% ovoid, 43% limoniform (obovoid, subglobose, ellipsoid)	57.3% ovoid, 42% limoniform (obpyriform)
apex	papillate	papillate, **semipapillate**	papillate	papillate	papillate	papillate	papillate, **few bipapillate**	papillate
lxb mean	**44.0 ± 6.1 x 30.8 ± 3.9**	**38.5±4.5 x 25.8±2.7**	43.3±6.1 x 29.5±3.5	**48.8±8.2 x 27.0±3.1**	42.7±4.0 x 29.7±2.8	38.7 ± 5.0 x 26.2 ± 3.3	38.3 ± 4.5 x 23.2 ± 2.9	**43.1 ± 6.2 x 27.1 ± 3.0**
range of isolate means	**39.2–49.6 x 27.3–33.7**	**37.1-39.3 x 24.4-26.6**	41.3-45.5 x 27.3-31.8	43.3-**54.9** x 25.7-29.3	41.9-43.4 x 28.6-31.5	37.3–40.7 x 25.0–27.9	33.6-41.3 x 20.5-25.6	41.1-46.5 x 26.1-28.2
total range	**27.4-59.4 x 19.0-40.0**	**26.7-52.1 x 17.4-32.1**	20.7-60.3 x 13.4-42.1	25.6-**69.1** x 17.4-39.4	30.5-55.0 x 21.3-35.7	26.3–64.3 x 17.6–40.7	19.3-62.6 x 9.2-36.7	28.3-64.9 x 21.1-36.5
l/b ratio	1.43 ± 0.13	1.50 ± 0.12	1.47 ± 0.15	**1.81 ± 0.24**	1.44 ± 0.14	**1.48 ± 0.12**	**1.66 ± 0.19**	1.60 ± 0.18
caducity	+	+	+	+	+	+	+	+
pedicels	**7.8 ± 4.1**	**6.9 ± 3.8**	4.0 ± 1.4	4.9 ± 1.6	3.6 ± 1.0	9.9 ± 2.7	7.4 ± 2.1	7.7 ± 3.3
internal proliferation	–	–	–	–	–	–	–	–
exitpores	4.7 ± 0.9	3.7 ± 0.5	5.3 ± 0.6	4.4 ± 0.9	5.6 ± 0.7	3.7 ± 0.7	3.3 ± 0.6	3.6 ± 0.5
sympodia	dense, 2-4 (5) sporangia	dense, 2-4 (5) sporangia	dense, 2-4 (5) sporangia	dense, **2-10 sporangia**	dense, 2-4 (5) sporangia	dense, **2-5 sporangia**	dense, **2-6 sporangia**	dense, **2-5 sporangia**
zoospore cysts	9.4 ± 0.9; **diplanetism**	9.6 ± 1.4; **diplanetism**	9.6 ± 1.4	9.9 ± 1.2; **diplanetism**	9.9 ± 1.6; **diplanetism**	8.0 ± 0.8; **diplanetism**	8.4 ± 0.7; **diplanetism**	9.2 ± 0.8; **diplanetism**
Breeding system	homothallic	homothallic	homothallic	homothallic	homothallic	homothallic	homothallic	homothallic
Oogonia					**golden-brown with age**			
mean diam	26.0 ± 2.6	23.6 ± 2.5	24.9 ± 2.6	27.3 ± 3.4	**30.1 ± 4.3**	24.9 ± 3.1	**28.1 ± 4.0**	25.4 ± 3.5
range of isolate means	25.4-26.9	23.0-24.3	24.1-25.5	25.9-28.5	**28.1-34.2**	23.6-25.8	**27.1-29.2**	23.2-25.5
total range	18.2-34.7	16.1-31.1	14.6-35.4	16.3-35.3	18.6-39.3	13.1-36.1	15.6-42.7	17.0-38.4
tapering base	**12.8% (0-28%)**	**9.3% (6-14%)**	**47.7%** (22-76%)	**87.5%** (72-96%)	**86%** (81-88%)	8.4% (4-14%)	12.4% (4-22%)	**-**
comma-shaped	39.6% (20-56%)	30.0% (24-38%)	26.7% (12-48%)	20.5% (14-28%)	**35.3%** (24-42%)	22.4% (16-32%)	25.7% (10-40%)	18.7% (12-26%)
elongated/excentric	**17.6% (10-30%)**	**15.3% (12-22%)**	**2.3% (0-4%)**	11.5% (4-18%)	16.0% (6-28%)	7.6% (4-14%)	16.4% (10-24%)	6.0% (4-10%)
Oospores								
plerotic oospores	99.6% (98-100%)	99.7% (99-100%)	88.0% (80-92%)	91% (86-96%)	99.6% (98-100%)	100%	**80.3%** (58-92%)	100%
mean diam	22.7 ± 2.1	20.7 ± 2.3	22.8 ± 2.4	24.4 ± 3.0	27.0 ± 3.7	21.9 ± 2.9	25.0 ± 3.6	22.5 ± 3.2
Total range	18.1-27.2	14.2-26.5	13.6-32.6	15.4-32.1	16.3-35.8	12.3-31.5	13.5-39.4	15.0-35.2
wall diam	1.96 ± 0.34	1.92 ± 0.45	1.8 ± 0.26	**1.61 ± 0.33**	2.07 ± 0.33	1.6 ± 0.27	1.75 ± 0.34	1.5 ± 0.23
oospore wall index	0.43 ± 0.05	0.45 ± 0.06	0.40 ± 0.04	**0.34 ± 0.07**	0.40 ± 0.06	0.38 ± 0.04	0.36 ± 0.04	0.35 ± 0.04
Abortion rate	20.6% (4-46%)	40.0% (19-82%)	**8.0% (6-10%)**	**65.5% (56-80%)**	**7.7% (6-10%)**	**24.4% (6-48%)**	16.8% (8-32%)	7.3% (2-12%)
Antheridia	**99.6% amphigynous**	**93.3% amphigynous**	100% amphigynous	100% amphigynous	**95.3% amphigynous**	100% amphigynous	100% amphigynous	100% amphigynous
size	11.6±2.0 x 9.4±1.3	10.9±2.0 x 8.5±1.2	12.7±2.2 x 9.5±1.1	13.7±3.6 x 9.8±1.7	14.6±2.9 x 9.6±1.3	11.4±2.1 x 9.8±1.3	12.2±2.2 x 10.1±1.6	11.4 ± 2.1 x 9.9 ± 1.4
Chlamydospores	–	–	–	–	–	–	–	–
size	–	–	–	–	–	–	–	–
Hyphal swellings	rare; ovoid, subglobose, limoniform; 12.1 ± 0.4	–	rare; subglob., irregular, limoniform, 10.4 ± 2.4	rare; subglob., irregular, limoniform, 10.3 ± 2.7	rare; (sub)globose, limoniform; 9.9 ± 2.1	–	–	–
Hyphal aggregations	+	+	+	+	+	+	+	+
Maximum temperature	20-<25	20-<25	20-<25	20-<25	20-<25	**>27.5-<30**	**>27.5-<30**	**>27.5-<30**
Optimum temperature	20	20	**20**	**15**	**15**	**25**	20	20
Growth rate at 20 °C	3.08 ± 0.42	3.69 ± 0.34	2.77 ± 0.07	1.57 ± 0.43	2.45 ± 0.41	2.77 ± 0.19	**3.36 ± 0.55**	**1.9 ± 0.09**
Growth rate at 25 °C	0	0	**0**	**0**	0.39 ± 0.13	2.87 ± 0.23	2.37 ± 0.29	**1.5 ± 0.31**

[a] Numbers of isolates included in the growth tests: *P. kernoviae* (Chile) = 5; *P. kernoviae* (Ireland) = 3; *P. chilensis* = 6; *P. pseudochilensis* = 6; *P. pseudokernoviae* = 3; *P. celebensis* = 5; *P. javanensis* = 10; *P. multiglobulosa* = 3.

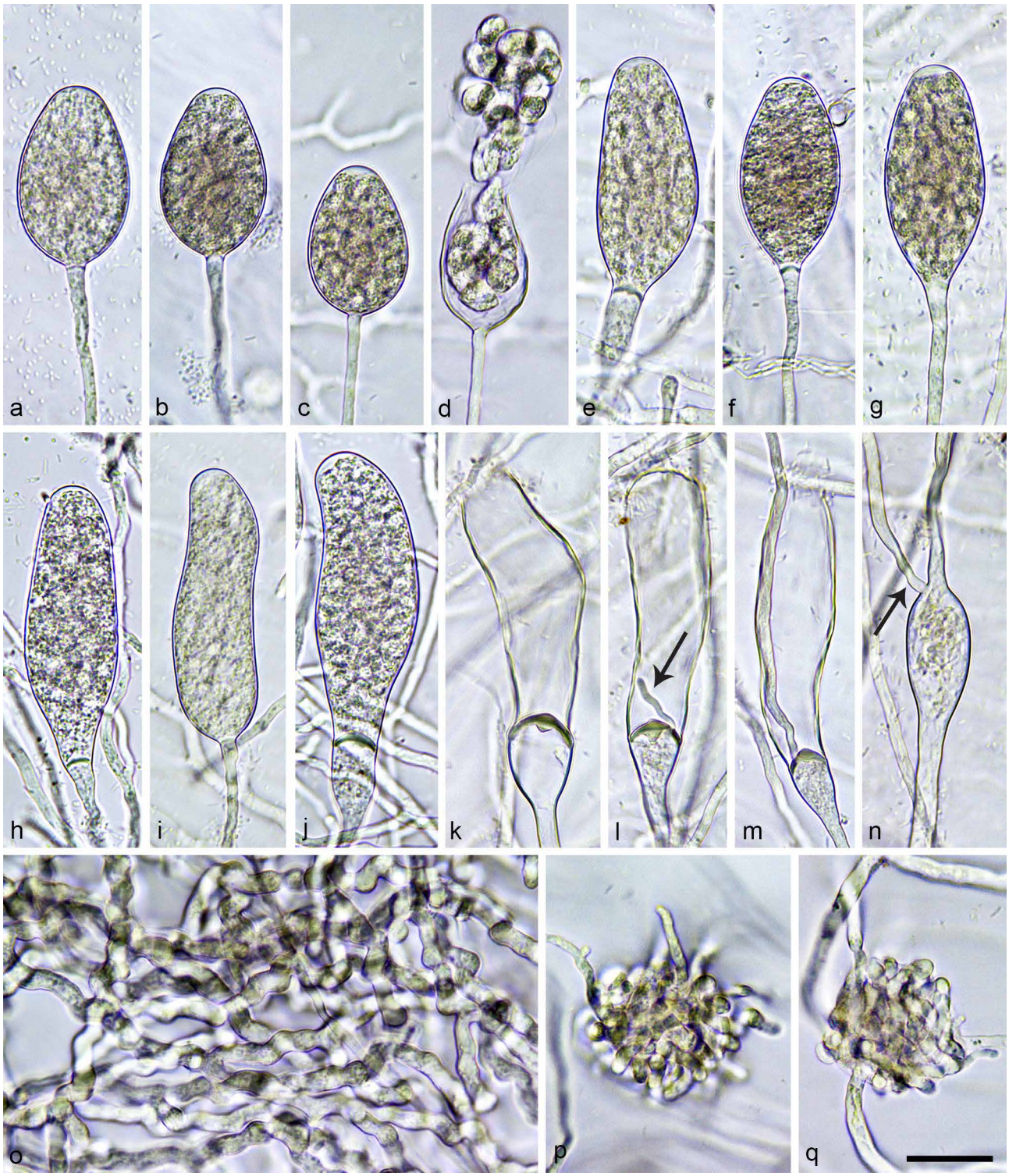

Fig. 4 Morphological structures of *Phytophthora ludoviciana*. a–m. Sporangia formed on V8-agar (V8A) flooded with soil extract; a–j. nonpapillate sporangia with a flat apex; a–c. ovoid; d. same ovoid sporangium as in c, releasing zoospores; e. elongated-ovoid with a conspicuous basal plug and widening of the sporangiophore towards the sporangial base; f. ellipsoid; g. elongated-ellipsoid; h. tubular with tapering base; i. tubular with curved apex; j. tubular with curved apex, a conspicuous basal plug and widening of the sporangiophore towards the sporangial base; k–m. tubular sporangia with conspicuous basal plugs and widening of the sporangiophores towards the sporangial base, empty after zoospore release; k. with curved asymmetric apex and sombrero-like basal plug; l. with sombrero-like basal plug and beginning internal extended proliferation (arrow); m. with curved base and internal extended proliferation; n. limoniform hyphal swelling with branching (arrow) of the sporangiophore; o. dense colony of undulating hyphae in V8A; p–q. compact hyphal aggregations in V8A. — Scale bar = 20 µm, applies to a–q.

reniform whilst motile (Fig. 4d), becoming spherical (av. diam = 9.2 ± 1.0 µm) on encystment. Sporangiophores sometimes branched at limoniform swellings (Fig. 4n). Hyphae were usually undulating and formed dense cultures (Fig. 4o) and small compact aggregations (Fig. 4p–q). Chlamydospores were not observed.

Oogonia, oospores & antheridia — All isolates of *P. ludoviciana* were sterile and did neither produce nor stimulate oogonia formation in mating tests with A1 and A2 tester strains of *P. cinnamomi*.

Colony morphology, growth rates & cardinal temperatures (Fig. 20, 23) — Colonies of *P. ludoviciana* were submerged and stellate on V8A, radiate with limited aerial mycelium on CA, and stoloniferous and dense felty on PDA (Fig. 20). On V8A maximum growth temperature was between 32.5 and < 35 °C. The isolates did not grow at 35 °C and did not resume growth

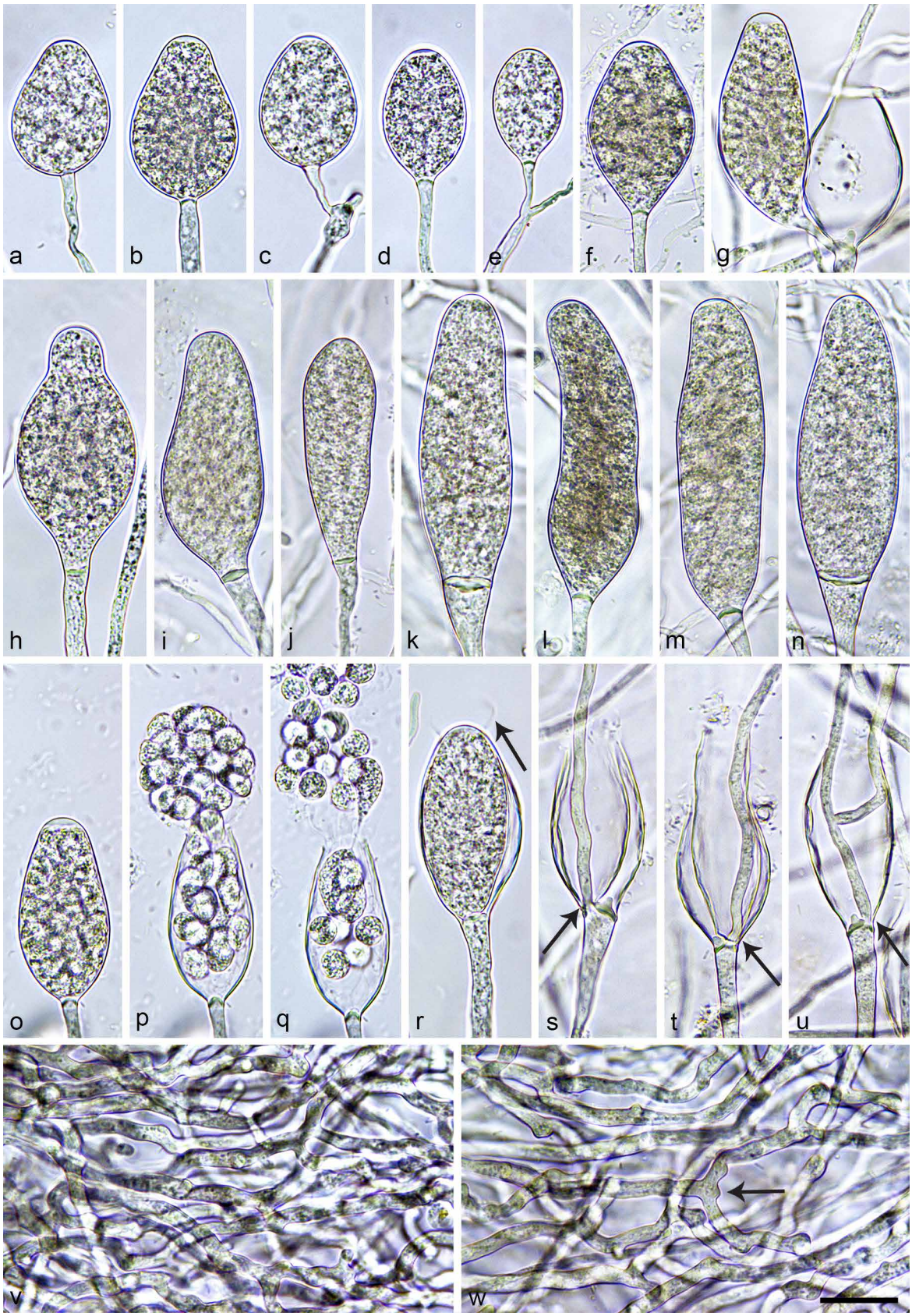

Fig. 5 Morphological structures of *Phytophthora procera*. a–u. Sporangia formed on V8-agar (V8A) flooded with soil extract; a–o, r. nonpapillate sporangia with a flat apex; a–c. ovoid; a–b. borne terminally; c. borne laterally; d. ellipsoid, borne terminally; e. ellipsoid, borne laterally; f. limoniform; g. ovoid empty sporangium after zoospore release, with a conspicuous basal plug, externally proferating with an elongated-ovoid sporangium; h. obpyriform; i. elongated-obpyriform, asymmetric, with a conspicuous basal plug; j. elongated club-shaped to pyriform; k. tubular with conspicuous basal plug and widening of the sporangiophore towards the sporangial base; l–m. tubular with curved apices and conspicuous basal plugs; n. elongated-ellipsoid with a conspicuous basal plug and widening of the sporangiophore towards the sporangial base; o. elongated-ovoid, differentiating zoospores; p–q. same sporangium as in o, releasing zoospores; r–u. empty sporangia after zoospore release; r. internal nested proliferation with new ellipsoid sporangium and relics of the evanescent vesicle still present (arrow); s–t. internal nested and extended proliferation with internal sporangiophore originating aside of the conspicuous basal plug (arrows); t. internal sporangium protruding out of the old sporangium; u. internal extended proliferation with internal sporangiophore originating aside of the conspicuous, sombrero-like basal plug (arrow) and branching inside the sporangium; v–w. dense undulating hyphal growth in V8A; w. sympodial hyphal branching (arrow). — Scale bar = 20 µm, applies to a–w.

when plates incubated for 5 d at 35 °C were transferred to 20 °C. *Phytophthora ludoviciana* had an optimum of growth at 27.5 °C with an average radial growth of 1.37 ± 0.07 mm/d but grew only slightly slower at 25 °C (Fig. 23). At 20 °C radial growth rates on V8A, CA and PDA were 0.95 ± 0.09 mm/d, 0.86 ± 0.06 mm/d and 0.44 ± 0.02 mm/d, respectively.

Additional specimen. USA, Louisiana, Archie, isolated from a naturally fallen leaf in a flooded swamp forest. Mar. 2020, *T. Corcobado & T. Májek*, LU038.

Phytophthora procera T. Jung, T. Corcobado, S. Raghuwinder & I. Milenković, *sp. nov.* — MycoBank MB 842944; Fig. 5

Etymology. Name refers to the slender shape of many sporangia (*procera* Lat. = slender).

Typus. USA, Louisiana, Archie, isolated from a naturally fallen leaf in a flooded swamp forest. Mar. 2020, *T. Corcobado & T. Májek* (holotype HNHM-MYC-009704, dried culture on V8A, Herbarium of the Hungarian Natural History Museum, Budapest, Hungary; ex-type culture CBS 149226 = NRRL 64144 = LU013). ITS and *cox1* sequences GenBank ON000767 and ON013833, respectively.

Sporangia, hyphae & chlamydospores (Fig. 5a–w) — Sporangia of *P. procera* were not observed on solid agar but were produced readily in non-sterile soil extract after 2–3 d. Sporangia were persistent with a nonpapillate flat apex (Fig. 5a–o, r) which was sometimes slightly curved (9.3 %; Fig. 5l–m). Sporangia were usually borne terminally on unbranched sporangiophores or infrequently laterally (Fig. 5c, e, g). Sporangiophores sometimes widened towards the sporangial base (Fig. 5k, n, s). Sporangial shapes were variable ranging from ovoid to elongated-ovoid (50 %; Fig. 5a–c, g, o–q), ellipsoid to elongated ellipsoid (30.7 %; Fig. 5d–e, n, r), tubular (8 %; Fig. 5k–m) and limoniform to elongated limoniform (8%; Fig. 5f) or less frequently obpyriform to elongated-obpyriform (2.0 %; Fig. 5h–i), clubshaped, ampulliform and pyriform (1.3 %; Fig. 5j). Sporangia often had a conspicuous (0.7–7.8 µm thickness), sometimes sombrero-like basal plug (Fig. 5g, i, k, m–n, s–u). Sporangial proliferation occurred usually internally in a nested (Fig. 5r–t), sometimes with the new sporangium protruding out of the previous sporangium (Fig. 5t), and/or extended way (Fig. 5s–u). Peculiarly, the sporangiophores for internal extended proliferation usually originated from beside the basal plug (Fig. 5s–u) and sometimes already branched inside the empty sporangium (Fig. 5u). Sometimes external proliferation of sporangia was also observed (Fig. 5g). Sporangial dimensions averaged 60.2 ± 11.3 × 25.2 ± 3.9 µm with an overall range of 29.1–92.6 × 12.7–33.5 µm and isolate means of 49.3–70.2 × 21.3–27.7 µm. The length/breadth ratio of the sporangia averaged 2.45 ± 0.61 with a range of isolate means of 1.88–2.89. Zoospores were discharged through an exit pore 6.7–15.8 µm wide (av. 10.3 ± 1.8 µm) (Fig. 5p–q, s–u). They were globose, limoniform or reniform whilst motile (Fig. 5p–q), becoming globose (av. diam = 10.2 ± 1.2 µm) on encystment. Hyphal swellings were very rarely formed and limoniform. Hyphae often branched sympodially and were usually undulating forming dense cultures (Fig. 5v–w). Chlamydospores were not observed.

Oogonia, oospores & antheridia — All isolates of *P. procera* were sterile and did neither produce nor stimulate oogonia formation in mating tests with A1 and A2 tester strains of *P. cinnamomi*.

Colony morphology, growth rates & cardinal temperatures (Fig. 20, 23) — Colonies of *P. procera* were submerged and radiate on V8A, petaloid with limited aerial mycelium on CA, and dense-felty, rosaceous with submerged margins on PDA (Fig. 20). On V8A the four tested isolates of *P. procera* had similar cardinal temperatures and growth rates and a broad optimum of growth at 20, 25 and 27.5 °C with average radial growth rates of 0.92 ± 0.11 mm/d, 1.07 ± 0.08 mm/d and 0.97 ± 0.19 mm/d, respectively. Minimum and maximum growth temperatures were below 10 °C and slightly above 32.5 °C, respectively (Fig. 23). None of the seven isolates was growing at 35 °C and they did not resume growth when plates incubated for 5 d at 35 °C were transferred to 20 °C. At 20 °C radial growth rates on CA and PDA were 0.89 ± 0.12 mm/d and 0.35 ± 0.11 mm/d, respectively.

Additional specimens. USA, Louisiana, Archie, isolated from naturally fallen leaves in a flooded swamp forest, Mar. 2020, *T. Corcobado & T. Májek*, LU007, LU010, LU056.

Phytophthora tenuimura T. Jung, T. Corcobado, T. Májek & M. Ferreira, *sp. nov.* — MycoBank MB 842945; Fig. 6

Etymology. Name refers to the thin oospore walls (*tenuis* Lat. = thin; *mura* Lat. = wall).

Typus. USA, Louisiana, Archie, isolated from a naturally fallen leaf in a flooded swamp forest. Mar. 2020, *T. Corcobado & T. Májek* (holotype HNHM-MYC-009709, dried culture on V8A, Herbarium of the Hungarian Natural History Museum, Budapest, Hungary; ex-type culture CBS 149227 = NRRL 64142 = LU052). ITS and *cox1* sequences GenBank ON000798 and ON013864, respectively.

Sporangia, hyphae & chlamydospores (Fig. 6a–o, w) — Sporangia of *P. tenuimura* were not observed on solid agar but were produced after 2–3 d in non-sterile soil extract. Sporangia were mostly borne terminally on unbranched sporangiophores (Fig. 6a–o) or very rarely laterally on short hyphae. Sporangia were non-caducous and nonpapillate with a flat apex (Fig. 6a–l). Sporangial shapes were ovoid to elongated-ovoid (55.2 %; Fig. 6a–f), ellipsoid to elongated-ellipsoid (40.8 %; Fig. 6h–k) or infrequently tubular (2.0 %; Fig. 6g), pyriform (1.2 %; Fig. 6l) and obovoid (0.8 %). Special features like a curved or asymmetric apex (15.6 %; Fig. 6f–g), lateral attachment of the sporangiophore to the sporangium (8.8 %; Fig. 6h) and a widening of the sporangiophore towards the sporangial base (0.4 %; Fig. 6i) were infrequently observed. Sporangia usually had an inconspicuous basal plug (0.7–2.9 µm thickness) but conspicuous basal plugs were infrequently observed (Fig. 6n–o). Sporangia proliferated internally in a nested way (Fig. 6l–m), sometimes with the new sporangium protruding out of the empty sporangium (Fig. 6l), and in an extended way (Fig. 6m, o), often with the new sporangiophore undulating (Fig. 6m, o). Zoospores were discharged through an exit pore 7.0–16.2 µm wide (av. 9.7 ± 2.0 µm) (Fig. 6m–o). They were usually limoniform to reniform whilst motile, becoming spherical (av. diam = 8.9 ± 1.2 µm) on encystment. Sporangial dimensions of five isolates averaged 45.7 ± 8.4 × 25.0 ± 2.3 µm (overall range 30.6–84.9 × 15.6–30.4 µm) with a range of isolate means of 40.1–54.5 × 23.6–25.8 µm. The length/breadth ratio averaged 1.83 ± 0.34 with a range of isolate means of 1.69–2.12. Hyphae showed undulating growth and formed dense colonies (Fig. 6w). Hyphal swellings and chlamydospores were not observed.

Oogonia, oospores & antheridia (Fig. 6p–v) — In single culture on V8A all seven isolates of *P. tenuimura* produced oogonia readily. Oogonia were borne terminally or laterally and had smooth (Fig. 6p–q, s–v) or sometimes slightly wavy walls (Fig. 6r). Oogonial shapes were globose to subglobose (78.5 %; Fig. 6p–s, u–v) or slightly excentric to elongated-ellipsoid (21.5 %; Fig. 6t, v), infrequently with a short tapering (2.0 %; Fig. 6s, u) or curved base (7.5 %; Fig. 6t). Oogonial stalks were sometimes intricate (Fig. 6r). Oogonia diameters of five isolates averaged 42.2 ± 6.3 µm with a wide overall range of 26.1–60.5 µm and a range of isolate means of 39.9–44.7 µm. Oospores were almost exclusively plerotic (98.0 %; Fig. 6p–v), globose (Fig. 6p–s, u–v) or ellipsoid (Fig. 6t, v), contained a large ooplast and often turned golden-brown with age, some-

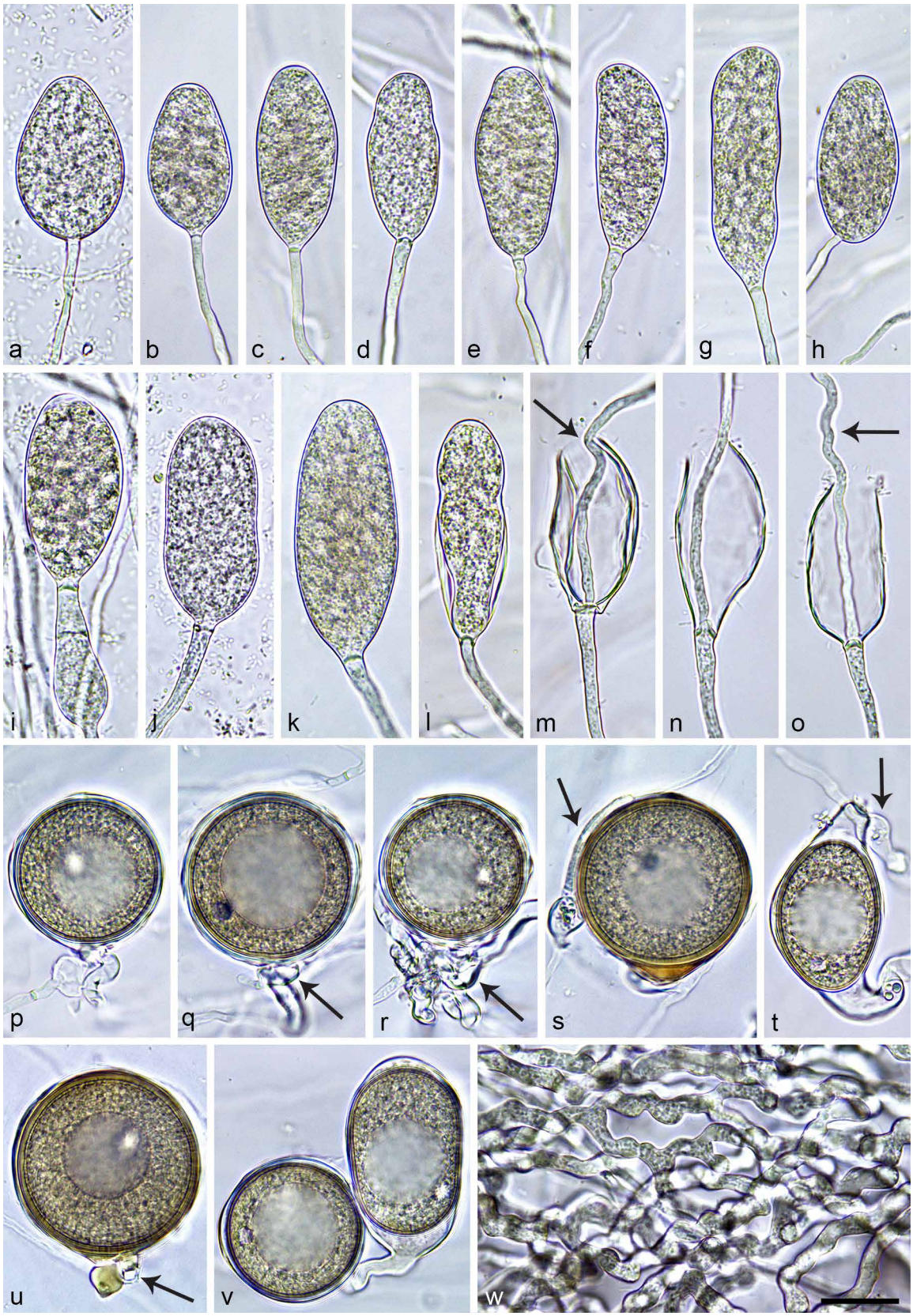

Fig. 6 Morphological structures of *Phytophthora tenuimura*. a–o. Sporangia formed on V8-agar (V8A) flooded with soil extract; a–k. nonpapillate sporangia with a flat apex; a–b. ovoid; c–e. elongated-ovoid; f. elongated-ovoid, slightly asymmetric with a curved apex; g. tubular with a curved apex; h. ellipsoid, laterally attached sporangiophore; i. ellipsoid with widening of the sporangiophore towards the sporangial base, shortly before release of the already differentiated zoospores; j. ellipsoid; k. elongated-ellipsoid; l–o. internal sporangial proliferation; l. nested proliferation with the new pyriform sporangium protruding out of the empty sporangium; m. nested and extended proliferation with undulating new sporangiophore (arrow); n. extended proliferation and conspicuous basal plug; o. extended proliferation with undulating new sporangiophore (arrow) and conspicuous basal plug; p–v. mature oogonia containing thick-walled plerotic oospores with large ooplasts, and paragynous antheridia, formed in single culture in V8A; p. globose oogonium with undulating stalk and terminal antheridium; q. globose oogonium with terminal antheridium (arrow); r. globose oogonium with wavy wall, intricated stalk and inconspicuous antheridium (arrow); s. globose oogonium with short tapering base, golden-brown colour of the oospore and oogonial base, and a tangentially aligned intercalary antheridium (arrow); t. excentric elongated oogonium with curved stalk, excentric elongated oospore and intercalary antheridium (arrow); u. globose oogonium with short tapering base, golden-brown colour of the oospore and oogonial base and inconspicuous antheridium (arrow); globose oogonium and ellipsoid oogonium with ellipsoid oospore; w. dense undulating hyphal growth in V8A. — Scale bar = 20 µm, applies to a–w.

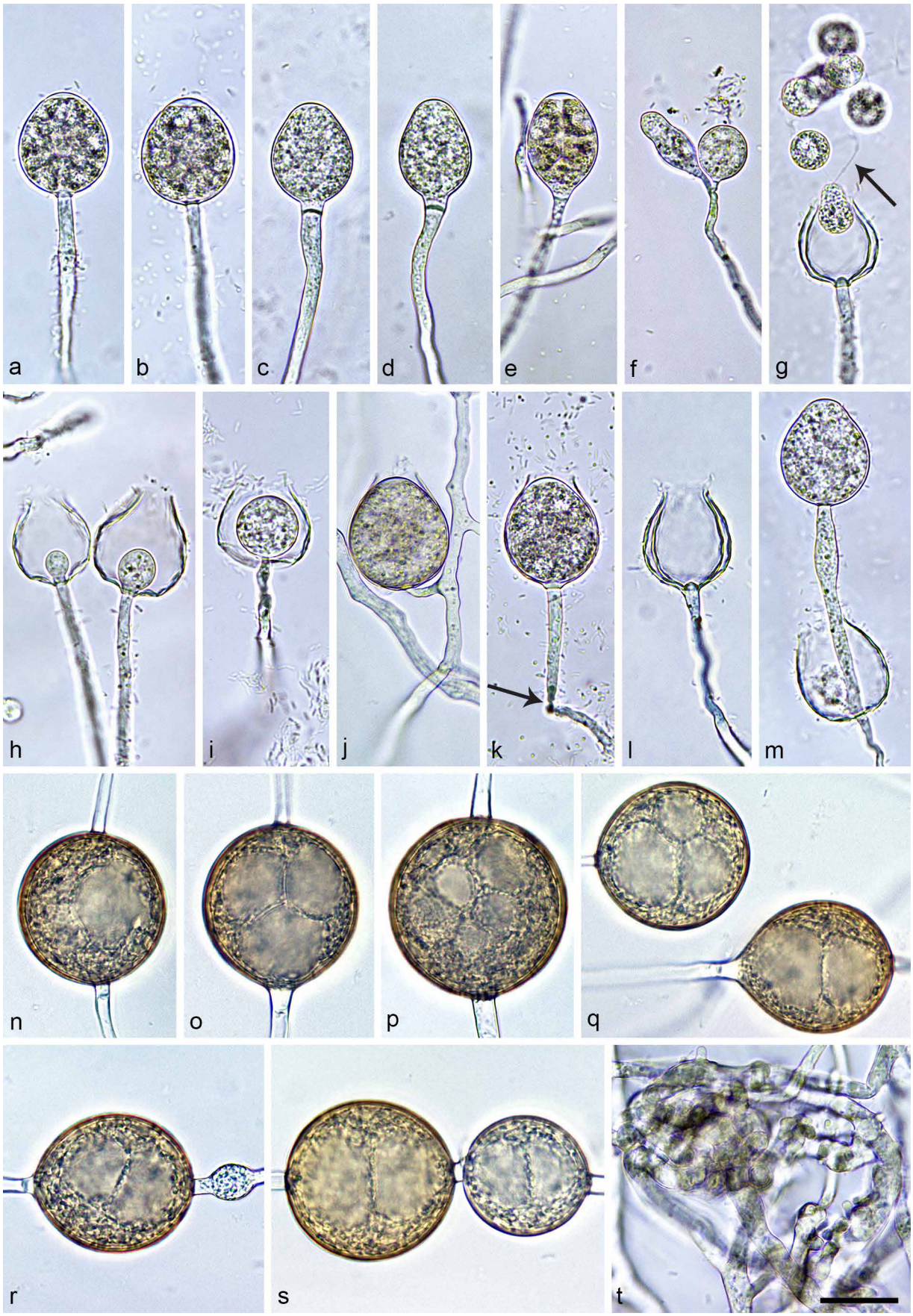

Fig. 7 Morphological structures of *Phytophthora pseudogallica*. a–m. Sporangia formed on V8 agar (V8A) flooded with soil extract; a–f. nonpapillate with flat apex; a–b. broad-ovoid with swollen apex before release of the already differentiated zoospores; c–d. ovoid. e. ovoid with slightly tapering base and swollen apex before release of the already differentiated zoospores; f. globose sporangium externally proliferating with an obpyriform sporangium; g. internal nested proliferation and release of zoospores, arrow points at flagellae; h–i. internal nested proliferation; j. internal nested proliferation of a laterally borne ovoid sporangium; k. internal nested proliferation and sporangiophore with conspicuous constriction (arrow); l. internal nested proliferation and undulating sporangiophore; m. ovoid sporangium internally proliferating in an extended way forming a new ovoid sporangium; n–s. golden-brown, thick-walled chlamydospores with multiple oil globules formed in V8A; n–p. globose intercalary; q. globose terminal (top) and subglobose intercalary (bottom); r. subglobose intercalary with a small hyphal swelling; s. globose, intercalary and catenulate; t. small dense hyphal aggregation. — Scale bar = 20 µm, applies to a–t.

times even staining the oogonial base (Fig. 6s, u). They had a mean diameter of 39.7 ± 5.8 µm (total range 24.4–54.2 µm), relatively thin walls (Fig. 6p–v) with an average thickness of 1.3 ± 0.2 µm (total range 0.9–1.6 µm) and a mean oospore wall index of 0.20 ± 0.03. With 11 % (6–16 %), mean oogonial abortion rate was low. Antheridia were formed terminally (Fig. 6p–q) or intercalary (Fig. 6s–t), in the latter case sometimes with the antheridial stalk tangentially aligning to the oogonium (Fig. 6s), and were exclusively paragynous (Fig. 6p–u), averaging 15.1 ± 3.5 × 9.7 ± 6.0 µm, with shapes ranging from clavate, subglobose to cylindrical.

Colony morphology, growth rates & cardinal temperatures (Fig. 20, 23) — Colonies of *P. tenuimura* had very limited aerial mycelium on V8A and CA with a radiate pattern on V8A and a chrysanthemum pattern on CA whereas colonies on PDA were dense-felty and stoloniferous (Fig. 20). Temperature-growth relations are shown in Fig. 23. All seven tested isolates had similar growth rates and cardinal temperatures. The maximum growth temperature was 30 – < 32.5 °C. Lethal temperature was 32.5 °C. The average radial growth rate at the optimum temperature of 27.5 °C was 1.17 ± 0.2 mm/d, but all isolates grew only slightly slower at 25 and 20 °C. At 20 °C radial growth rates on V8A, CA and PDA were 0.92 ± 0.14 mm/d, 0.94 ± 0.12 mm/d and 0.4 ± 0.05 mm/d, respectively.

Additional specimens. USA, Louisiana, Archie, isolated from naturally fallen leaves in a flooded swamp forest, Mar. 2020, *T. Corcobado & T. Májek*, LU050, LU051, LU065, LU066, LU073, LU074.

Phytophthora pseudogallica T. Jung, N.M. Chi, Brasier & I. Milenković, *sp. nov.* — MycoBank MB 842950; Fig. 7

Etymology. Name refers to the morphological similarity to *P. gallica*.

Typus. Vietnam, Sapa, isolated from a fallen leaf in a stream running through an evergreen cloud forest, 2017, *T. Jung & N.M. Chi* (holotype HNHM-MYC-009706, dried culture on V8A, Herbarium Hungarian Natural History Museum; ex-type culture CBS 149206 = NRRL 64136 = VN861). ITS and *cox1* sequences GenBank ON000774 and ON013840, respectively.

Sporangia, hyphae & chlamydospores (Fig. 7a–t) — Sporangia of *P. pseudogallica* were not formed on solid agar but were produced after 2–3 d in non-sterile soil extract. Sporangia were non-caducous, nonpapillate with a flat apex (Fig. 7a–f, j–k, m) and an inconspicuous basal plug (0.8–1.8 µm thickness). They were borne terminally on unbranched sporangiophores (Fig. 7a–e, g–i, k–m) or occasionally on short lateral branches (Fig. 7j) or in small sympodia (Fig. 7f). Sporangiophores sometimes had a conspicuous constriction (Fig. 7k) and were occasionally undulating (Fig. 7l). Sporangial shapes were mostly ovoid to broad-ovoid (94.5 %; Fig. 7a–e, j–k, m) and less frequently globose to subglobose (4.5 %; Fig. 7f) or obpyriform (1.0 %; Fig. 7f). Sporangia commonly proliferated internally in both a nested (Fig. 7g–l) and extended way (Fig. 7m). External proliferation was occasionally observed (Fig. 7f). Sporangia were small with mean dimensions of 25.2 ± 2.7 × 21.3 ± 2.5 µm (overall range 19.4–33.7 × 13.0–29.5 µm) and a range of isolate means of 24.3–26.7 × 20.1–22.8 µm. The length/breadth ratio averaged 1.2 ± 0.1 with a range of isolate means of 1.18–1.21. Zoospores of *P. pseudogallica* were discharged through an exit pore 5.0–13.0 µm wide (8.6 ± 1.5 µm). They were subglobose, limoniform or reniform whilst motile, becoming spherical (av. diam = 11.5 ± 1.7 µm) on encystment. Small hyphal swellings were only rarely observed (Fig. 7r). All isolates formed in V8A occasionally small dense hyphal aggregations (Fig. 7t) and abundantly chlamydospores. Chlamydospores were globose (91 %; Fig. 7n–q, s) to subglobose (9 %; Fig. 7q–s), mostly borne intercalary, often in chains (catenulate), (Fig. 7n–s) or less frequently terminal (Fig. 7q). They usually contained multiple lipid globules and turned golden-brown with age. Chlamydospores were large averaging 47.3 ± 11.7 µm diam (total range 20.2–78.2 µm) and had relatively thick walls of 1.8 ± 0.4 µm.

Oogonia, oospores & antheridia — All isolates of *P. pseudogallica* were sterile and did neither produce nor stimulate oogonia formation in mating tests with A1 and A2 tester strains of *P. cinnamomi*.

Colony morphology, growth rates & cardinal temperatures (Fig. 20, 23) — Colonies were striate on V8A with white aerial mycelium in the centre and appressed to submerged margins, uniform and dense-felty on CA, and stoloniferous dense-felty on PDA (Fig. 20). Temperature-growth relations are shown in Fig. 23. *Phytophthora pseudogallica* had a maximum growth temperature between 25 and < 27.5 °C and an optimum for growth at 20 °C with a radial growth rate of 1.63 ± 0.18 mm/d but isolates were growing only slightly slower at 15 and 25 °C with radial growth rates of 1.51 ± 0.16 and 1.53 ± 0.23 mm/d, respectively. All isolates resumed growth when plates incubated for 5 d at 27.5 were transferred to 20 °C. Lethal temperature was between 27.5 and 30 °C. On CA and PDA radial growth rates at 20 °C were 0.43 ± 0.01 mm/d and 0.4 ± 0.07 mm/d, respectively.

Additional specimens. Vietnam, Sapa, isolated from fallen leaves in a stream running through an evergreen cloud forest, 2017, *T. Jung & N.M. Chi*, VN910, VN920, VN922.

Phytophthora scandinavica T. Jung, I. Milenković, M.A. Redondo, T. Corcobado, *sp. nov.* — MycoBank MB 842951; Fig. 8

Etymology. Name refers to the origin of all known isolates in the Scandinavian country Sweden (*scandinavica* Lat. = from Scandinavia).

Typus. Sweden, Kiruna area, isolated from riverbank soil, Sept. 2017, *I. Milenković & T. Corcobado* (holotype HNHM-MYC-009708, dried culture on V8A, Herbarium of the Hungarian Natural History Museum, Budapest, Hungary; ex-type culture CBS 149204 = NRRL 66990 = SW325). ITS and *cox1* sequences GenBank ON000786 and ON013852, respectively.

Sporangia, hyphal swellings & chlamydospores (Fig. 8a–l) — Sporangia of *P. scandinavica* were not observed on solid agar but were produced abundantly after 1–2 d in non-sterile soil extract. Sporangia were non-caducous with a nonpapillate (Fig. 8a–e, j), sometimes pointed apex (Fig. 8d, g), developing a swollen apex before zoospore release (Fig. 8f–g). Sporangia were ovoid to broad-ovoid (70.8 %; Fig. 8a–d, g–h) or obpyriform (29.2 %; Fig. 8e–f, j) and usually borne terminally on unbranched sporangiophores or infrequently on short lateral hyphae. In all isolates internal nested proliferation (Fig. 8i–j) was common and external proliferation occurred occasionally (Fig. 8i) whereas internal extended proliferation was not observed. Sporangial dimensions of *P. scandinavica* averaged 52.9 ± 6.6 × 37.1 ± 4.2 µm (overall range 35.5–72.4 × 28.3–50.8 µm) with isolate means of 51.0–55.9 × 36.1–38.3 µm. The length/breadth ratio of the sporangia averaged 1.43 ± 0.14 with a range of isolate means of 1.38–1.48. Zoospores were discharged through exit pores of 8.6–20.0 µm width (av. 13.2 ± 2.6 µm; Fig. 8h–j). They were limoniform to reniform whilst motile, becoming spherical (av. diam = 13.7 ± 1.4 µm) on encystment. In both liquid culture and solid agar inflated, tubular, irregular to coralloid hyphal swellings were intercalary and laterally formed (Fig. 8k–l). Chlamydospores were not observed.

Oogonia, oospores & antheridia (Fig. 8m–t) — All isolates of *P. scandinavica* produced oogonia in single culture on V8A which matured within 2–3 wk. Oogonia were smooth-walled, borne terminally or laterally and had globose to subglobose (66.4 %; Fig. 8m–p) or excentric, elongated or comma-like (33.6 %; Fig. 8q–t) shapes, sometimes with a short tapering base (5.6 %; Fig. 8r–s). Oogonial diameters averaged 40.5 ± 6.4 µm (overall range 19.1–64.4 µm and range of

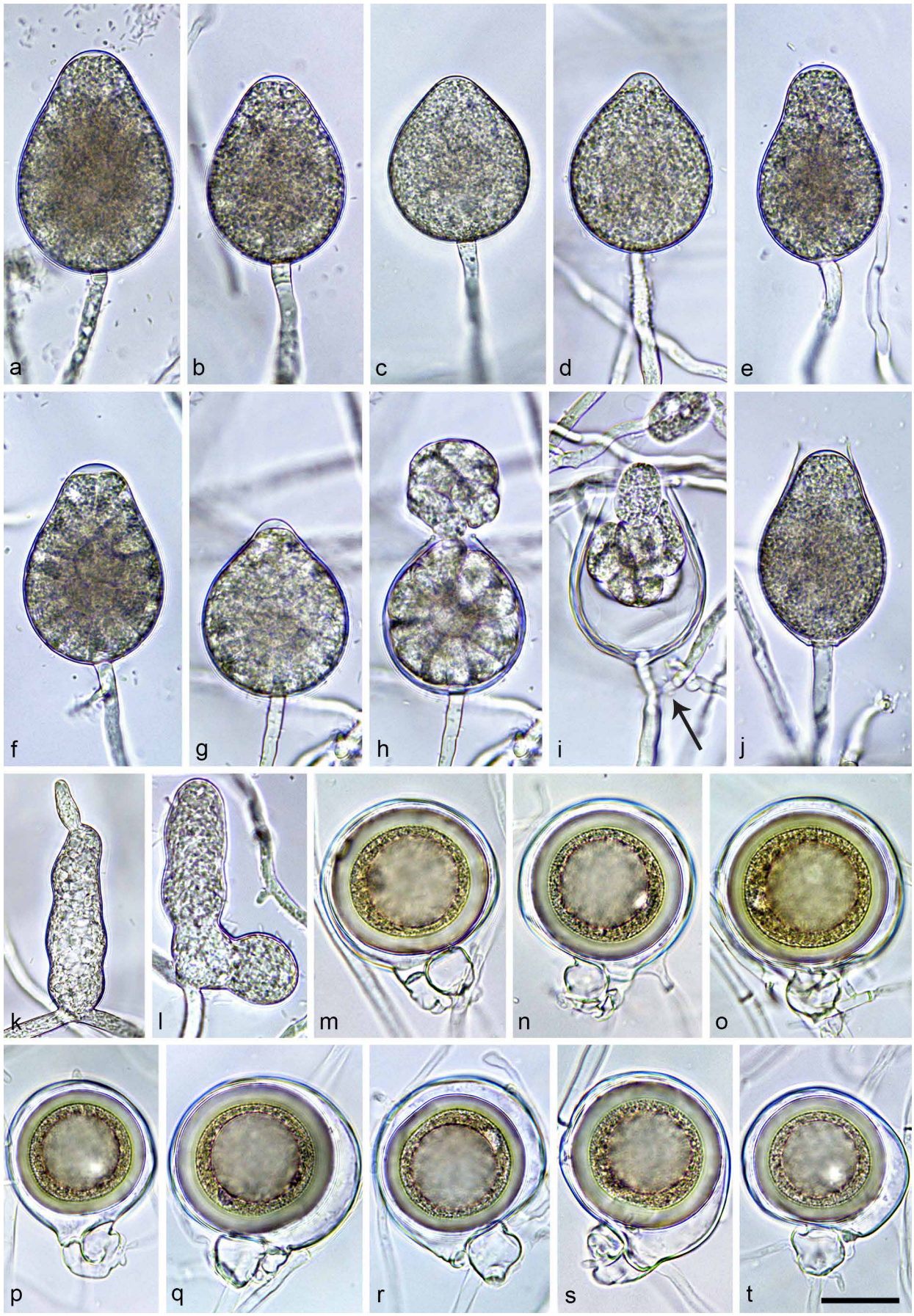

Fig. 8 Morphological structures of *Phytophthora scandinavica*. a–j. Sporangia formed on V8 agar (V8A) flooded with soil extract; a–e. nonpapillate; a–c. ovoid with flat apex; d. ovoid with pointed apex; e. obpyriform with flat apex; f. obpyriform with swollen apex before zoospore release; g. ovoid with pointed and swollen apex before zoospore release; h. ovoid, releasing zoospores; i. ovoid, releasing zoospores, with internal nested and external (arrow) proliferation; j. obpyriform, internal nested proliferation; k–l. irregular-tubular hyphal swellings in V8A; k. intercalary; l. lateral; m–t. mature smooth-walled oogonia formed in single culture in V8A, with thick-walled oospores containing large ooplasts and paragynous antheridia; m. globose oogonium with near-plerotic oospore; n–p. globose to subglobose oogonia with aplerotic oospores; q–r. excentric oogonia with aplerotic oospores; s–t. excentric comma-shaped oogonia with aplerotic oospores. — Scale bar = 25 µm, applies to a–t.

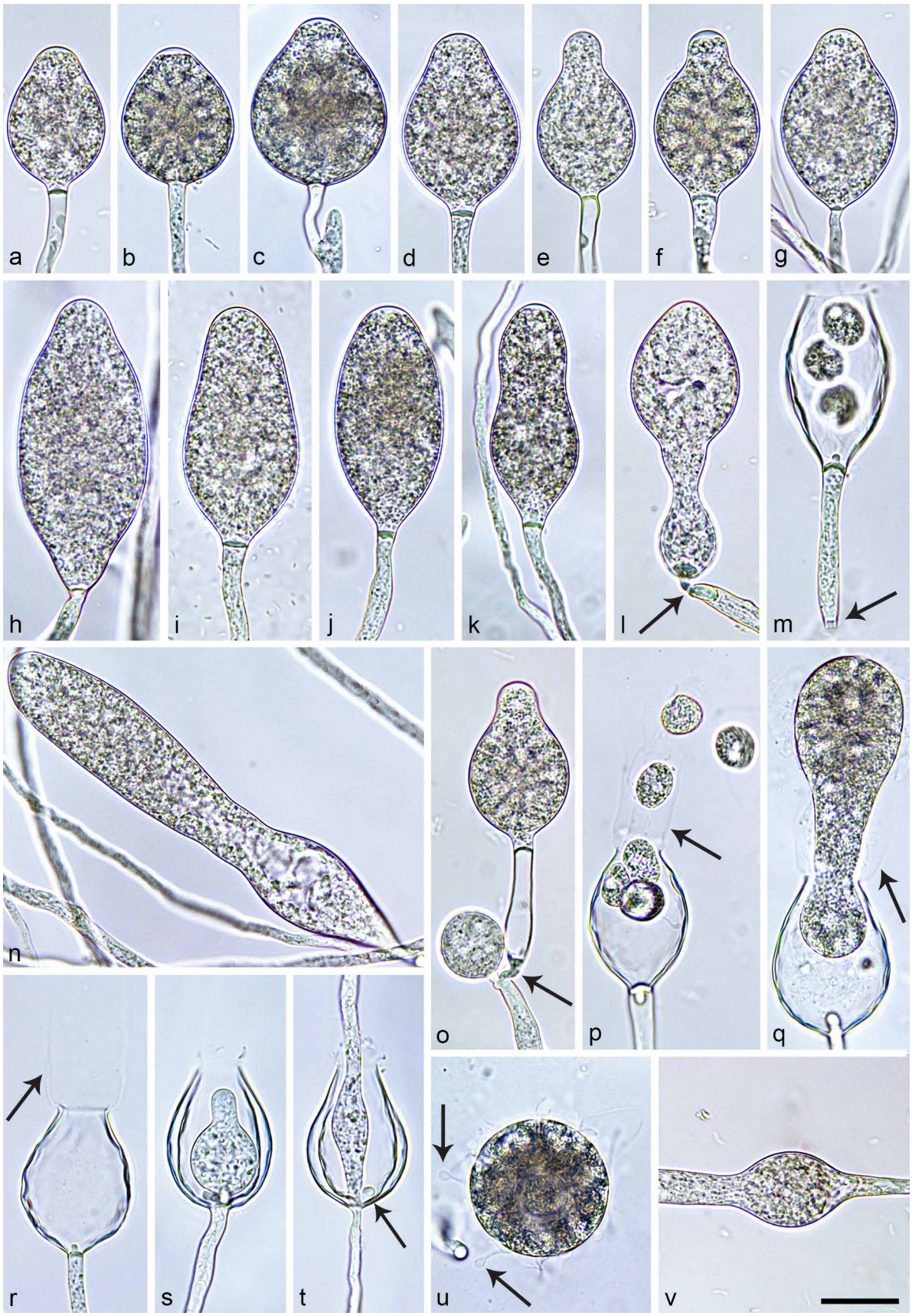

Fig. 9 Morphological structures of *Phytophthora subarctica*. a–t. Sporangia formed on V8-agar (V8A) flooded with soil extract; a–l, n–o. nonpapillate sporangia with a flat apex; a. ovoid; b. ovoid, before release of zoospores; c. broad-ovoid, on a short lateral hypha; d. ovoid; e. obpyriform; f. obpyriform, before release of zoospores; g. limoniform; h. elongated-limoniform; i. elongated-ovoid; j. ellipsoid; k. elongated-obpyriform; l. ampulliform with a thick basal plug containing a conspicuous constriction (arrow); m. with conspicuous basal plug, after release of all but three zoospores, caducous having been shed at a sporangiophore constriction (arrow); n. elongated-ampulliform to tubular; o. obpyriform sporangium with long pedicel, a constriction in the basal plug of the pedicel (arrow), and external proliferation just below the basal plug; p. sporangium with conspicuous basal plug releasing zoospores through evanescent vesicle (arrow); q. sporangium with conspicuous basal plug releasing incompletely differentiated cytoplasm through evanescent vesicle (arrow); r. empty sporangium with conspicuous basal plug after zoospore release, with evanescent vesicle (arrow); s. internal nested proliferation; t. internal nested and extended proliferation and conspicuous basal plug (arrow); u. released, incompletely differentiated cytoplasm with multiple flagella with coiled ends (arrows); v. limoniform hyphal swelling. — Scale bar = 20 µm, applies to a–v.

isolate means 38.8–42.5 µm). Oospores were predominantly aplerotic (86.8 %; Fig. 8n–t) or less frequently near-plerotic (13.2 %; Fig. 8m), globose to slightly subglobose, contained a large ooplast and turned slightly golden-brown with age (Fig. 8m–t). They had a mean diameter of 39.2 ± 6.8 µm (total range 16.8–51.7 µm), thick walls (av. 3.1 ± 0.9 µm, total range 1.3–5.3 µm) and a mean oospore wall index of 0.45 ± 0.06. Mean oogonial abortion rate was 20 % (12–24 %). Antheridia were formed terminally or laterally (Fig. 8m) and were exclusively paragynous, usually inserted very close to the oogonial base (Fig. 8m–t), averaging 15.1 ± 2.9 × 11.7 ± 2.1 µm, with shapes ranging from cubic, subglobose to cylindrical, sometimes with finger-like hyphal projections (10 %).

Colony morphology, growth rates & cardinal temperatures (Fig. 21, 23) — All five *P. scandinavica* isolates examined formed on V8A and CA faintly petaloid colonies with submerged margins and limited aerial mycelium in the centre, and stoloniferous, dense-felty colonies on PDA (Fig. 21). On V8A, the maximum temperature for growth was in three of the five tested isolates between 27.5 and 30 °C while the other two isolates showed very slow growth at 30 °C. None of the isolates was growing at 32.5 °C (Fig. 23) but they resumed growth when plates incubated for 5 d at 32.5 °C were transferred to 20 °C. Lethal temperature was between 32.5 and 35 °C. The average radial growth rate was 4.7 ± 0.06 mm/d at the optimum temperature of 20 °C and only marginally lower at 25 °C (4.6 ± 0.04 mm/d) (Fig. 23). On CA and PDA radial growth rates at 20 °C were 2.96 ± 0.17 mm/d and 1.49 ± 0.12 mm/d, respectively.

Additional specimens. Sweden, Kiruna area, isolated from riverbank soil, Sept. 2017, *I. Milenković & T. Corcobado*, SW314, SW315, SW316, SW326, SW327.

Phytophthora subarctica T. Jung, T. Corcobado, J. Oliva & I. Milenković, *sp. nov.* — MycoBank MB 843134; Fig. 9

Etymology: Name refers to the origin of all known isolates from the subarctic zone in northern Sweden.

Typus. Sweden, Kiruna area, isolated from a forest stream using a *Fagus sylvatica* leaf as bait, Sept. 2017, *I. Milenković & T. Corcobado* (holotype HNHM-MYC-020632, dried culture on V8A, Herbarium of the Hungarian Natural History Museum, Budapest, Hungary; ex-type culture CBS 148850 = NRRL 64339 = SW176). ITS and *cox1* sequences GenBank ON000790 and ON013856, respectively.

Sporangia, hyphae & chlamydospores (Fig. 9a–v) — Sporangia of *P. subarctica* were not observed on solid agar but were produced readily in non-sterile soil extract after 1–2 d. Sporangia were non-caducous with a nonpapillate and mostly flat apex (Fig. 9a–l, n–o). Sporangia were usually borne terminally on unbranched sporangiophores (Fig. 9a–b, d–l) or infrequently on short lateral sporangiophores (Fig. 9c). Sporangiophores sometimes showed a conspicuous constriction near the sporangial base (Fig. 9l, o) where they were easily shed (Fig. 9m). Sporangial shapes were ovoid (37.2 %; Fig. 9a–b, d), broad-ovoid (20.0 %; Fig. 9c), elongated-ovoid (15.6 %; Fig. 9i), limoniform to elongated limoniform (7.2 %; Fig. 9g–h), ampulliform to elongated ampulliform (7.2 %; Fig. 9l, n), obpyriform to elongated obpyriform (6.1 %; Fig. 9e–f, k, o), pyriform (3.3 %) or ellipsoid to elongated ellipsoid (2.8 %; Fig. 9j). After zoospore release a conspicuous basal plug was observed in 62.2 % of sporangia (Fig. 9m, p–t). Sporangia proliferated internally, in both a nested (Fig. 9s–t) or an extended way (Fig. 9t) often with the new sporangiophore emerging beside the conspicuous basal plug, and infrequently externally (Fig. 9o). Sporangial dimensions averaged 53.8 ± 11.5 × 31.6 ± 4.1 µm with an overall range of 32.7–127.6 × 16.3–39.5 µm and isolate means of 43.5–58.2 × 29.2–34.1 µm. The length/breadth ratio of the sporangia averaged 1.73 ± 0.46 with a range of isolate means of 1.49–1.90. Zoospores were discharged through an exit pore 7.4–15.0 µm wide (av. 10.4 ± 1.7 µm) (Fig. 9m, p–t) and an evanescent vesicle (Fig. 9p–t). They were limoniform to reniform whilst motile (Fig. 9m, p), becoming spherical (av. diam = 10.6 ± 0.9 µm) on encystment. Sometimes sporangia released incompletely differentiated cytoplasm (Fig. 9q) which immediately became spherical and had multiple flagella, often with coiled ends (Fig. 9u). Infrequently limoniform swellings were found on sporangiophores (Fig. 9v). Chlamydospores were not observed.

Oogonia, oospores & antheridia — All isolates of *P. subarctica* were sterile and did neither produce nor stimulate oogonia formation in mating tests with A1 and A2 tester strains of *P. cinnamomi*.

Colony morphology, growth rates & cardinal temperatures (Fig. 21, 23) — Colonies of *P. subarctica* were appressed to submerged with limited aerial mycelium in the centre on V8A and CA, radiate on V8A and faintly radiate on CA, and stoloniferous and dense felty with very slow growth on PDA (Fig. 21). On V8A *P. subarctica* had an optimum of growth at 25 °C with an average radial growth of 1.31 ± 0.16 mm/d (Fig. 23). Maximum growth temperature was between 30 and 32.5 °C. None of the isolates was growing at 32.5 °C and they did not resume growth when plates incubated for 5 d at 32.5 °C were transferred to 20 °C. At 20 °C radial growth rates on V8A, CA and PDA were 1.21 ± 0.14 mm/d, 1.15 ± 0.17 mm/d and 0.2 ± 0.11 mm/d, respectively.

Additional specimens. Sweden, Kiruna area, isolated from a forest stream using *F. sylvatica* leaves as baits, Sept. 2017, *I. Milenković & T. Corcobado*, SW639, SW640, SW641.

Phytophthora tonkinensis T. Jung, N.M. Chi, Scanu & I. Milenković, *sp. nov.* — MycoBank MB 843135; Fig. 10

Etymology. Name refers to the origin of all known isolates in northern Vietnam (Tonkin is a previous name for the three northernmost regions of Vietnam).

Typus. Vietnam, Sapa, isolated from a fallen leaf in a stream running through an evergreen cloud forest, 2017, *T. Jung & N.M. Chi* (holotype HNHM-MYC-009701, dried culture on V8A, Herbarium Hungarian Natural History Museum, Budapest, Hungary; ex-type culture CBS 148852 = NRRL 64356 = VN859). ITS and *cox1* sequences GenBank ON000799 and ON013865, respectively.

Sporangia, hyphae & chlamydospores (Fig. 10a–n, v–w) — Sporangia of *P. tonkinensis* were not observed on solid agar but were produced after 2–4 d in non-sterile soil extract. Sporangia were borne on unbranched sporangiophores, mostly terminally (Fig. 10a–b, d–h, j, l, n) or less frequently laterally on short hyphae (Fig. 10c, i, m). Sporangia were non-caducous, nonpapillate with a flat apex (Fig. 10a–i). Sporangial shapes were ovoid to broad-ovoid (61 %; Fig. 10a–c, e–g), subglobose (36.4 %; Fig. 10d, h) or infrequently obpyriform (1.3 %) and ellipsoid (1.3 %; Fig. 10i). Sporangia usually proliferated internally in both a nested (Fig. 10l–m) and extended way (Fig. 10n). Zoospores were discharged through an exit pore 5.8–14.7 µm wide (av. 9.8 ± 1.7 µm) (Fig. 10j, l–n). They were usually binucleate, limoniform to reniform whilst motile, becoming spherical (av. diam = 10.4 ± 1.0 µm) on encystment (Fig. 10j–k). Sporangial dimensions of four isolates averaged 29.0 ± 3.2 × 23.7 ± 3.1 µm (overall range 19.5–37.1 × 14.5–31.6 µm) with a range of isolate means of 27.8–29.8 × 23.0–24.0 µm. The length/breadth ratio averaged 1.23 ± 0.15 with a range of isolate means of 1.16–1.30. Hyphae were often irregular and coralloid (Fig. 10v) sometimes forming dense aggregations (Fig. 10w). Hyphal swellings and chlamydospores were not observed.

Oogonia, oospores & antheridia (Fig. 10o–u) — In single culture on V8A all four isolates of *P. tonkinensis* produced oo-

Fig. 10 Morphological structures of *Phytophthora tonkinensis*. a–n. Sporangia and zoospores formed on V8 agar (V8A) flooded with soil extract; a–d. non-papillate sporangia with flat apex; a–b. ovoid, terminal; c. subglobose, lateral; d. ovoid, on lateral hypha; e–i. nonpapillate terminal sporangia with swollen apex before release of the already differentiated zoospores; e–g. ovoid; h. subglobose; i. ellipsoid; j. sporangium releasing zoospores; k. binucleate zoospores with long flagella (arrow); l. terminal sporangia with internal nested proliferation; m. lateral sporangium with beginning nested proliferation; n. sporangium with internal extended proliferation; o–u. mature oogonia with oospores containing large ooplasts, formed in single culture in V8A; o–p. with amphigynous unicellular antheridia with finger-like projections; o. globose, smooth-walled with plerotic oospore; p. slightly excentric, smooth-walled with near-plerotic oospore; q–u. with paragynous antheridia; q. globose, smooth-walled with tapering base and plerotic oospore; r. elongated, smooth-walled with curved base and near-plerotic oospore; s. excentric, with wavy wall, tapering base, aplerotic oospore and intercalary antheridium; t. globose, with wavy wall and plerotic oospore; u. globose, with wavy golden-brown wall and aplerotic oospore; v. coralloid hyphae; w. dense hyphal aggregation. — Scale bar = 20 µm, applies to a–w.

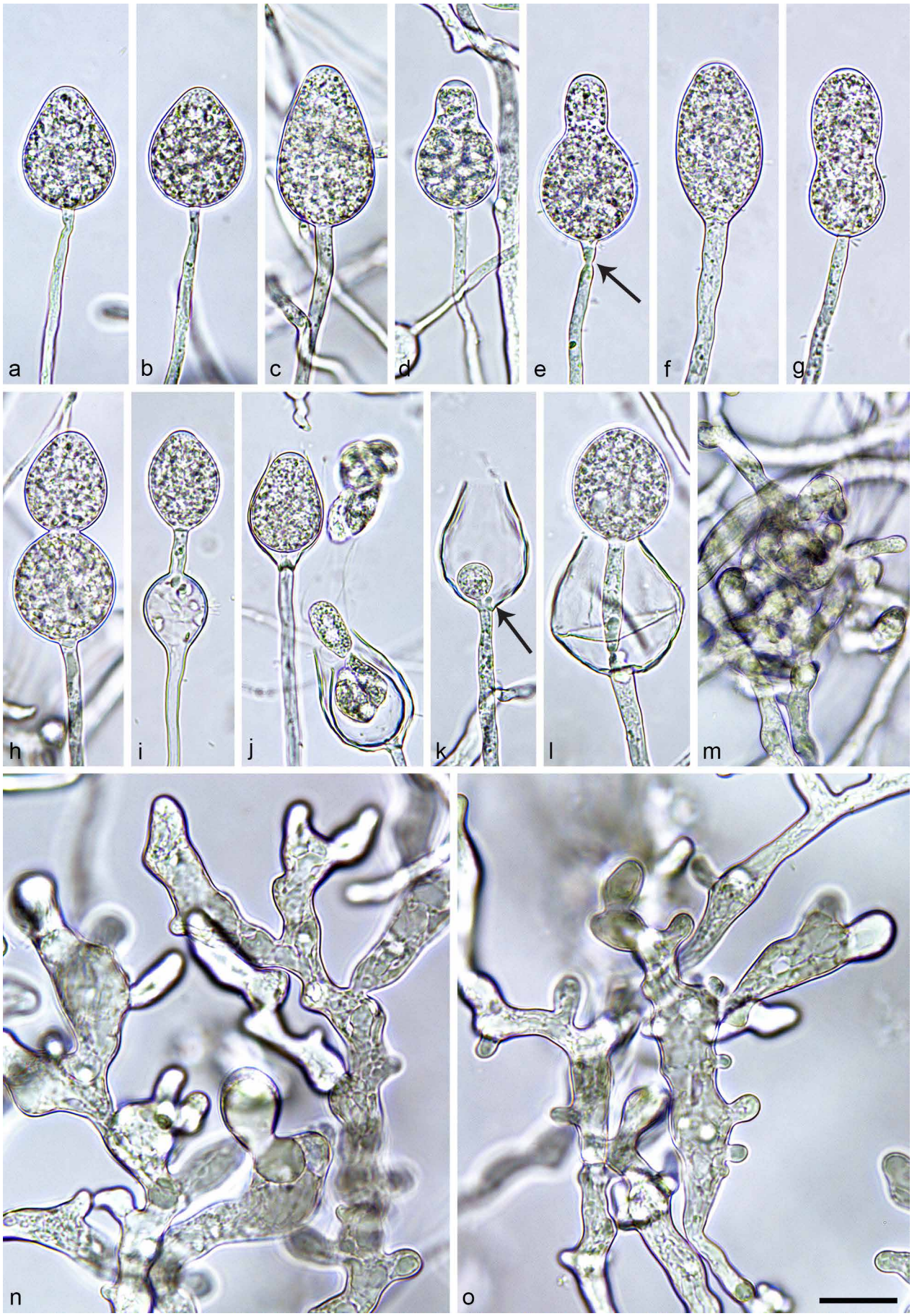

Fig. 11 Morphological structures of *Phytophthora ukrainensis*. a–l. Sporangia formed on V8-agar (V8A) flooded with soil extract; a–c, e–j. nonpapillate sporangia; a–b. ovoid; c. elongated-ovoid; d. obpyriform, with swollen apex before release of zoospores; e. obpyriform with a thick basal plug containing a conspicuous constriction (arrow); f. ellipsoid; g. peanut-shaped; h. ampulliform; i. ovoid sporangium and subglobose hyphal swelling; j. internal nested proliferation and release of zoospores; k. beginning internal nested proliferation with the new sporangiophore originating beside a conspicuous basal plug (arrow); l. internal extended proliferation with the new sporangiophore originating beside a conspicuous basal plug; m. hyphal aggregation; n–o. inflated coralloid hyphae. — Scale bar = 20 µm, applies to a–o.

gonia mainly in the centre of the colony and in fertile patches. Oogonia were borne terminally or laterally and had globose to subglobose (77.0 %; Fig. 10o, q–r, t–u) or slightly excentric or elongated (23.0 %; Fig. 10p, s) shapes, sometimes with a tapering (11.0 %; Fig. 10q–s) or curved base (13.5 %; Fig. 10r). Oogonial diameters averaged 46.2 ± 6.2 µm (overall range 30.3–59.1 µm and range of isolate means 45.1–48.4 µm). Oospores were near-plerotic to plerotic (69.0 %; Fig. 10o, q–r, t) or partly to fully aplerotic (31.0 %; Fig. 10p, s, u), globose, contained a large ooplast and often turned golden-brown with age (Fig. 10o–u). They had a mean diameter of 42.9 ± 5.5 µm (total range 28.4–56.9 µm), smooth (Fig. 10o–r) to slightly wavy walls (Fig. 10s–u) with an average thickness of 1.6 ± 0.3 µm (total range 1.1–3.0 µm) and a mean oospore wall index of 0.24 ± 0.03. With 6.3 % (4–8 %), mean oogonial abortion rate was low. Antheridia were formed terminally or laterally (Fig. 10o–r, t–u), often with a finger-like projection (Fig. 10o–p), or sometimes intercalary (Fig. 10s) and were predominantly paragynous (98.0 %; Fig. 10i–m) or infrequently amphigynous and unicellular (2.0 %; Fig. 10o–p), averaging 14.1 ± 2.2 × 10.8 ± 2.0 µm, with shapes ranging from clavate, subglobose to cylindrical.

Colony morphology, growth rates & cardinal temperatures (Fig. 21, 23) — Colonies on V8A and CA were appressed with very limited aerial mycelium and irregular margins, uniform on V8A and with faintly striate and dendroid sectors on CA; on PDA almost no growth (Fig. 21). Temperature-growth relations are shown in Fig. 23. All four isolates had similar growth rates and cardinal temperatures. The maximum growth temperature was between 20 and 25 °C. All isolates resumed growth when plates incubated for 5 d at 27.5 °C were transferred to 20 °C. Lethal temperature was between 27.5 and 30 °C. The average radial growth rate at the optimum temperature of 20 °C was 1.13 ± 0.1 mm/d but all isolates grew only slightly slower at 10 and 15 °C. On CA and PDA radial growth rates at 20 °C were 1.02 ± 0.2 mm/d and 0.17 ± 0.03 mm/d, respectively.

Additional specimens. Vietnam, Sapa, isolated from fallen leaves in a stream running through an evergreen cloud forest, 2017, *T. Jung & N.M. Chi*, VN1106, VN1107, VN1108, VN1109.

Phytophthora ukrainensis I. Milenković, T. Jung, T. Corcobado, I. Matsiakh, *sp. nov.* — MycoBank MB 843136; Fig. 11

Etymology. Name refers to the origin of most known isolates in Ukraine.

Typus. Ukraine, Lviv region, Ivano-Frankove, isolated from a naturally fallen *Quercus* leaf in the Vereshchytsia River, Aug. 2019, *I. Milenković*, *T. Corcobado & I. Matsiakh* (holotype HNHM-MYC-009710, dried culture on V8A, Herbarium of the Hungarian Natural History Museum, Budapest, Hungary; ex-type culture CBS 148851 = NRRL 64255 = UA373). ITS and *cox1* sequences GenBank ON000805 and ON013871, respectively.

Sporangia, hyphae & chlamydospores (Fig. 11a–o) — Sporangia were not observed on solid agar but were produced abundantly within 1–2 d in non-sterile soil extract. Sporangia were usually borne terminally on unbranched sporangiophores (Fig. 11a–j) and proliferated internally in both a nested (Fig. 11j–k) and extended way (Fig. 11l) with the new sporangiophore originating aside of a conspicuous basal plug (Fig. 11k–l). External proliferation was only rarely observed. Sporangia were non-caducous and nonpapillate (Fig. 11a–j), often becoming semipapillate-like before releasing zoospores (Fig. 11d). Sporangia were ovoid, elongated-ovoid or broad-ovoid (73.6 %; Fig. 11a–c, i–l), obpyriform (23.6 %; Fig. 11d–e) and infrequently ellipsoid (0.8 %; Fig. 11f), subglobose (0.8 %), peanut-like (0.6 %; Fig. 11g) or ampulliform (0.6 %; Fig. 11h). Some sporangia had a thick basal plug containing a conspicuous constriction (Fig. 11e). Sporangia were small averaging 35.9 ± 4.7 × 26.2 ± 3.4 µm with an overall range of 26.3–58.2 × 18.7–36.3 µm and isolate means of 34.0–38.1 × 23.5–29.9 µm. Mean length/breadth ratio of the sporangia was 1.38 ± 0.19 with a range of isolate means of 1.28–1.60. Zoospores were discharged through exit pores 5.3–15.0 µm wide (av. 8.4 ± 1.5 µm) (Fig. 11j–l). They were limoniform to reniform whilst motile, becoming spherical (av. diam = 10.4 ± 1.1 µm) on encystment. In liquid culture all isolates formed occasionally subglobose to limoniform swellings on sporangiophores (av. diam = 9.1 ± 1.5 µm; Fig. 11i). In solid V8A hyphae were often inflated and coralloid (Fig. 11n–o) and sometimes formed small hyphal aggregations (Fig. 11m).

Colony morphology, growth rates & cardinal temperatures (Fig. 21, 23) — All five *P. ukrainensis* isolates examined formed on V8A and CA colonies with limited aerial mycelium in the centre, striate on V8A and radiate on CA, and stoloniferous, dense-felty colonies on PDA (Fig. 21). Temperature-growth relations on V8A are shown in Fig. 23. The isolate from northern Sweden had slightly lower maximum and optimum temperatures for growth than the Ukrainian isolates. The Ukrainian isolates had their maximum between 32.5 and 35 °C and the isolates did not resume growth when plates incubated for 5 d at 35 °C were transferred to 20 °C. Their optimum temperature was 32.5 °C with a radial growth rate of 3.5 ± 0.12 mm/d. The Swedish isolate had a maximum temperature between 30 and 32.5 °C with 32.5 °C being lethal and an optimum temperature of 30 °C with a radial growth rate of 3.1 ± 0.28 mm/d (Fig. 23). At 20 °C radial growth rates of the Ukrainian and Swedish isolates on V8A, CA and PDA were 1.48 ± 0.21 mm/d, 2.62 ± 0.08 mm/d and 0.84 ± 0.37 mm/d, respectively.

Additional specimens. Sweden, Kiruna area, isolated from a forest stream using a *Quercus robur* leaf as bait, Sept. 2017, *I. Milenković & T. Corcobado*, SW154. – Ukraine, Lviv region, Ivano-Frankove, isolated from naturally fallen *Quercus* leaves in the Vereshchytsia River, Aug. 2019, *I. Milenković*, *T. Corcobado & I. Matsiakh*, UA376, UA430, UA431, UA432, UA433.

Phytophthora chilensis T. Jung, M. Horta Jung, A. Durán & I. Milenković, *sp. nov.* — MycoBank MB 842946; Fig. 12

Etymology. Name refers to the origin of all known isolates in Chile.

Typus. Chile, Parque Oncol, isolated from a stream running through a Valdivian rainforest using a *Rhododendron* leaf as bait, Nov. 2014, *T. Jung*, *A. Durán & E. Sanfuentes* (holotype HNHM-MYC-009700, dried culture on V8A, Herbarium of the Hungarian Natural History Museum, Budapest, Hungary; ex-type culture CBS 148797 = NRRL 64353 = CL165). ITS and *cox1* sequences GenBank ON000726 and ON013792, respectively.

Sporangia, hyphae & chlamydospores (Fig. 12a–k, v) — Sporangia of *P. chilensis* were observed on solid agar and were produced abundantly in non-sterile soil extract after 1–2 d. Sporangia were borne terminally (Fig. 12a–d, f) or laterally in dense sympodia of 2–5 sporangia (Fig. 12f) although a few lateral-sessile sporangia were present in all isolates (Fig. 12e, g). Sporangia were papillate (Fig. 12a–j) and caducous (Fig. 12g–k) with short pedicels averaging 4.0 ± 1.4 µm (Fig. 12a–d, f–k). Sporangial shapes ranged from ovoid (64.0 %; Fig. 12a–b, e–g, i–j), broad-ovoid (23.3 %; Fig. 12c–d) and elongated ovoid (4.3 %; Fig. 12h) to limoniform (3.3 %), obpyriform (2.1 %; Fig. 12g) or subglobose, ellipsoid and obovoid (each 1.0 %). Most sporangia had a conspicuous basal plug which protruded into the empty sporangium (Fig. 12g). Sporangia proliferated exclusively externally (Fig. 12a–d, f). Sporangial dimensions of six isolates of *P. chilensis* averaged 43.3 ± 6.1 × 29.5 ± 3.5 µm (overall range 20.7–60.3 × 13.4–42.1 µm) with a range of isolate means of 41.3–45.5 × 27.3–31.8 µm. The length/breadth ratio averaged 1.47 ± 0.15 with a range of isolate means of 1.39–1.71. Zoospores of *P. chilensis* were discharged directly through a narrow exit pore 3.2–6.9 µm wide (av. 5.3 ± 0.6 µm) (Fig. 12g, k). They were limoniform to reniform whilst motile, becoming spherical (av. diam = 9.6 ± 1.4 µm) on encystment. Small subglobose,

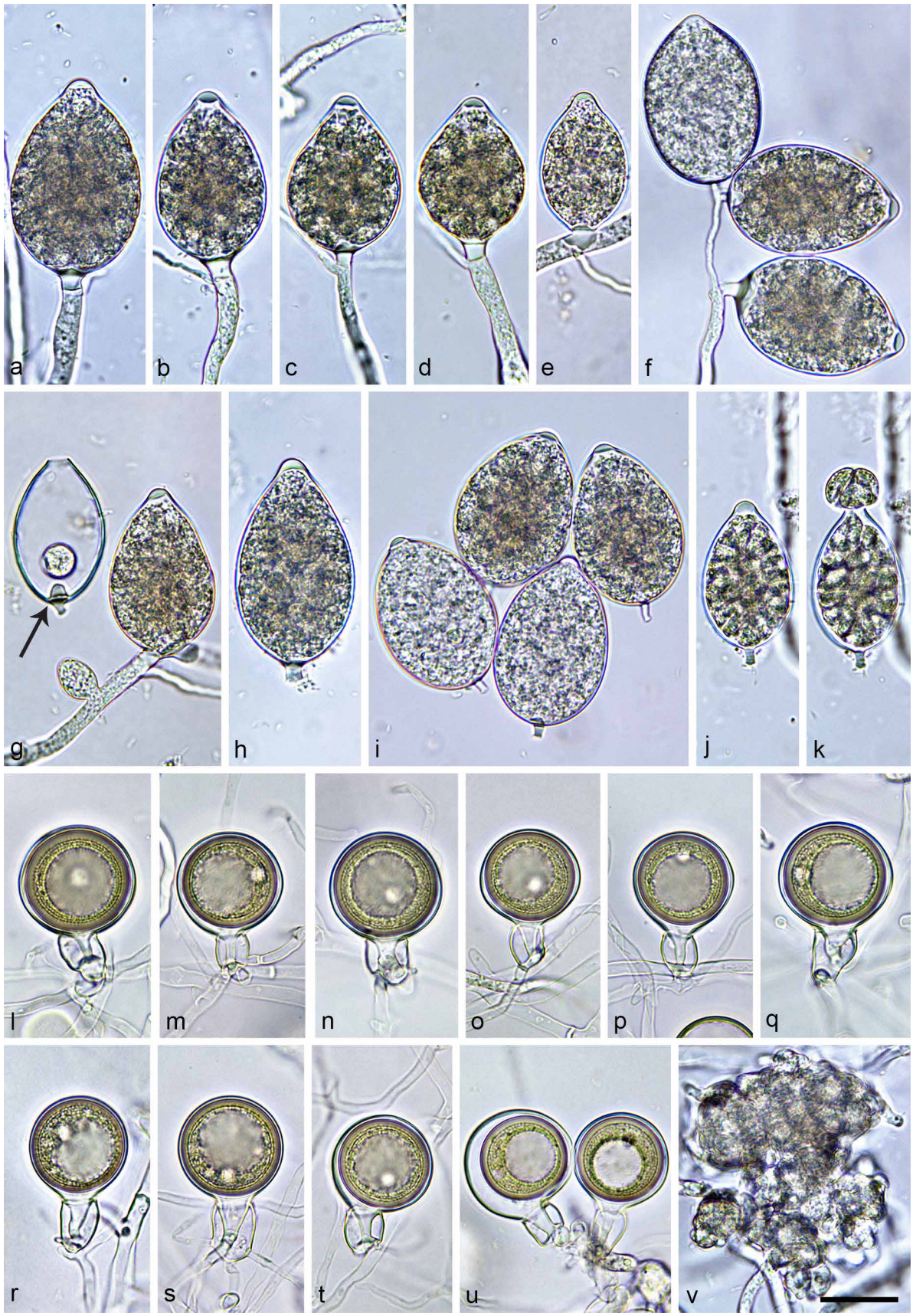

Fig. 12 Morphological structures of *Phytophthora chilensis*. a–k. Sporangia with short pedicels formed on V8 agar (V8A) flooded with soil extract; a–j. papillate sporangia; a. ovoid terminal; b–d. ovoid terminal with external proliferation; e. ovoid, lateral-sessile with conspicuous basal plug protruding into the sporangiophore; f. dense sympodium of three sporangia; g. slightly obpyriform, lateral-sessile sporangium with small ovoid hyphal swelling beside it and ovoid caducous sporangium with conspicuous basal plug (arrow), after release of most zoospores; h. elongated-ovoid caducous sporangium; i. ovoid caducous sporangia. j. ovoid caducous sporangium, differentiating zoospores; k. same sporangium as in j, releasing zoospores; l–u. mature smooth-walled oogonia formed in single culture in solid V8A, with oospores, containing large ooplasts, and amphigynous antheridia; j–t. globose oogonia with plerotic oospores; l. non-tapering base, bicellular antheridium; m–n. non-tapering bases, unicellular antheridia; o–s. tapering funnel-like bases, unicellular antheridia; t. slightly comma-shaped, tapering base and bicellular antheridium; u. excentric slightly comma-shaped oogonium with tapering base, aplerotic oospore and bicellular antheridium (left), and globose oogonium with tapering base, plerotic oospore and unicellular antheridium (right); v. dense compact hyphal aggregation in solid V8A. — Scale bar = 20 µm, applies to a–v.

limoniform or irregular swellings of 10.4 ± 2.4 µm were infrequently observed on sporangiophores (Fig. 12g). All isolates formed dense hyphal aggregations (Fig. 12v). Chlamydospores were not produced by any isolate.

Oogonia, oospores & antheridia (Fig. 12l–u) — Gametangia were readily produced in single culture by all isolates of *P. chilensis* on V8A within 1 wk and matured within 2–3 wk. Oogonia were borne terminally or laterally, smooth-walled, with round base and thin or thick stalk (Fig. 12l–n) or with tapering sometimes funnel-like base (on av. 44.7 %; Fig. 12o–u). They were predominantly globose to subglobose (av. 96.7 %; Fig. 12l–u) or sometimes excentric (av. 2.3 %; Fig. 12u). On average 26.7 % of oogonia were slightly comma-shaped (Fig. 12t–u). Oogonial diameters averaged 24.9 ± 2.6 µm (overall range 14.6–35.4 µm and range of isolate means 24.1–25.5 µm). Oospores had a mean diameter of 22.8 ± 2.4 µm (total range 13.6–32.6 µm), were globose and mostly plerotic (88 %; Fig. 12l–u) or less frequently aplerotic (12 %; Fig. 12u) and contained a large ooplast (Fig. 12l–u). The oospores had walls with a thickness of 1.8 ± 0.26 µm and an oospore wall index of 0.40 ± 0.04. Oogonial abortion rate was low (on. av. 8 %; 6–10 %). The antheridia averaged 12.7 ± 2.2 × 9.5 ± 1.1 µm were exclusively amphigynous with cylindrical or irregular shapes (Fig. 12l–u), unicellular (Fig. 12m–s) or less frequently bicellular with the basal cell being much smaller (Fig. 12l, t–u).

Colony morphology, growth rates & cardinal temperatures (Fig. 22, 24) — All six *P. chilensis* isolates formed after 10 d similar colonies on the three different agar media (Fig. 22). Colonies on V8A and CA were appressed with limited aerial mycelium, faintly striate to radiate with irregular margins on V8A and faintly radiate on CA, while colonies on PDA were dense-felty with radiating raised lobes separated by irregular trenches. The temperature-growth relations on V8A are shown in Fig. 24. Five of the six isolates had similar growth rates at all temperatures and an optimum temperature of 20 °C while isolate CL171 had an optimum temperature of 15 °C. The maximum growth temperature for all isolates was between 20 and 25 °C. None of the isolates was able to grow at 25 °C. Lethal temperature was 25 °C for isolates CL165, CL169, CL170 and CL171, and 30 °C for isolates CL166 and CL172. At 20 °C radial growth rates on V8A, CA and PDA were 2.77 ± 0.07 mm/d, 2.43 ± 0.1 mm/d and 0.62 ± 0.14 mm/d, respectively.

Additional specimens. Chile, Parque Oncol, isolated from streams running through Valdivian rainforests using *Rhododendron* leaves as baits, Nov. 2014, *T. Jung*, *A. Durán & E. Sanfuentes*, CL166, CL169, CL170, CL171, CL172.

Phytophthora pseudochilensis T. Jung, M. Horta Jung, E. Sanfuentes & I. Milenković, *sp. nov.* — MycoBank MB 842947; Fig. 13

Etymology. Name refers to the morphological similarity to *P. chilensis*.

Typus. Chile, Parque Oncol, isolated from a stream running through a Valdivian rainforest using a *Rhododendron* leaf as bait, Nov. 2014, *T. Jung*, *A. Durán & E. Sanfuentes* (holotype HNHM-MYC-009705, dried culture on V8A, Herbarium of the Hungarian Natural History Museum, Budapest, Hungary; ex-type culture CBS 148798 = NRRL 64352 = CL168). ITS and *cox1* sequences GenBank ON000773 and ON013839, respectively.

Sporangia, hyphae & chlamydospores (Fig. 13a–j, s–t) — Sporangia of *P. pseudochilensis* were produced abundantly in non-sterile soil extract after 1–2 d and were also observed on solid V8A. Sporangia were borne usually in dense sympodia of 2–10 sporangia (Fig. 13c–d, j) or infrequently terminally on unbranched sporangiophores (Fig. 13b). Sporangia were papillate (Fig. 13a, c, g) or semipapillate (Fig. 13b, e–f, h, j), sometimes with a slightly asymmetric apex and an inclined papilla (4.5 %; Fig. 13g, i) or a laterally displaced apex (Fig. 13h), and caducous (Fig. 13d–i) with short pedicels averaging 4.9 ± 1.6 µm (Fig. 13a–b, e–j). Sporangial shapes ranged from ovoid (49.0 %; Fig. 13a, c–d) and elongated-ovoid (25.0 %; Fig. 13e–h, j) to obpyriform (9.5 %; Fig. 13b), limoniform (8.0 %; Fig. 13c–d), ellipsoid and elongated-ellipsoid (4.5 %; Fig. 13d, i) and obovoid (4.0 %). Most sporangia had an inconspicuous basal plug which did not protrude into the empty sporangium (Fig. 13i–j). Sporangia proliferated exclusively externally (Fig. 13a, d, j). Sporangial dimensions of six isolates of *P. pseudochilensis* averaged 48.8 ± 8.2 × 27.0 ± 3.1 µm (overall range 25.6–69.1 × 17.4–39.4 µm) with a range of isolate means of 43.3–54.9 × 25.7–29.3 µm. The length/breadth ratio averaged 1.81 ± 0.24 with a range of isolate means of 1.69–1.94. Zoospores were limoniform to reniform whilst motile, becoming spherical (av. diam = 9.9 ± 1.2 µm) on encystment and were discharged directly through a narrow exit pore 2.5–6.3 µm wide (av. 4.4 ± 0.9 µm) (Fig. 13i–j). Cysts germinated directly or indirectly by releasing a secondary zoospore (diplanetism). All isolates produced in solid V8A coralloid or irregular lateral hyphae (Fig. 13s) and hyphal aggregations (Fig. 13t), and in liquid culture infrequently subglobose, limoniform or irregular swellings (10.3 ± 2.7 µm diam). Chlamydospores were not observed.

Oogonia, oospores & antheridia (Fig. 13k–r) — Gametangia were readily produced in single culture by all isolates of *P. pseudochilensis* on V8A within 1 wk and matured within 2–3 wk. Oogonia were borne laterally or less frequently terminally, smooth-walled, globose to subglobose with a tapering often funnel-like (87.5 %; Fig. 13l–r) or sometimes a round base (12.5 %; Fig. 13k). On average 20.5 % of oogonia were comma-shaped (Fig. 13r). Oogonial diameters were averaging 27.3 ± 3.4 µm with an overall range of 16.3–35.3 µm and a range of isolate means of 25.9–28.5 µm. Oospores were globose, mostly near plerotic to plerotic (91.0 %; Fig. 13k–n, q–r) or less frequently aplerotic (9.0 %; Fig. 13o–q), and contained a large ooplast (Fig. 13k–r). Oospore diameters averaged 24.4 ± 3.0 µm (total range 15.4–32.1 µm). Oospores had walls with a diameter of 1.61 ± 0.33 µm and an oospore wall index of 0.34 ± 0.07. With on average 65.5 % (56–80 %) the oogonial abortion rate was high. The antheridia were amphigynous, almost exclusively unicellular, with cylindrical or irregular shapes (Fig. 13k–r) and sometimes finger-like projections (Fig. 13l, o), averaging 13.7 ± 3.6 × 9.8 ± 1.7 µm.

Colony morphology, growth rates & cardinal temperatures (Fig. 22, 24) — Colonies of *P. pseudochilensis* were loose and appressed to submerged with scarce aerial mycelium and a dendroid to stoloniferous pattern with irregular margins on V8A, uniform and appressed with limited aerial mycelium on CA, and dense-felty with irregular raised lobes separated by irregular trenches and irregular feathery margins on PDA (Fig. 22). The temperature-growth relations on V8A are shown in Fig. 24. All six isolates had similar growth rates at all temperatures and identical cardinal temperatures for growth with a low optimum of 15 °C and a maximum between 20 and 25 °C. None of the isolates was able to grow at 25 °C but they resumed growth when plates incubated for 5 d at 25 °C were transferred to 20 °C. Lethal temperature was between 25 and 27.5 °C. Radial growth rates at 15 and 20 °C were 2.39 ± 0.22 mm/d and 1.57 ± 0.43 mm/d, respectively (Fig. 24). On CA and PDA radial growth rates at 20 °C were 1.8 ± 0.03 mm/d and 0.65 ± 0.03 mm/d, respectively.

Additional specimens. Chile, Parque Oncol, isolated from a stream running through a Valdivian rainforest using *Rhododendron* leaves as baits, Nov. 2014, *T. Jung*, *A. Durán & E. Sanfuentes*, CL335, CL336, CL337, CL338, CL339.

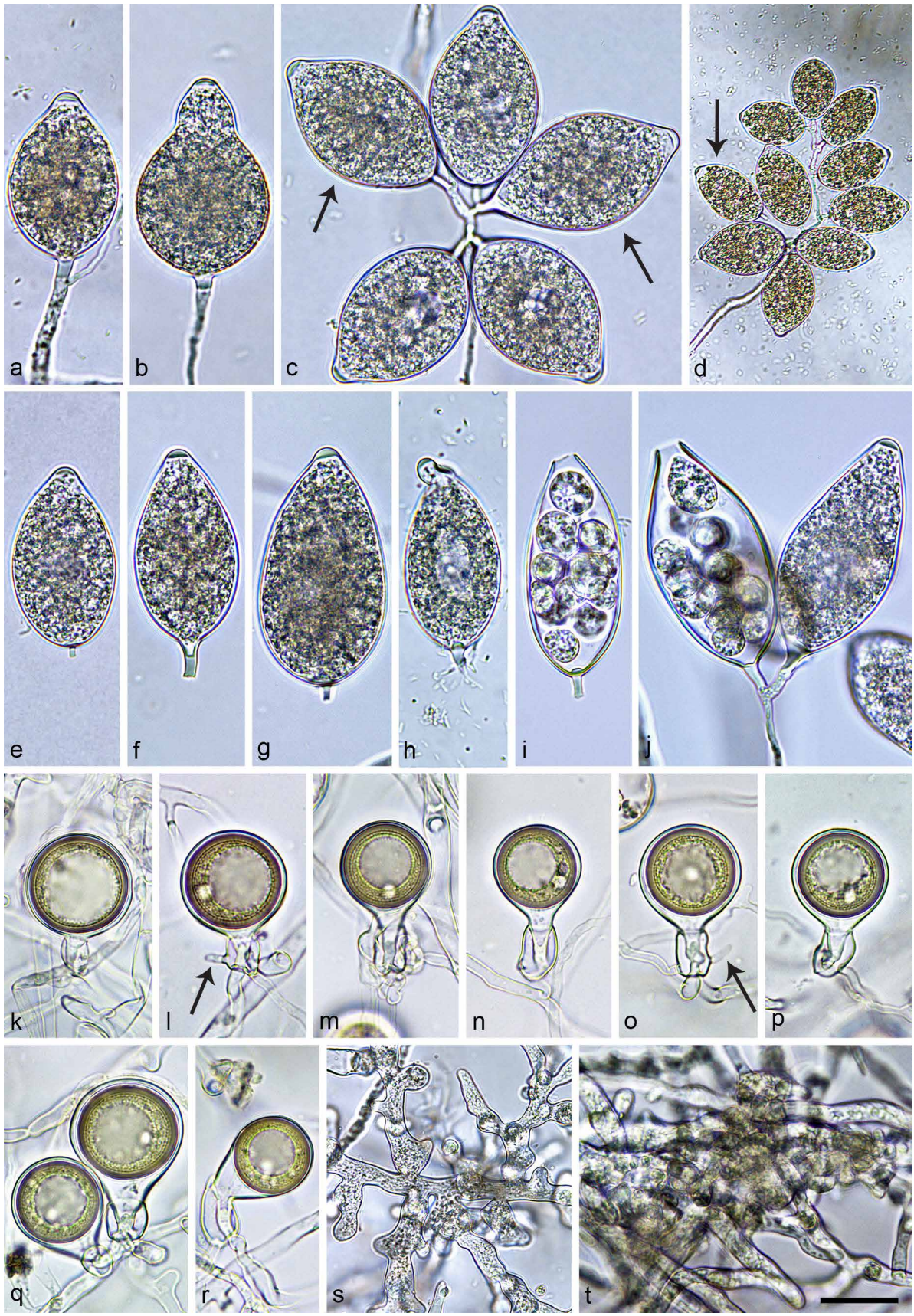

Fig. 13 Morphological structures of *Phytophthora pseudochilensis*. a–j. Sporangia with short pedicels formed on V8 agar (V8A) flooded with soil extract; a. ovoid, papillate, terminal, with external proliferation; b. obpyriform, semipapillate, terminal; c. dense sympodium of two liminoform (arrows) and three ovoid papillate sporangia; d. dense sympodium of ten mainly ovoid or limoniform sporangia except of one ellipsoid sporangium which has already been shed (arrow); e–i. caducous sporangia; e–f. elongated-ovoid, semipapillate; g. elongated-ovoid, papillate with slightly asymmetric apex and inclined papilla; h. elongated-ovoid, semipapillate with a laterally displaced apex; i. elongated-ellipsoid sporangium with slightly asymmetric apex which failed to release all zoospores; j. sympodium of two elongated-ovoid sporangia, one mature and semipapillate and one releasing zoospores; k–r. mature smooth-walled oogonia formed in single culture in solid V8A, with oospores, containing large ooplasts, and amphigynous unicellular antheridia; k. non-tapering base; l–r. tapering funnel-like oogonial bases; l. near plerotic oospore and antheridium with finger-like projection (arrow); m–n. plerotic oospore; o. aplerotic oospore and antheridium with finger-like projection (arrow); p. aplerotic oospore; q. two oogonia with near plerotic (left) and aplerotic (right) oospores; r. comma-shaped oogonium with plerotic oospore; s. coralloid irregular lateral hyphae in solid V8A; t. hyphal aggregation in solid V8A. — Scale bar = 20 µm, applies to all except of d where it is 50 µm.

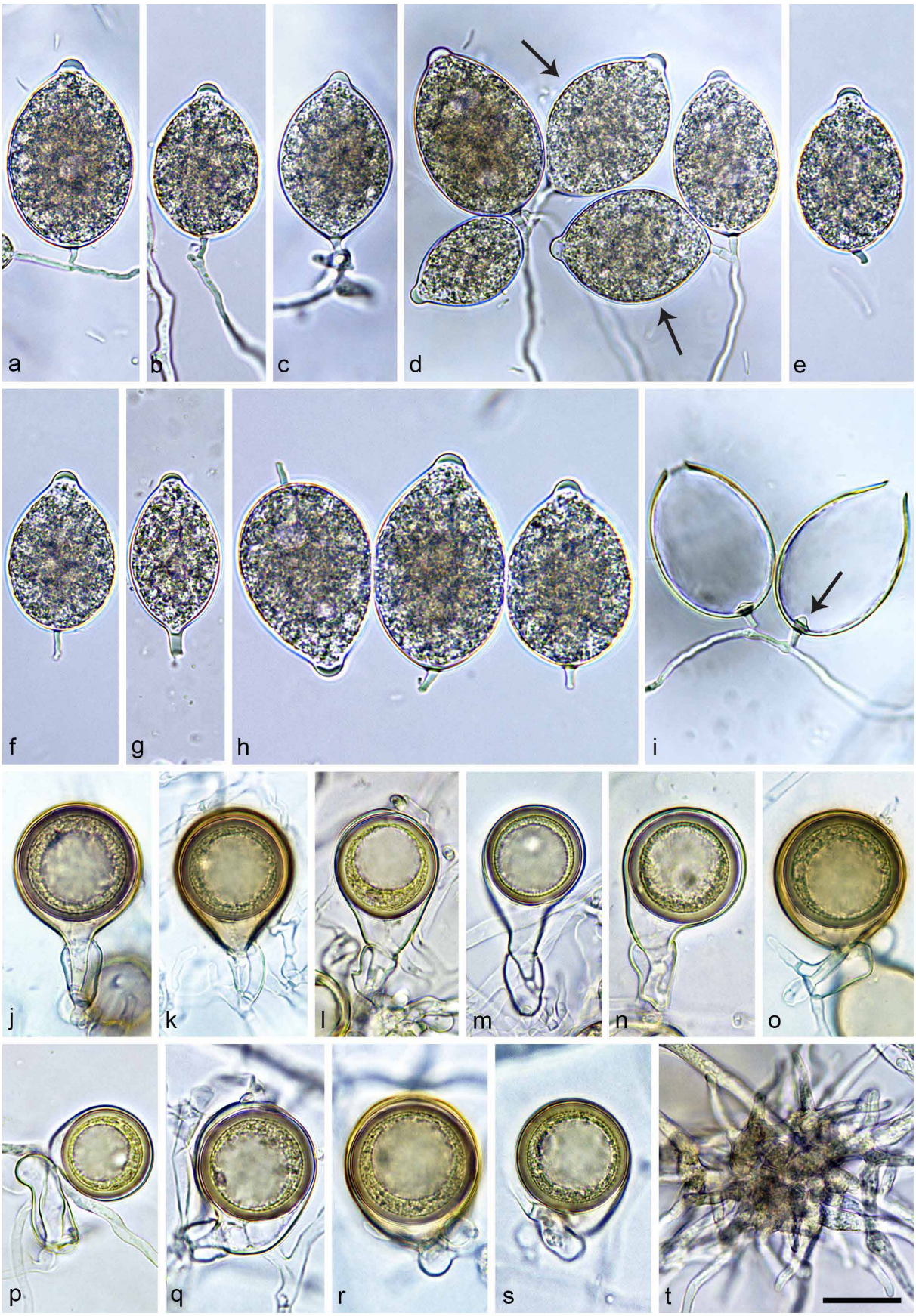

Fig. 14 Morphological structures of *Phytophthora pseudokernoviae*. a–i. Sporangia with short pedicels formed on V8 agar (V8A) flooded with soil extract; a–h. papillate sporangia; a. ovoid lateral, in a beginning sympodium; b. ovoid with beginning external proliferation; c. limoniform; d. ovoid and limoniform (arrows) sporangia in two sympodia of three (left) and two sporangia (right); e–f. ovoid, caducous; g. limoniform, caducous; h. ovoid, caducous; i. two empty sporangia after zoospore release, one just being shed (left) and the other one lateral with conspicuous basal plug protruding into the sporangium (arrow); j–s. mature smooth-walled oogonia formed in solid V8A, with plerotic or near plerotic oospores containing large ooplasts; j–q. with amphigynous unicellular antheridia; j–n. globose oogonia with tapering funnel-like bases; j–k. golden-brown; n. comma-shaped; o. golden-brown subglobose oogonium with rounded comma-shaped base and finger-like projection at the antheridium; p. subglobose oogonium with rounded base, extremely comma-shaped; q. elongated oogonium with tapering base, comma-shaped; r. golden-brown subglobose oogonium with tapering base and paragynous antheridium; s. globose oogonium with tapering base and paragynous antheridium; t. dense hyphal aggregation in solid V8A. — Scale bar = 20 µm, applies to a–t.

Phytophthora pseudokernoviae T. Jung, M. Horta Jung, A. Durán & E. Sanfuentes, *sp. nov.* — MycoBank MB 842949; Fig. 14

Etymology. Name refers to the morphological similarity to *P. kernoviae*.

Typus. Chile, Parque Oncol, isolated from a naturally fallen necrotic leaf of *Drimys winteri* in a Valdivian rainforest, Nov. 2014, *T. Jung*, *A. Durán & E. Sanfuentes* (holotype HNHM-MYC-009707, dried culture on V8A, Herbarium of the Hungarian Natural History Museum, Budapest, Hungary; ex-type culture CBS 148796 = NRRL 64351 = CL012). ITS and *cox1* sequences GenBank ON000780 and ON013846, respectively.

Sporangia, hyphae & chlamydospores (Fig. 14a–i, t) — Sporangia of *P. pseudokernoviae* were observed on solid agar and were produced abundantly in non-sterile soil extract after 1–2 d. Sporangia were mostly borne laterally or infrequently terminally in dense sympodia of 2–5 sporangia (Fig. 14a, d, i). Sporangia were exclusively papillate (Fig. 14a–h) and caducous (Fig. 14e–i) with short pedicels averaging 3.6 ± 1.0 µm (Fig. 14a–i). Sporangial shapes showed low variability and were predominantly ovoid (88.0 %; Fig. 14a–b, d–f, h–i) or less frequently limoniform (12.0 %; Fig. 14c–d, g). Sporangia often had a conspicuous basal plug which protruded into the empty sporangium (Fig. 14i) and proliferated exclusively externally (Fig. 14a–b, d). Sporangial dimensions of three isolates of *P. pseudokernoviae* averaged 42.7 ± 4.0 × 29.7 ± 2.8 µm with an overall range of 30.5–55.0 × 21.3–35.7 µm and a range of isolate means of 41.9–43.4 × 28.6–31.5 µm. The length/breadth ratio averaged 1.44 ± 0.14 with a range of isolate means of 1.38–1.50. Zoospores of *P. pseudokernoviae* were discharged through a narrow exit pore 4.3–7.2 µm wide (av. 5.6 ± 0.7 µm) (Fig. 14i). They were limoniform to reniform whilst motile, becoming spherical (av. diam = 9.9 ± 1.6 µm) on encystment. Cysts germinated directly or indirectly by releasing a secondary zoospore (diplanetism). Small subglobose, limoniform or irregular swellings of 9.9 ± 2.1 µm were infrequently formed on sporangiophores. All isolates produced dense hyphal aggregations (Fig. 14t). Chlamydospores were not observed.

Oogonia, oospores & antheridia (Fig. 14j–s) — Gametangia were readily produced in single culture by all isolates of *P. pseudokernoviae* in V8A within 1 wk and matured within 2–3 wk. Oogonia were borne terminally or laterally, smooth-walled, predominantly with a tapering often funnel-like (86.0 %; Fig. 14k–o, r–t) or less frequently with a rounded base (14.0 %; Fig. 14p–q) which in 35.3 % of oogonia was also comma-shaped curved (Fig. 14o, q–r). They were predominantly globose to subglobose (av. 84.0 %; Fig. 14j–k, o–p, r–s) or sometimes elongated or excentric (16.0 %; Fig. 14l–n, q), sometimes turning golden-brown with age (Fig. 14j–k, o, r). Oogonial diameters averaged 30.1 ± 4.3 µm with an overall range of 18.6–39.3 µm and a range of isolate means 28.1–34.2 µm. Oospores contained a large ooplast and were globose and almost exclusively plerotic or near-plerotic (99.6 %; Fig. 14j–s) with a mean diameter of 27.0 ± 3.7 µm (total range 16.3–35.8 µm). Oospores had wall diameters of 2.1 ± 0.33 µm and an oospore wall index of 0.40 ± 0.06. Oogonial abortion rate was low (on. av. 7.7 %; 6–10 %). The antheridia were predominantly amphigynous unicellular (95.3 %) with cylindrical or slightly irregular shapes (Fig. 14j–q) or occasionally paragynous (4.7 %; Fig. 14r–s), averaging 14.6 ± 2.9 × 9.6 ± 1.3 µm.

Colony morphology, growth rates & cardinal temperatures (Fig. 22, 24) — After 10 d growth at 20 °C colonies of *P. pseudokernoviae* on V8A and CA were appressed with limited aerial mycelium, uniform to faintly striate on V8A and faintly radiate on CA, whereas colonies on PDA were dense-woolly and faintly petaloid (Fig. 22). At 25 °C all three isolates showed very slow growth for 5 d and then stopped growing suggesting a maximum temperature of growth slightly below 25 °C. The isolates did not resume growth when the plates were transferred to 20 °C. With mean radial growth rates of 2.47 ± 0.62 mm/d and 2.45 ± 0.41 mm/d at 15 and 20 °C, respectively, *P. pseudokernoviae* had a broad optimum of growth (Fig. 24). On CA and PDA radial growth rates at 20 °C were 1.93 ± 0.11 mm/d and 1.0 ± 0.07 mm/d, respectively.

Additional specimens. Chile, Parque Oncol, isolated from a naturally fallen necrotic leaf of *D. winteri* in a Valdivian rainforest, Nov. 2014, *T. Jung*, *A. Durán & E. Sanfuentes*, CL013; isolated from a stream running through a Valdivian rainforest using a *Nothofagus obliqua* leaf as bait, Nov. 2014, *T. Jung*, *A. Durán & E. Sanfuentes*, CL156.

Phytophthora celebensis T. Jung, M. Junaid, N. Nasri & I. Milenković, *sp. nov.* — MycoBank MB 843002; Fig. 15

Etymology. Name refers to the origin of all known isolates in Sulawesi (Celebes is a previous name of Sulawesi).

Typus. Indonesia, South Sulawesi Province, District of Tana Toraja, isolated from a naturally fallen leaf floating in a stream running through a submontane tropical rainforest, May 2019, *T. Jung*, *M. Junaid & N. Nasri* (holotype HNHM-MYC-021540, dried culture on V8A, Herbarium of the Hungarian Natural History Museum, Budapest, Hungary; ex-type culture CBS 148800 = SL092). ITS and *cox1* sequences GenBank ON000720 and ON013786, respectively.

Sporangia, hyphae & chlamydospores (Fig. 15a–h, s) — Sporangia of *P. celebensis* were observed on solid agar and were produced abundantly in non-sterile soil extract after 1–2 d. Sporangia were borne terminally (Fig. 15a–b, h) or laterally (Fig. 15b, h), often in dense sympodia of 2–5 sporangia (Fig. 15b, h). Spor angia were papillate (Fig. 15a–f, h) and caducous (Fig. 15b–h) with short to medium-length pedicels averaging 9.9 ± 2.7 µm (Fig. 15a–h). Sporangial shapes ranged from ovoid (48.8 %; Fig. 15a–d) and broad-ovoid (4.0 %; Fig. 15e) to limoniform (41.6 %; Fig. 15h), obovoid (3.4 %; Fig. 15f), ellipsoid (1.0 %), subglobose (0.8 %) and pyriform (0.4 %). Sometimes sporangia were laterally attached to the sporangiophore (7.6 %; Fig. 15a) or had an inconspicuous basal plug (10.8 %; Fig. 15f). Sporangial proliferation was exclusively external. Sporangial dimensions of five isolates averaged 38.7 ± 5.0 × 26.2 ± 3.3 µm (overall range 26.3–64.3 × 17.6–40.7 µm) with a range of isolate means of 37.3–40.7 × 25.0–27.9 µm. The length/breadth ratio averaged 1.48 ± 0.12 with a range of isolate means of 1.44–1.54. Zoospores of *P. celebensis* were discharged directly through narrow exit pores 2.1–5.1 µm wide (av. 3.7 ± 0.7 µm) (Fig. 15g). They were limoniform to reniform whilst motile, becoming spherical (av. diam = 8.0 ± 0.8 µm) on encystment. Cysts germinated directly or indirectly by releasing a secondary zoospore (diplanetism). All isolates formed dense hyphal aggregations (Fig. 15s). Hyphal swellings and chlamydospores were not observed.

Oogonia, oospores & antheridia (Fig. 15i–r) — Gametangia were readily produced in single culture by all isolates of *P. celebensis* in V8A within 1 wk and matured within 2–3 wk. Oogonia were borne terminally or laterally, smooth-walled, globose to subglobose (92.4 %; Fig. 15i–p, r) or rarely slightly excentric or elongated (7.6 %; Fig. 15q), mostly with round base and thin stalk (91.6 %; Fig. 15i–o) or with short tapering base (8.4 %; Fig. 15p–r). On average 22.4 % of oogonia were slightly bending to comma-shaped (Fig. 15q–r). Oogonial diameters averaged 24.9 ± 3.1 µm (overall range 13.1–36.1 µm and range of isolate means 23.6–25.8 µm). Oospores had a mean diameter of 21.9 ± 2.9 µm (total range 12.3–31.5 µm), were globose and plerotic to near-plerotic and contained a large ooplast (Fig. 15i–r). The oospores had walls with a diameter of 1.6 ± 0.27 µm and an oospore wall index of 0.38 ± 0.04. Oogonial abortion rate was 24.4 % (6–48 %). The antheridia averaged 11.4 ± 2.1 × 9.8 ± 1.3 µm and were exclusively amphigynous unicellular with cylindrical, subglobose or square shapes (Fig. 15i–r).

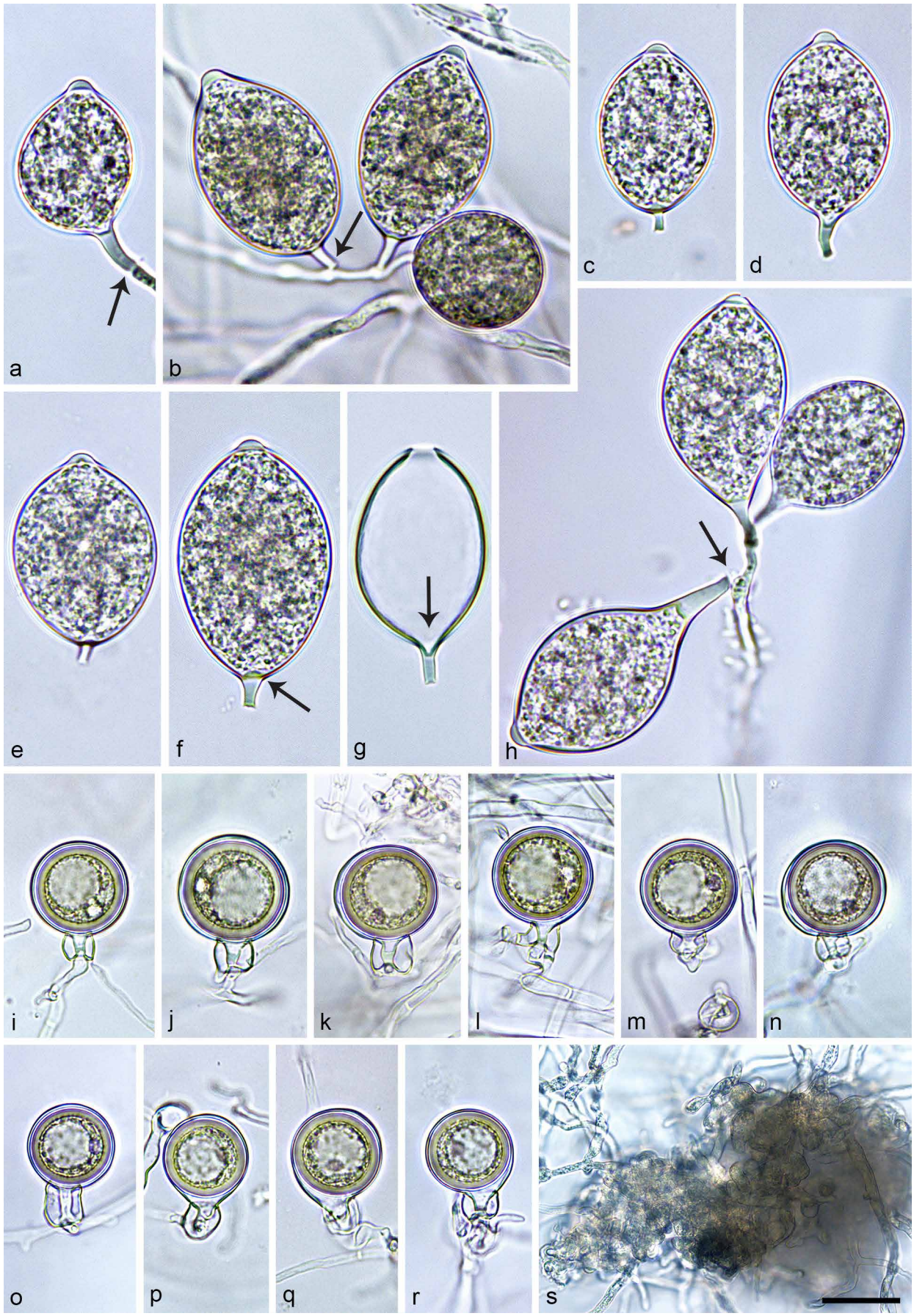

Fig. 15 Morphological structures of *Phytophthora celebensis*. a–h. Sporangia with mostly medium-length pedicels formed on V8 agar (V8A) flooded with soil extract; a–f. papillate; a. ovoid, slightly asymmetric, with laterally attached sporangiophore; b. sympodium with one immature and two ovoid sporangia, one of them caducous (arrow); c–d. ovoid, caducous; e. broad-ovoid, caducous; f. obovoid with inconspicuous basal plug (arrow), caducous; g. ovoid, caducous, after release of zoospores, without protruding basal plug (arrow); h. sympodium with one immature and two limoniform sporangia, one of them caducous (arrow); i–r. mature oogonia formed in single culture in solid V8A, with thick-walled plerotic or near-plerotic oospores, containing large ooplasts, and amphigynous unicellular antheridia; i–n. with round bases and short tapering stalks; o. with round base and medium-length stalk; p–r. with short, tapering bases; q–r. slightly bending to comma-shaped; s. dense hyphal aggregation in solid V8A. — Scale bar = 20 µm, applies to a–s.

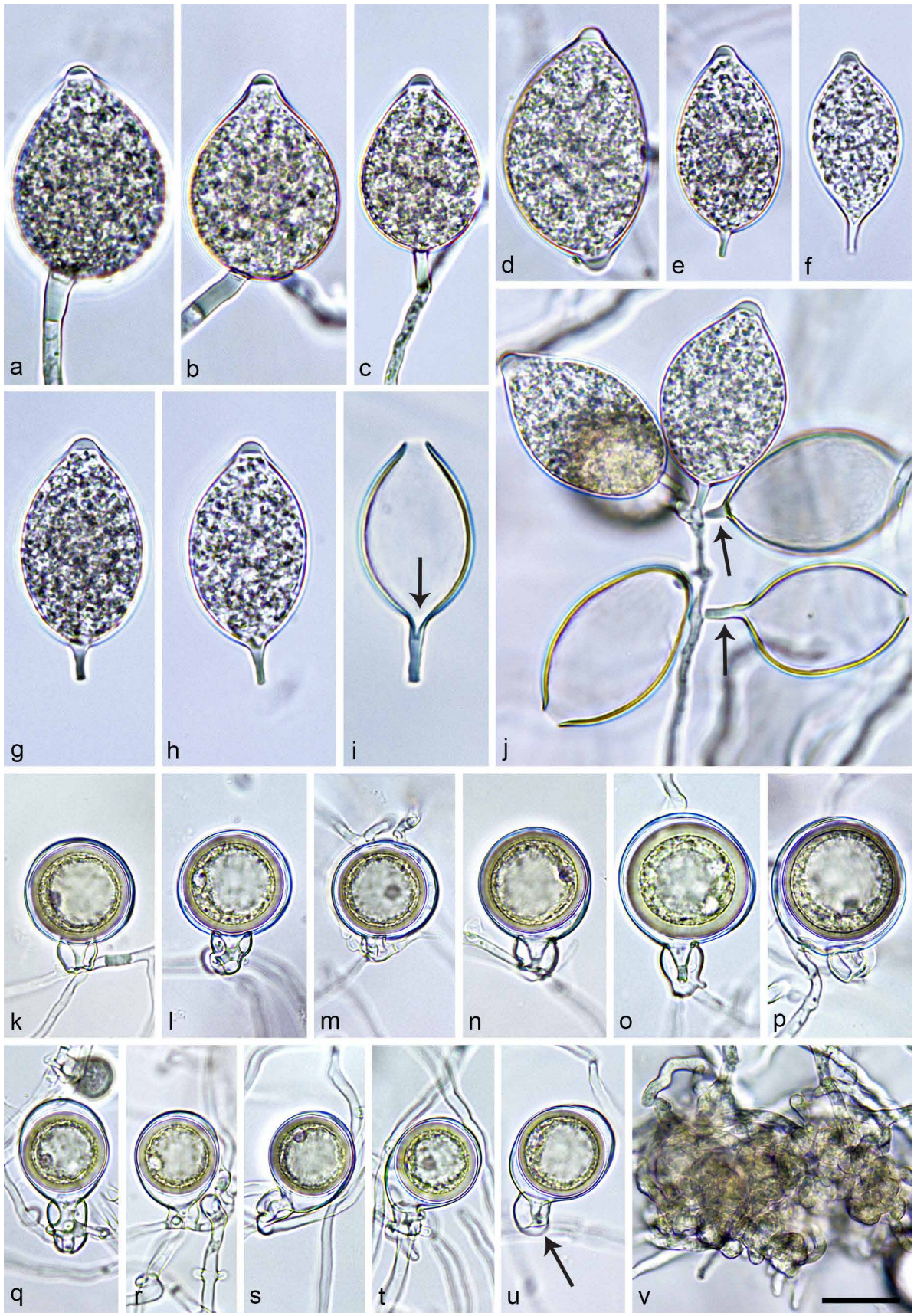

Fig. 16 Morphological structures of *Phytophthora javanensis*. a–j. Sporangia with short to medium-length pedicels formed on V8 agar (V8A) flooded with soil extract; a–h. papillate; a. ovoid, terminal, sporangiophore laterally attached; b. ovoid, intercalary; c. ovoid, lateral; d. limoniform, bipapillate; e. slender-ovoid, caducous; f. limoniform, caducous; g–i. slender-ovoid, caducous; i. empty after release of zoospores, without basal plug (arrow); j. sympodium with two ovoid papillate sporangia and three empty sporangia after release of zoospores, one of the latter persistent with inconspicuous basal plug, two caducous (arrows) without basal plugs; k–u. mature oogonia formed in single culture in solid V8A, with thick-walled oospores, containing large ooplasts; k–t. amphigynous unicellular antheridia; k–l. globose with round bases, short tapering stalks and plerotic or near-plerotic oospores; m. subglobose with round base, short stalk and aplerotic oospore; n. subglobose with short tapering base and plerotic oospore; o. subglobose with short tapering stalk and slightly aplerotic oospore; p. subglobose to slightly excentric with round base and slightly aplerotic oospore; q. elongated with tapering base and aplerotic oospore; r. slightly elongated with tapering base and slightly aplerotic oospore; s–u. slightly elongated, comma-shaped with tapering bases and slightly aplerotic oospores; u. amphigynous bicellular antheridium with small basal cell (arrow); v. dense hyphal aggregation in solid V8A. — Scale bar = 20 µm, applies to a–v.

Colony morphology, growth rates & cardinal temperatures (Fig. 22, 24) — All isolates of *P. celebensis* formed after 10 d similar colonies on the three different agar media. Colonies were appressed with limited aerial mycelium and a dendroid growth pattern on V8A and CA, and dense-woolly and uniform on PDA (Fig. 22). The temperature-growth relations on V8A are shown in Fig. 24. On V8A *P. celebensis* had an optimum temperature of 25 °C with a radial growth rate of 2.9 ± 0.23 mm/d. The maximum growth temperature for all isolates was between 27.5 and 30 °C. None of the isolates was able to grow at 30 °C and isolates did not resume growth when plates incubated for 5 d at 30 °C were transferred to 20 °C. On V8A, CA and PDA radial growth rates at 20 °C were 2.77 ± 0.19 mm/d, 2.3 ± 0.09 mm/d and 1.0 ± 0.05 mm/d, respectively.

Additional specimens. Indonesia, South Sulawesi Province, District of Tana Toraja, isolated from naturally fallen leaves floating in a stream running through a submontane tropical rainforest, May 2019, *T. Jung*, *M. Junaid & N. Nasri*, SL091, SL540, SL541, SL542.

Phytophthora javanensis T. Jung, M. Junaid, N. Nasri & M. Horta Jung, *sp. nov.* — MycoBank MB 842954; Fig. 16

Etymology. Name refers to the origin of the first isolates in Java.

Typus. Indonesia, Java, Gunung Puntang, Bandung area, isolated from a naturally fallen leaf floating in a stream running through a submontane tropical rainforest, Feb. 2019, *T. Jung*, *M. Junaid & N. Nasri* (holotype HNHM-MYC-009702, dried culture on V8A, Herbarium of the Hungarian Natural History Museum, Budapest, Hungary; ex-type culture CBS 149203 = NRRL 64129 = JV025a). ITS and *cox1* sequences GenBank ON000750 and ON013816, respectively.

Sporangia, hyphae & chlamydospores (Fig. 16a–j, v) — Sporangia of *P. javanensis* were observed on solid agar and were produced abundantly in non-sterile soil extract after 1–2 d. Sporangia were borne terminally (Fig. 16a, j), laterally (Fig. 16c, j), often in dense sympodia of 2–6 sporangia (Fig. 16j), or infrequently intercalary (Fig. 16b). Sporangia were exclusively papillate (Fig. 16a–h, j), sometimes bipapillate (Fig. 16d), and caducous (Fig. 16e–j) with short to medium-length pedicels averaging 7.4 ± 2.1 µm (Fig. 16a–j). Sporangial shapes showed low variability and were mostly ovoid (53.6 %; Fig. 16a–c, e, g–h) or limoniform (43.0 %; Fig. 16d, f, i) and infrequently obovoid (1.6 %), ellipsoid (1.0 %) or subglobose (0.8 %). Sporangia usually had no conspicuous basal plug (Fig. 16i–j), were sometimes laterally attached (3.6 %; Fig. 16a) and proliferated exclusively externally. Sporangial dimensions of ten isolates of *P. javanensis* averaged 38.3 ± 4.5 × 23.2 ± 2.9 µm with an overall range of 19.3–62.6 × 9.2–36.7 µm and a range of isolate means of 33.6–41.3 × 20.5–25.6 µm. The length/breadth ratio averaged 1.66 ± 0.19 with a range of isolate means of 1.54–1.81. Zoospores were discharged through a narrow exit pore 1.9–8.3 µm wide (av. 3.3 ± 0.6 µm) (Fig. 16i–j). They were limoniform to reniform whilst motile, becoming spherical or ellipsoid (av. diam = 8.4 ± 0.7 µm) on encystment. Cysts germinated directly or indirectly by releasing a secondary zoospore (diplanetism). All isolates produced dense hyphal aggregations (Fig. 16v). Hyphal swellings or chlamydospores were not observed.

Oogonia, oospores & antheridia (Fig. 16k–u) — All 10 isolates of *P. javanensis* produced in single culture on V8A within 1 wk abundant gametangia which matured within 2–3 wk. Oogonia were borne terminally or laterally, smooth-walled, predominantly with rounded bases (87.6 %; Fig. 16k–m, p) or less frequently with slightly tapering bases (12.4 %; Fig. 16n–o, q–u). On average 25.7 % of oogonia were slightly bending to comma-shaped (Fig. 16s–u). They were predominantly globose to subglobose (83.6 %; Fig. 16k–p) or sometimes elongated (16.4 %; Fig. 16q–u). Oogonial diameters averaged 28.1 ± 4.0 µm with an overall range of 15.6–42.7 µm and a range of isolate means of 27.1–29.2 µm. Oospores contained almost exclusively a single large ooplast and were globose, plerotic to near-plerotic (80.3 %; Fig. 16k–l, n) or less frequently slightly aplerotic (19.7 %; Fig. 16m, o–u) with a mean diameter of 25.0 ± 3.6 µm (total range 13.5–39.4 µm). Oospores had wall diameters of 1.75 ± 0.34 µm and an oospore wall index of 0.36 ± 0.04. Oogonial abortion rate was 16.8 % (8–32 %). The antheridia were predominantly amphigynous unicellular (99.0 %; Fig. 16k–t) or rarely bicellular with the basal cell being considerably smaller (1.0%; Fig. 16u) averaging 12.2 ± 2.2 × 10.1 ± 1.6 µm. Antheridial shapes were cylindrical, ovoid or square.

Colony morphology, growth rates & cardinal temperatures (Fig. 22, 24) — All *P. javanensis* isolates formed on V8A and CA dendroid to stoloniferous colonies with limited aerial mycelium, while colonies on PDA were dense-woolly and uniform (Fig. 22). All ten isolates had a maximum temperature of growth between 27.5 and 30 °C. The lethal temperature was 30 °C for isolates from Java and 32.5 °C for isolates from Sulawesi. At the optimum temperature of 20 °C the average radial growth rate was 3.36 ± 0.55 mm/d (Fig. 24) with the five isolates from Sulawesi showing faster growth (3.81 ± 0.38 mm/d) than the five isolates from Java (2.91 ± 0.14 mm/d). At 20 °C radial growth rates on CA and PDA were 2.97 ± 0.16 mm/d and 1.28 ± 0.06 mm/d, respectively, for the Java isolates, and 3.27 ± 0.11 mm/d and 1.4 ± 0.09 mm/d, respectively, for the Sulawesi isolates.

Additional specimens. Indonesia, Java, Gunung Puntang, Bandung area, isolated from naturally fallen leaves floating in a stream running through a submontane tropical rainforest, Feb. 2019, *T. Jung*, *M. Junaid & N. Nasri*, JV025b, JV191, JV192, JV193; South Sulawesi Province, District of Tana Toraja, isolated from naturally fallen leaves floating in a stream running through a submontane tropical rainforest, May 2019, *T. Jung*, *M. Junaid & N. Nasri* SL081, SL084, SL537, SL538, SL539.

Phytophthora multiglobulosa T. Jung, M. Junaid, M. Horta Jung & I. Milenković, *sp. nov.* — MycoBank MB843003; Fig. 17

Etymology. Name refers to the presence of multiple lipid globules in many oospores.

Typus. Indonesia, South Sulawesi Province, District of North Toraja, isolated from a naturally fallen leaf floating in a stream running through a tropical hill rainforest, May 2019, *T. Jung*, *M. Junaid & N. Nasri* (holotype HNHM-MYC-021539, dried culture on V8A, Herbarium of the Hungarian Natural History Museum, Budapest, Hungary; ex-type culture CBS 148799 = SL005). ITS and *cox1* sequences GenBank ON000763 and ON013829, respectively.

Sporangia, hyphae & chlamydospores (Fig. 17a–h, s) — Sporangia of *P. multiglobulosa* were observed on solid agar and were produced abundantly in non-sterile soil extract after 1–2 d. Sporangia were borne terminally (Fig. 17a–c, f, h) or laterally (Fig. 17d, f, h), often in dense sympodia of 2–5 sporangia (Fig. 17h). Sporangia were papillate with shallow papillae (Fig. 17a–e, h) and caducous (Fig. 17e, g–h) with short to medium-length pedicels averaging 7.7 ± 3.3 µm (Fig. 17a–h). Sporangial shapes were ovoid (57.3 %; Fig. 17a–d, f–h), limoniform (42.0 %; Fig. 17e, h) or infrequently obpyriform (0.7 %). Some sporangia had an inconspicuous basal plug (Fig. 17g–h) and sometimes laterally attached sporangiophores (6.0 %; Fig. 17b–c). Sporangial proliferation was exclusively external (Fig. 17c, f). Sporangial dimensions of three isolates averaged 43.1 ± 6.2 × 27.1 ± 3.0 µm (overall range 28.3–64.9 × 21.1–36.5 µm) with a range of isolate means of 41.1–46.5 × 26.1–28.2 µm. The length/breadth ratio averaged 1.60 ± 0.18 with a range of isolate means of 1.55–1.66. Zoospores of *P. multiglobulosa* were discharged directly through narrow exit pores 2.2–4.8 µm wide (av. 3.6 ± 0.5 µm) (Fig. 17f–h). They were limoniform to reniform whilst motile, becoming spherical (av. diam = 9.2 ± 0.8 µm) on encystment. Cysts germinated directly

Fig. 17 Morphological structures of *Phytophthora multiglobulosa*. a–h. Sporangia with short to medium-length pedicels formed on V8 agar (V8A) flooded with soil extract; a–e. papillate; a. ovoid, terminal; b. ovoid, slightly asymmetric with laterally attached sporangiophore; c. ovoid with laterally attached sporangiophore and external proliferation (arrow); d. ovoid, lateral; e. ovoid to limoniform, caducous; f. ovoid releasing zoospores, with external proliferation; g. ovoid, empty after release of zoospores, with inconspicuous basal plug, caducous; h. dense sympodium with two ovoid papillate sporangia and two empty caducous sporangia (arrows) after release of zoospores, one limoniform (left) and the other one ovoid (right); i–r. mature globose to subglobose oogonia with round non-tapering bases, containing thick-walled plerotic or near-plerotic oospores, formed in single culture in solid V8A; i–j. oogonia with oospores containing a single large ooplast; i. bicellular antheridium with small basal cell (arrow); j–r. unicellular antheridia; k–p. oogonia with oospores containing multiple lipid globules; n–o. slightly leaning oogonia; p. comma-shaped oogonium; q–r. comma-shaped oogonia with oospores containing a single large ooplast; s. dense hyphal aggregation in solid V8A. — Scale bar = 20 µm, applies to a–s.

or indirectly by releasing a secondary zoospore (diplanetism). All isolates formed dense hyphal aggregations (Fig. 17s). Hyphal swellings and chlamydospores were not observed.

Oogonia, oospores & antheridia (Fig. 17i–r) — Gametangia were readily produced in single culture by all isolates of *P. multiglobulosa* on V8A within 1 wk and matured within 2–3 wk. Oogonia were borne terminally or laterally, smooth-walled, globose or infrequently subglobose with round base and thin stalk (Fig. 17i–r). On average 18.7 % of oogonia were comma-shaped (Fig. 17p–r). Oogonial diameters averaged 25.4 ± 3.5 µm (overall range 17.0–38.4 µm and range of isolate means 23.2–25.5 µm). Oospores had a mean diameter of 22.5 ± 3.2 µm (total range 15.0–35.2 µm), were globose, plerotic or near-plerotic (Fig. 17i–r) and contained a single large ooplast (62 %; Fig. 17i–j, q–r) or multiple lipid globules (38 %; Fig. 17k–p). The oospores had walls with a diameter of 1.5 ± 0.23 µm and an oospore wall index of 0.35 ± 0.04. Oogonial abortion rate was low (on. av. 7.3 %; 2–12 %). The antheridia averaged 11.4 ± 2.1 × 9.9 ± 1.4 µm were exclusively amphigynous with mostly cylindrical (Fig. 17i–r), unicellular (Fig. 17j–r) or infrequently bicellular with the basal cell being much smaller (Fig. 17i).

Colony morphology, growth rates & cardinal temperatures (Fig. 22, 24) — *Phytophthora multiglobulosa* formed submerged to appressed colonies with a radiate pattern and irregular margins on V8A and CA, and dense-woolly uniform colonies on PDA (Fig. 22). The temperature-growth relations on V8A are shown in Fig. 24. On V8A the maximum growth temperature was between 27.5 and 30 °C. All isolates failed to resume growth when plates incubated for 5 d at 30 °C were transferred to 20 °C. Average radial growth rates at the optimum of 20 °C on V8A, CA and PDA were 1.91 ± 0.09 mm/d, 1.88 ± 0.08 mm/d and 0.59 ± 0.06 mm/d, respectively.

Additional specimens. Indonesia, South Sulawesi Province, District of North Toraja, isolated from naturally fallen leaves floating in a stream running through a tropical hill rainforest, May 2019, *T. Jung*, *M. Junaid & N. Nasri*, SL006, SL007.

NOTES

Across the 11 259-character alignment of LSU, ITS, *βtub*, *hsp90*, *tigA*, *rpl10*, *tef-1α*, *enl*, *ras-ypt1*, *cox1*, *nadh1* and *rps10* the seven known and 14 new *Phytophthora* species from Clade 10 differed from each other at 36–1 179 positions (Table 3) corresponding to sequence differences of 0.32–10.49 % (Table 4). The seven known Clade 10 species *P. boehmeriae*, *P. gallica*, *P. gondwanensis*, *P. intercalaris*, *P. kernoviae*, *P. morindae* and *P.* taxon boehmeriae-like had 65, 33, 64, 78, 44, 77 and 39 unique polymorphisms, respectively. The 14 new Clade 10 species *P. celebensis*, *P. chilensis*, *P. javanensis*, *P. ludoviciana*, *P. multiglobulosa*, *P. procera*, *P. pseudochilensis*, *P. pseudogallica*, *P. pseudokernoviae*, *P. scandinavica*, *P. subarctica*, *P. tenuimura*, *P. tonkinensis* and *P. ukrainensis* had 28, 11, 15, 56, 8, 73, 23, 82, 20, 100, 53, 46, 125 and 64 unique polymorphisms, respectively. The 14 new Clade 10 species and the known Clade 10 species *P. gallica*, *P. intercalaris*, *P. gondwanensis* and *P. kernoviae* showed distinctive colony morphologies on V8A, CA and PDA at 20 °C (Fig. 20–22). In addition, the 14 new species can be separated from each other and from other Clade 10 species by a combination of morphological and physiological characters of which the most discriminating are highlighted in bold in Table 6–8.

Phytophthora intercalaris differs from all other species in Clade 10 by being heterothallic and in producing ornamented oogonia with a 100 % abortion rate (Yang et al. 2016). The production of chlamydospores discriminates *P. pseudogallica*, informally designated as *P.* taxon gallica-like 1 in Jung et al. (2020), from all other Clade 10 species with nonpapillate sporangia except of *P. intercalaris*, *P. gallica* and *P. afrocarpa* (Jung & Nechwatal 2008, Yang et al. 2016, Bose et al. 2021; Table 6–8). Although *P. pseudogallica* and *P. gallica* are both sterile and produce chlamydospores of similar size they can be easily distinguished by the lower maximum temperature for growth and the much smaller sporangial size and l/b ratio in *P. pseudogallica* and the much higher proportion of obpyriform sporangia in *P. gallica* (Table 6). *Phytophthora pseudogallica* differs from *P. afrocarpa* by having a lower maximum temperature for growth, much bigger chlamydospores, and sporangia with a lower l/b ratio and both nested and extended proliferation (Table 6). Furthermore, *P. pseudogallica* shows on CA at 20 °C the slowest growth of all 18 Clade 10 species tested. The homothallic breeding system of *P. tonkinensis*, informally designated as *P.* taxon gallica-like 2 by Jung et al. (2020), and the production of chlamydospores in *P. pseudogallica* discriminate these co-occurring sister species. Moreover, unlike *P. pseudogallica*, *P. tonkinensis* forms coralloid to irregular hyphal swellings, has a lower maximum temperature for growth and is unable to grow at 25 °C (Table 6–7; Fig. 7, 10, 23). *Phytophthora tonkinensis* differs from *P. scandinavica* by having a lower maximum temperature for growth, much slower growth rates, much smaller sporangia, thinner oospore walls and lower oospore wall index. *Phytophthora scandinavica* co-occurs with the sterile *P. subarctica* and *P. ukrainensis* in boreal streams in Sweden and can be discriminated easily from them by its homothallic breeding system and by having lower maximum and optimum temperatures for growth (Table 6–7; Fig. 8–9, 11, 23). In *P. ukrainensis* the single isolate SW154 from a boreal stream in Sweden shares the same morphological characteristics as the Ukrainian isolates but has lower optimum (30 vs 32.5 °C) and maximum temperatures for growth (30–32.5 vs 32.5–35 °C). *Phytophthora subarctica* and *P. ukrainensis* can be distinguished by the larger sporangial dimensions and l/b ratio in *P. subarctica*, and the production of coralloid to irregular hyphal swellings, and higher maximum and optimum temperatures for growth in *P. ukrainensis*. The North American *P. ludoviciana* and *P. procera* differ from *P. subarctica* and *P. ukrainensis* by having undulating hyphal growth. In addition, *P. subarctica* and the Ukrainian isolates of *P. ukrainensis* have higher maximum temperatures for growth. Furthermore, *P. procera* has larger sporangia with much higher l/b ratio. *Phytophthora tenuimura* is discriminated from *P. subarctica* and *P. ukrainensis* by having undulating hyphal growth and a homothallic breeding system (Table 6–7; Fig. 4–7, 9, 11, 23). *Phytophthora ludoviciana*, *P. procera* and *P. tenuimura* co-occur in a swamp forest in Louisiana. While *P. tenuimura* can easily be distinguished from the other two sterile species by being homothallic and having a lower maximum temperature for growth, *P. procera* differs from *P. ludoviciana* in producing much larger sporangia with much higher l/b ratio and by its lower optimum temperature for growth (Table 6; Fig. 4–7, 23).

In Subclade 10c, the four known species *P. boehmeriae*, *P. morindae*, *P. gondwanensis* and *P. kernoviae* and the six new species *P. chilensis*, *P. pseudochilensis*, *P. pseudokernoviae*, *P. celebensis*, *P. javanensis* and *P. multiglobulosa* all share a homothallic breeding system and the production of caducous papillate sporangia enabling an aerial lifestyle. *Phytophthora morindae* differs from the other nine papillate Clade 10 species by the production of sporangia with the highest l/b ratio and the longest pedicels which are often formed in umbellate sympodia (Nelson & Abad 2010; Table 7–8). For *P. boehmeriae* most published morphological and physiological information dates from pre-molecular times and, thus, it cannot be excluded that they might partly have come from other Clade 10 species. For instance, isolates from brown rot of orange fruits in Argentina, originally assigned to *P. boehmeriae* (Frezzi 1941, 1950, Erwin &

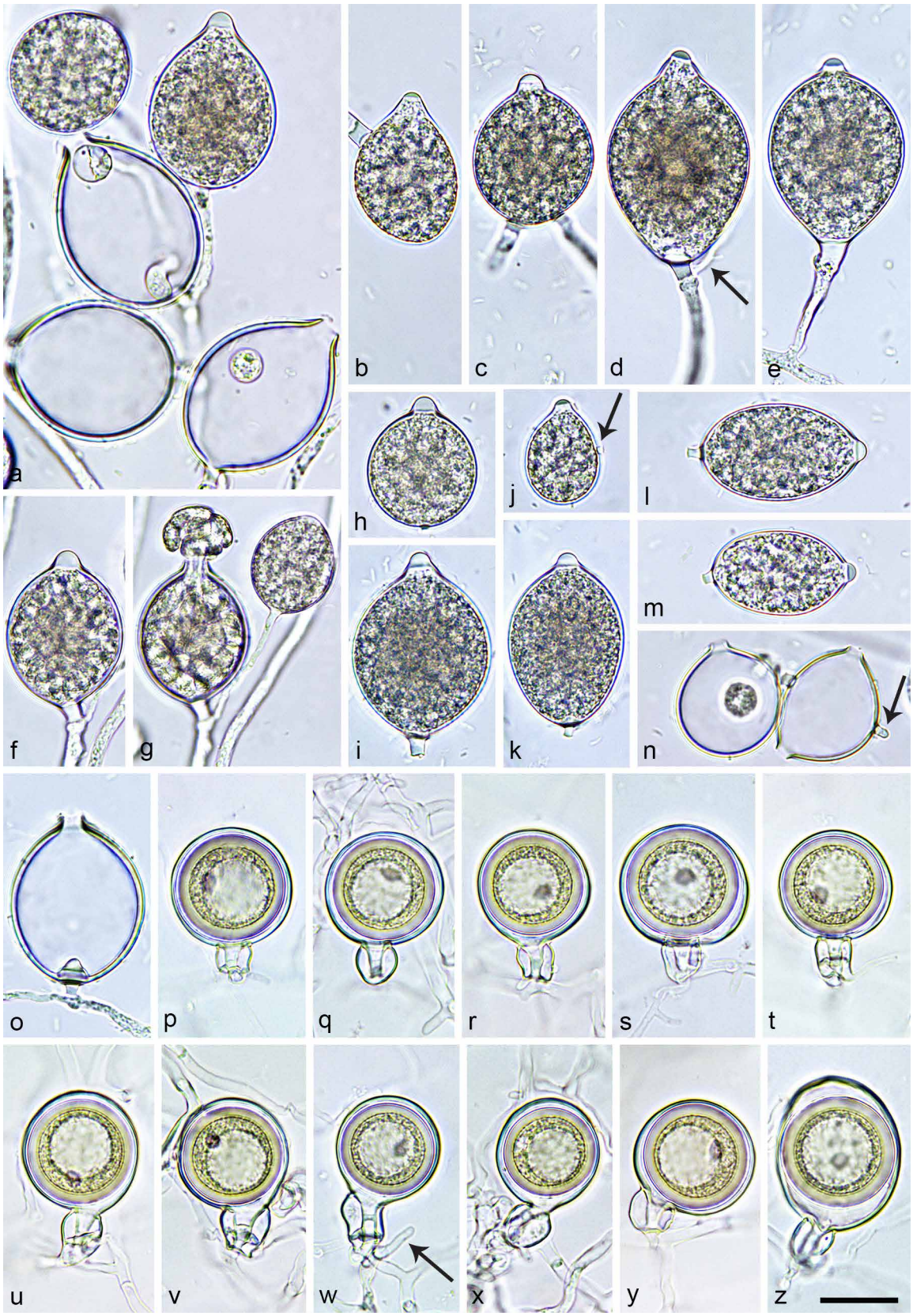

Fig. 18 Morphological structures of *Phytophthora gondwanensis*. a–o. Sporangia with short pedicels formed on V8 agar (V8A) flooded with soil extract; a. dense sympodium with an immature sporangium (top), a mature, ovoid sporangium with prominent papilla and three ovoid empty sporangia without basal plugs after release of zoospores; b–m. papillate sporangia; b. ovoid with laterally attached sporangiophore; c. subglobose, intercalary; d. limoniform, terminal with external proliferation (arrow); e. broad-pyriform, lateral; f–g. ovoid releasing zoospores, with external proliferation; h–n. caducous; h. globose with very short pedicel; i. broad-ovoid; j. ovoid with laterally attached very short pedicel (arrow); k. broad-ellipsoid; l. elongated-ovoid to ellipsoid; m. ellipsoid; n. empty caducous sporangia after zoospore release, one globose to subglobose, the other one limoniform, formerly bipapillate with two exit pores and short hyphal projection (arrow); o. ovoid, empty lateral sporangium after zoospore release, with conspicuous protruding basal plug; p–z. mature smooth-walled oogonia with thick-walled globose oospores containing large ooplasts, and amphigynous antheridia, formed in single culture in solid V8A; p–t. globose to subglobose oogonia with round non-tapering bases and near-plerotic to plerotic oospores; p–s. unicellular antheridia; t. bicellular antheridium; u–w. slightly leaning to comma-shaped oogonia with short tapering bases, near-plerotic to plerotic oospores and bicellular antheridia; w. antheridium with finger-like projection (arrow); x. comma-shaped oogonium with slightly aplerotic oospore and unicellular antheridium; y. comma-shaped oogonium with plerotic oospore and unicellular antheridium; z. elongated oogonium with aplerotic oospore and unicellular antheridium. — Scale bar = 20 µm, applies to a–z.

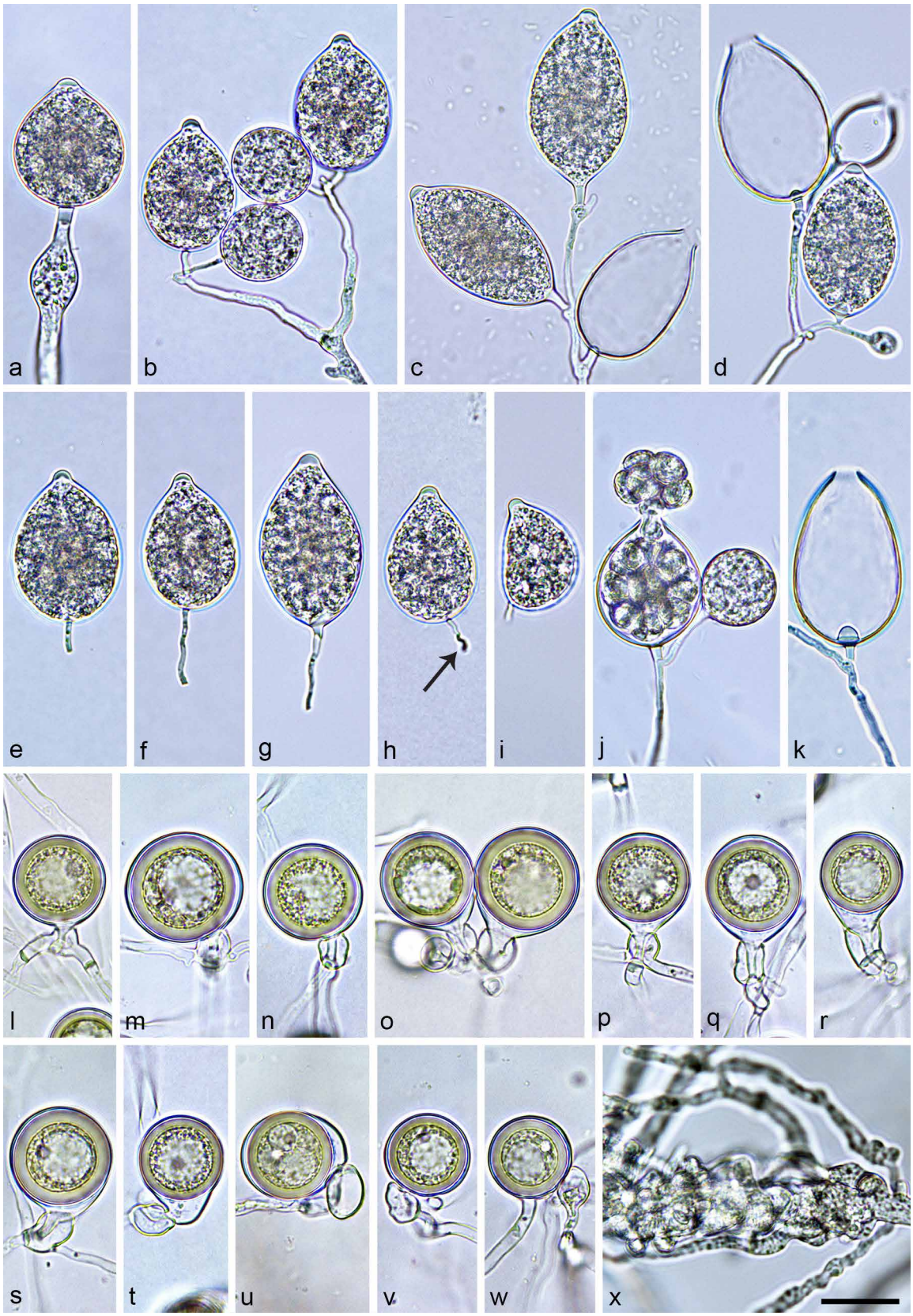

Fig. 19 Morphological structures of *Phytophthora kernoviae*. a–k. Sporangia with pedicels of variable length formed on V8 agar (V8A) flooded with soil extract; a. broad-ovoid, terminal with short pedicel and a sporangiophore swelling; b. two sympodia, each with one immature and one ovoid papillate sporangium; c. sympodium with a limoniform papillate sporangium (left), an ovoid papillate sporangium (top) and an ovoid empty sporangium after zoospore release, with inconspicuous basal plug; d. sympodium with an immature growing sporangium and three ovoid sporangia, one of them papillate and two empty after release of their zoospores; e–i. papillate caducous sporangia; e. ovoid with medium-length pedicel; f. ovoid with long pedicel; g. elongated-ovoid with long pedicel; h. ovoid with laterally attached, medium-length undulating (arrow) pedicel; i. asymmetric mouse-shaped with short pedicel; j. ovoid, releasing zoospores, with external proliferation; k. elongated-ovoid lateral, empty after zoospore release with conspicuous protruding basal plug; l–w. mature smooth-walled oogonia formed in solid V8A, with plerotic oospores containing large ooplasts; l–q. with amphigynous unicellular antheridia; l. globose with round non-tapering base; m–n. globose, slightly leaning, with round non-tapering bases; o–q. globose to subglobose with tapering bases; r. slightly elongated with tapering funnel-like base and amphigynous bicellular antheridium; s–u. comma-shaped with amphigynous unicellular antheridia; t. with tapering base; u. with multiple lipid globules; v–w. globose oogonia with paragynous antheridia; x. lateral hyphae entangling the primary hypha forming an aggregation, in solid V8A. — Scale bar = 20 µm, applies to a–x.

Ribeiro 1996), were recently demonstrated by multigene phylogenetic analysis to belong to an unknown taxon closely related to *P. boehmeriae* and, hence, re-designated as *P.* taxon boehmeriae-like (Yang et al. 2017). Also, multiple isolates from Australia, China, Brazil and South Africa originally identified as *P. boehmeriae* were re-assigned to *P. gondwanensis* confirming Burgess et al. (2021). Therefore, only morphological and physiological data published for the ex-type isolate from Taiwan (Tucker 1931) and for *P. boehmeriae* isolates from chili pepper in India (Chowdappa et al. 2014) can be used for comparisons. The sister species *P. boehmeriae* and *P.* taxon boehmeriae-like are morphologically similar. The ex-type isolate of *P. boehmeriae* differs from *P.* taxon boehmeriae-like mainly by the on average larger chlamydospores (41.2 vs 29.5 µm) and sporangia (51.8 × 40.1 vs 42 × 34 µm) (Tucker 1931, Frezzi 1950, Erwin & Ribeiro 1996). However, the sporangia of 43 Indian isolates of *P. boehmeriae* were on average considerably smaller (35.3 × 20.5 µm) than sporangia of the ex-type isolate and those of *P.* taxon boehmeriae-like. The closely related *P.* taxon koreanensis from *Ailanthus altissima* in Korea (isolate KACC40173) had sporangia of similar size as *P.* taxon boehmeriae-like (44 × 32.7 µm; Kim & Kim 2004). Therefore, the true morphometric differences between the three sister species remain unclear. *Phytophthora boehmeriae* differs clearly from all other papillate Clade 10 species, except *P.* taxon boehmeriae-like, by producing chlamydospores and growing faster between 20 and 25 °C, and, in addition, from *P. morindae*, *P. kernoviae*, *P. celebensis*, *P. javanensis* and *P. multiglobulosa* by having shorter pedicels (Tucker 1931, Chowdappa et al. 2014; Table 7–8). In addition, the occurrence of bipapillate sporangia discriminates *P. boehmeriae* from the four species of the *P. kernoviae* complex and from *P. celebensis* and *P. multiglobulosa*. *Phytophthora* taxon boehmeriae-like differs from all other papillate Clade 10 species, except *P. boehmeriae*, by the production of chlamydospores (Frezzi 1950, Erwin & Ribeiro 1996).

For *P. gondwanensis* morphology and optimum temperature for growth of the isolates from the Japanese Amami island examined in the present study (Fig. 18, 24) were in accordance with the original description from New South Wales (Crous et al. 2015), except that in the Japanese isolates the sporangia were on average longer (44.7 ± 3.9 vs 39.3 ± 5.2 µm) and showed a higher l/b ratio (1.6 vs 1.2). For *P. kernoviae* the morphology and cardinal temperatures of the isolates from Chile and Ireland examined in the present study (Fig. 19, 24) were in accordance with the original species description from the UK (Brasier et al. 2005) apart from the slightly lower maximum temperature for growth (< 25 vs 26 °C), the thinner oospore walls (c. 2.0 vs 3.5 µm) and the infrequent occurrence of some paragynous antheridia in all Chilean and Irish isolates. The Chilean isolates had on average larger sporangia and oogonia and showed slightly slower growth than the Irish isolates (Table 8). *Phytophthora kernoviae* can be discriminated from its co-occurring sister species *P. chilensis*, *P. pseudochilensis* and *P. pseudokernoviae* by the occurrence of asymmetric mouse-shaped sporangia and by having longer sporangial pedicels and much smaller proportions of oogonia with tapering bases. Moreover, *P. kernoviae* differs from *P. chilensis* by its almost exclusive production of plerotic oospores with higher abortion rates and by producing besides amphigynous also a few paragynous antheridia; from *P. pseudochilensis* by having smaller sporangia with lower l/b ratio, higher oospore wall index, lower oospore abortion rate and higher optimum temperature for growth; and from *P. pseudokernoviae* by having on average smaller oogonia with higher oospore abortion rate, more variable sporangial shapes, and lower maximum and higher optimum temperatures for growth (Table 8; Fig. 12–14, 19, 24). *Phytophthora pseudochilensis* is distinguished from both *P. chilensis* and *P. pseudokernoviae* by having on average larger sporangia with less prominent papillae and higher l/b ratio, larger sympodia containing higher numbers of sporangia, oospores with thinner walls, lower oospore wall index and much higher abortion rates, and slower growth. Compared to *P. chilensis*, both *P. pseudochilensis* and *P. pseudokernoviae* have much higher proportions of oogonia with tapering bases and lower optimum temperatures for growth. In addition, *P. pseudokernoviae* differs from both *P. chilensis* and *P. pseudochilensis* by its larger oogonia which are more frequently comma-shaped, the occurrence of paragynous antheridia and a higher optimum temperature for growth (Table 8; Fig. 12–14, 24). Collectively, *P. chilensis*, *P. pseudochilensis* and *P. pseudokernoviae* are discriminated from *P. gondwanensis* by having higher proportions of plerotic oospores, much lower proportions of elongated or excentric oogonia, much lower optimum and maximum temperatures for growth and slower growth rates at 20 °C and above (Table 7–8; Fig. 12–14, 18, 24).

The three Clade 10c species from tropical rainforests in Indonesia, *P. celebensis*, *P. javanensis* and *P. multiglobulosa*, differ from the four species of the *P. kernoviae* complex from temperate Valdivian rainforests by their higher maximum temperatures for growth (Table 8; Fig. 24). Further, they have on average longer sporangial pedicels than *P. chilensis*, *P. pseudochilensis* and *P. pseudokernoviae* and higher optimum temperatures for growth than *P. pseudochilensis* and *P. pseudokernoviae* (Table 8; Fig. 12–17, 19, 24). *Phytophthora celebensis*, *P. javanensis* and *P. multiglobulosa* are distinguished from the subtropical *P. gondwanensis* by their lower maximum and optimum temperatures for growth and much slower growth above 20 °C (Table 7–8; Fig. 24). *Phytophthora javanensis* isolates from Java and Sulawesi share the same morphological characters and cardinal temperatures but isolates from Sulawesi show faster growth between 10 and 25 °C (Fig. 24). *Phytophthora javanensis* differs from both *P. celebensis* and *P. multiglobulosa* by the occurrence of aplerotic oospores and bipapillate sporangia, and by having on average larger oogonia and faster growth at 20 °C. In addition, *P. celebensis* is discriminated from both *P. javanensis* and *P. multiglobulosa* by its higher optimum temperature for growth and by having on average slightly longer pedicels, whereas *P. multiglobulosa* is distinguished from *P. celebensis* and *P. javanensis* by its larger sporangia and considerably slower growth rates between 10 and 27.5 °C (Table 8; Fig. 15–17, 24).

DISCUSSION

During extensive surveys of *Phytophthora* diversity performed between 2011 and 2019 three described and 14 previously unknown *Phytophthora* species from phylogenetic Clade 10 were isolated from natural or semi-natural forests and rivers in Chile, Croatia, Czech Republic, Indonesia, Ireland, Japan, Louisiana, Serbia, Sweden, Ukraine and Vietnam. Based on differences in morphology of asexual and sexual structures, colony morphology, temperature-growth relations and multigene phylogenetic analyses of sequence data from nine nuclear and three mitochondrial gene loci, the 14 new *Phytophthora* species are described here as *P. celebensis*, *P. chilensis*, *P. javanensis*, *P. ludoviciana*, *P. multiglobulosa*, *P. procera*, *P. pseudochilensis*, *P. pseudogallica*, *P. pseudokernoviae*, *P. scandinavica*, *P. subarctica*, *P. tenuimura*, *P. tonkinensis* and *P. ukrainensis*. This triples the number of known extant species in Clade 10.

These new species were recovered from forest streams (*P. celebensis*, *P. chilensis*, *P. javanensis*, *P. multiglobulosa*, *P. pseudochilensis*, *P. pseudogallica*, *P. subarctica*, *P. tonkinensis* and *P. ukrainensis*); an inundated swamp forest (*P. ludoviciana*, *P. procera* and *P. tenuimura*); or the riverbank of a forest stream (*P. scandinavica*). Their hosts are largely unknown and no visi-

bly acute disease symptoms were observed at the sample locations, suggesting host-pathogen equilibrium resulting from long-term co-evolution. The exception was the aerial pathogen *P. pseudokernoviae*, which was isolated from necrotic lesions on both attached mature and freshly fallen, senescent *Drimys winteri* leaves in late spring/early summer. This is the period when the leaf area in the Chilean Valdivian rainforest stands reaches its annual maximum due to the co-occurrence of old and freshly emerged foliage (Adami et al. 2018). The optimum growth temperature of *P. pseudokernoviae* is 15 °C, close to the average long term Valdivian temperatures during November and December of c. 13–16 °C. This suggests ecological adaptation of this aerial pathogen to the specific conditions of this ecosystem, with the *D. winteri* leaf lesions being annual seasonal infections. A similar seasonality on senescent foliage has been proposed for the airborne wide-host range pathogen *P. ramorum* in its native habitat in the East Asian laurosilva forests (Jung et al. 2021). Interestingly, Sanfuentes et al. (2016) isolated *P. kernoviae* from *D. winteri* leaf litter in a Valdivian rainforest in May 2012, the beginning of the winter season. Whether host stress resulting from *P. pseudokernoviae*- and *P. kernoviae*- induced leaf infections exacerbate the forest dieback and mortality caused by the introduced *P. cinnamomi* (lineage PcG2-A2; Jung et al. 2018a, Shakya et al. 2021) or *vice versa* requires investigation. The apparent co-evolution of the 14 new Clade 10 species with their associated flora and the fact that no similar DNA sequence data from other regions of the world has been submitted to GenBank suggest that they are native inhabitants of their respective habitats.

Our surveys provide further insights into the global biogeography of Clade 10. It occurs naturally in all continents other than Antarctica, but most species appear to have rather limited distri-

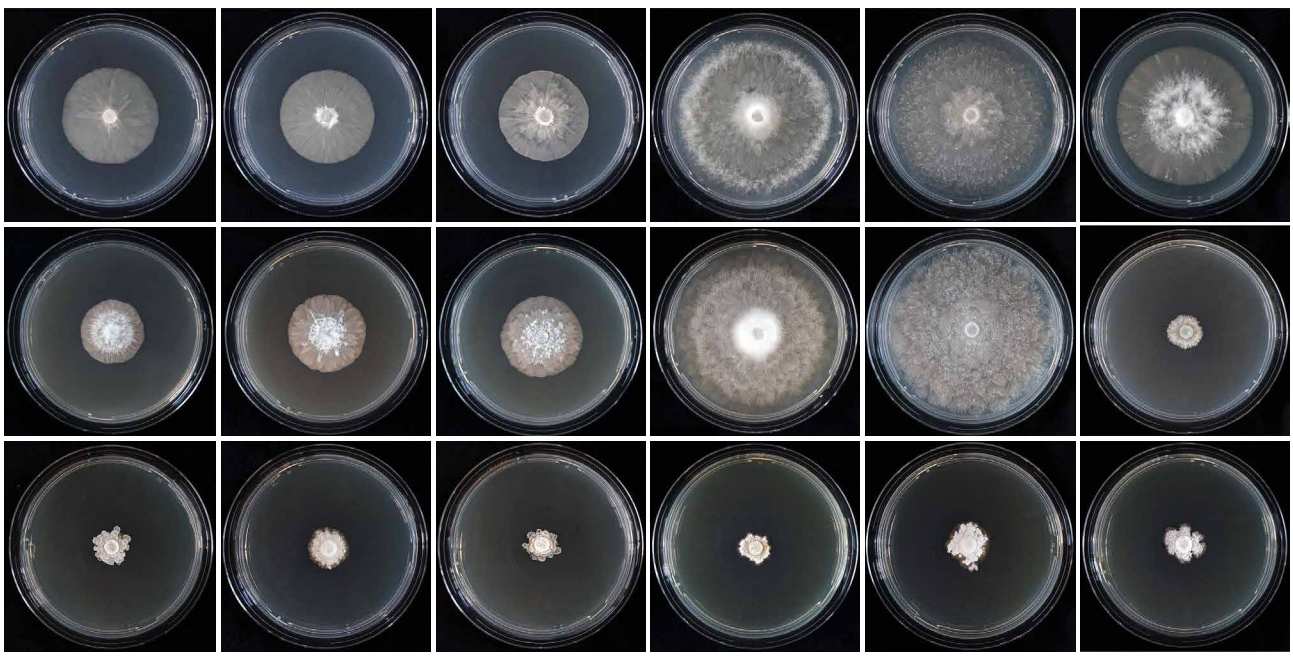

Fig. 20 Colony morphology of *Phytophthora ludoviciana*, *P. procera*, *P. tenuimura*, *P. gallica*, *P. intercalaris* and *P. pseudogallica* after 14 d growth (from left to right) at 20 °C on V8 agar, carrot juice agar and potato-dextrose agar (from top to bottom).

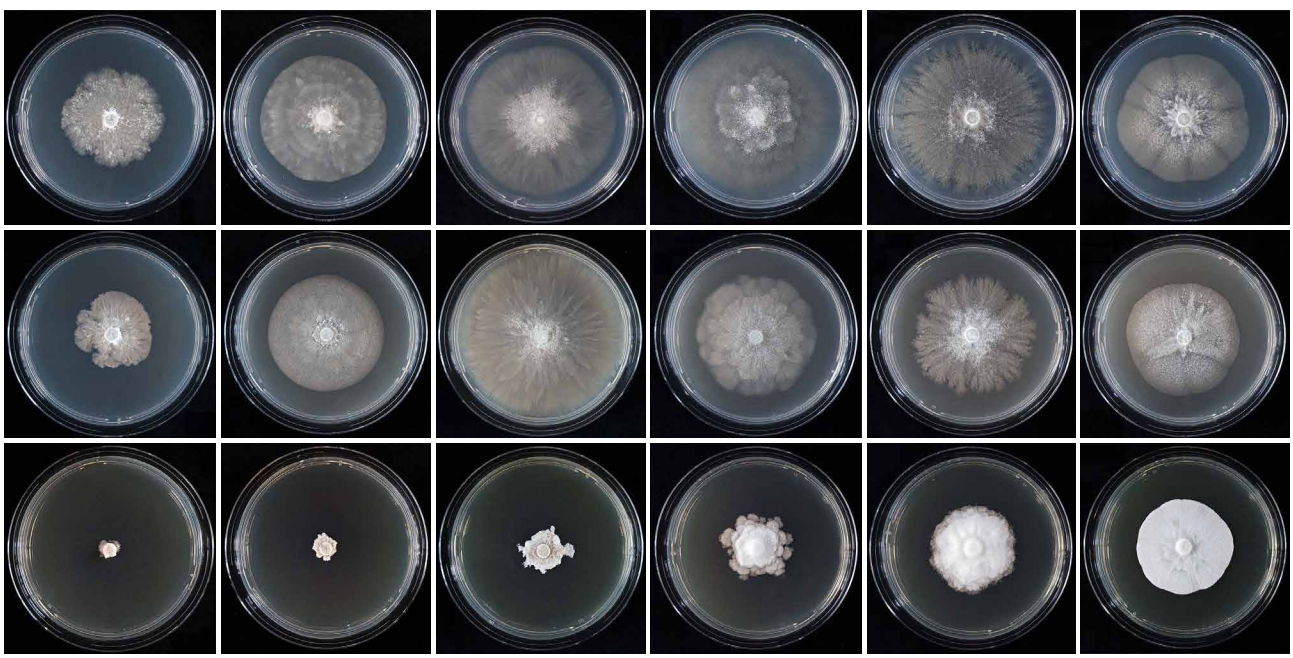

Fig. 21 Colony morphology of *Phytophthora tonkinensis*, *P. subarctica* and *P. ukrainensis* after 14 d growth, and of *P. scandinavica*, *P. gondwanensis* and *P. kernoviae* after 10 d growth (from left to right) at 20 °C on V8 agar, carrot juice agar and potato-dextrose agar (from top to bottom).

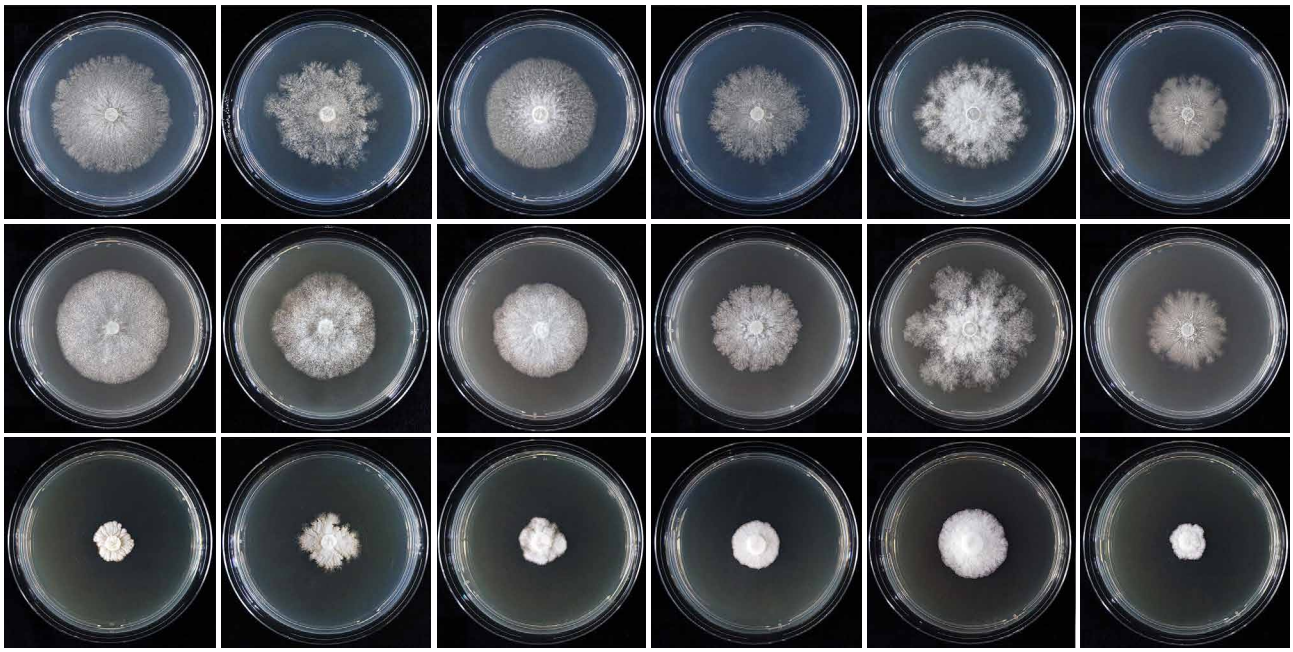

Fig. 22 Colony morphology of *Phytophthora chilensis*, *P. pseudochilensis*, *P. pseudokernoviae*, *P. celebensis*, *P. javanensis* and *P. multiglobulosa* after 10 d growth (from left to right) at 20 °C on V8 agar, carrot juice agar and potato-dextrose agar (from top to bottom).

butions and across large areas Clade 10 appears to be absent. Equally, there are several notable Clade 10 hotspots. These are the Valdivian rainforests, where the four airborne species from the *P. kernoviae* complex co-occur; the inundated swamp forest in Louisiana inhabited by *P. ludoviciana*, *P. procera* and *P. tenuimura*; boreal streams in northern Sweden hosting *P. scandinavica*, *P. subarctica* and *P. ukrainensis*; streams in montane cloud forests in northern Vietnam with co-occurrence of *P. pseudogallica* and *P. tonkinensis*; and Sulawesi where the airborne species *P. celebensis*, *P. javanensis* and *P. multiglobulosa* occur in tropical hill and submontane rainforests. Another hotspot may be the afrotemperate forests of the Western and Eastern Cape regions in South Africa, where the previously unknown *P. afrocarpa* and *P.* taxon canthium were found (Oh et al. 2013, Bose et al. 2021).

In contrast, in most temperate regions of Europe, with the exception of the British Isles where the introduced *P. kernoviae* is present, and Ukraine where we found *P. ukrainensis*, *P. gallica* is currently the only recorded Clade 10 species (Jung et al. 1996, 2000, Hansen & Delatour 1999, Jönsson et al. 2003, Jung & Blaschke 2004, Jung 2009, O'Hanlon et al. 2016, Milenković et al. 2018, Redondo et al. 2018a, b, Corcobado et al. 2020, Matsiakh et al. 2020, this study). In temperate regions of the Eastern USA *P. intercalaris*, the undescribed but closely related *P.* taxon Maryland 6, and *P. gallica* have been recovered infrequently from streams and irrigation reservoirs in several states but in forest soils no Clade 10 species have been detected (Balci et al. 2007, Shrestha et al. 2013, Jones et al. 2014, Yang et al. 2016). In early surveys of temperate Western North America no Clade 10 species were obtained (Reeser et al. 2011, Hansen et al. 2012a), but more recently *P. gallica* has been isolated, though only sporadically, from rhizosphere soil and water around riparian *Alnus* trees (Sims et al. 2015).

In China, *P.* taxon gallica-like 3 was recently found in the cold-temperate north eastern region, whereas in the temperate far western Tian Shan mountains in Xinjiang and in the mountains of Yunnan in the south west no Clade 10 species were recovered (Huai et al. 2013, Xu et al. 2019). Other regions apparently also devoid of Clade 10 species are: the temperate regions of eastern Australia (Burgess et al. 2017, Kaliq et al. 2019); the Mediterranean regions of Europe (Vettraino et al. 2002, 2005, Balci & Halmschlager 2003, Català et al. 2015, Scanu et al. 2015, Jung et al. 2019, Seddaiu et al. 2020); the southwestern USA (Hansen et al. 2012a, Stamler et al. 2016, Frankel et al. 2020); Western Australia (Hüberli et al. 2013, Burgess et al. 2017) with the exception of sporadic isolation of *P. gondwanensis* (Burgess et al. 2021); and the tropical and subtropical lowland rainforests and monsoon forests in Taiwan (Jung et al. 2017a), Vietnam (Jung et al. 2020), Hainan (Zeng et al. 2009), Borneo and Sumatra (T. Jung, A. Durán & M. Junaid, unpublished results), Guyana (Legeay et al. 2020) and Central America and Peru (T. Jung, Y. Balci & K. Broders, unpublished results).

The evolutionary history of Clade 10 is characterised by an early, two-step divergence into three subclades (Fig. 2, 3) with considerable differences in phenotype, lifestyle and current distribution. The earliest diverged Subclade 10a comprises the aquatic *P. ludoviciana*-*P. procera*-*P. tenuimura* cluster from Louisiana. In being genetically distant by 8.5–10.6 % from all other Clade 10 species across the alignment, and in having persistent nonpapillate often elongated sporangia and undulating *Pythium*-like hyphae, these three species were very distinct. Subclade 10b comprises eight soil- or waterborne species with persistent nonpapillate sporangia that are either sexually sterile, have a homothallic breeding system, or in just one case (*P. intercalaris*) a heterothallic breeding system. Subclade 10b also includes two undescribed taxa with unknown biological properties, *P.* taxon Maryland 6 from Maryland, and *P.* taxon gallica-like 3 from North-eastern China. Subclade 10b has a Laurasian and mostly Holarctic distribution with three notable exceptions: *P. pseudogallica* and *P. tonkinensis*, which co-occur in a forest stream at 2 000 m altitude on Fansipan mountain in northern Vietnam, and technically fall within the Oriental biogeographic realm though adjacent to the Holarctic zone; and *P. afrocarpa* in Western Cape Province (Bose et al. 2021), the southernmost Afrotropical biogeographic region.

In contrast, Subclade 10c comprises ten aerial papillate species with homothallic breeding systems; together with the informally designated *P.* taxon boehmeriae-like which is also papillate aerial and homothallic and *P.* taxon canthium with unknown biological properties. Subclade 10c shows a disjunct Gondwanan and circum-Pacific distribution with *P. chilensis*, *P. kernoviae*,

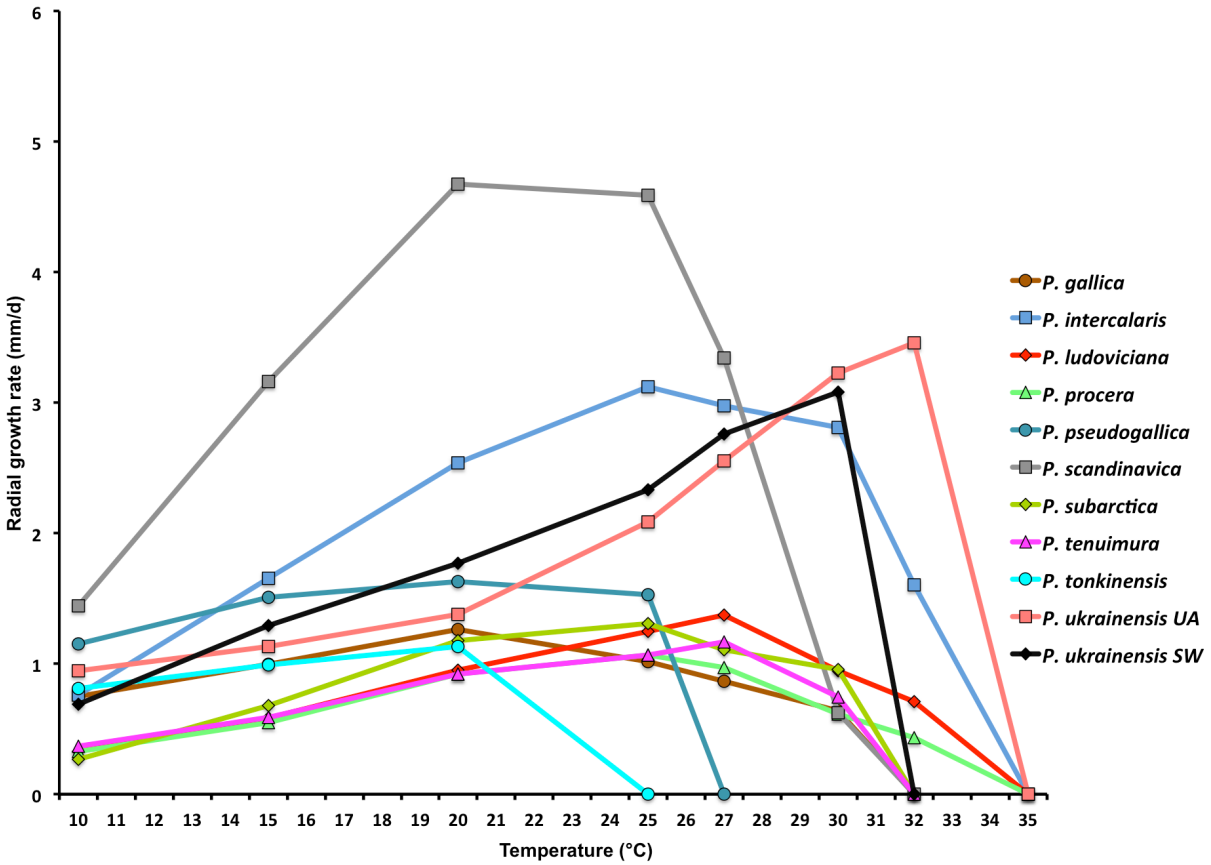

Fig. 23 Mean radial growth rates of two known and eight new *Phytophthora* species from Subclades 10a, i.e., *P. ludoviciana* (2 isolates), *P. procera* (4 isolates) and *P. tenuimura* (7 isolates), and 10b, i.e., *P. gallica* (3 isolates), *P. intercalaris* (1 isolate), *P. pseudogallica* (4 isolates), *P. scandinavica* (5 isolates), *P. subarctica* (4 isolates), *P. tonkinensis* (5 isolates) and *P. ukrainensis* (4 isolates), on V8 agar at different temperatures.

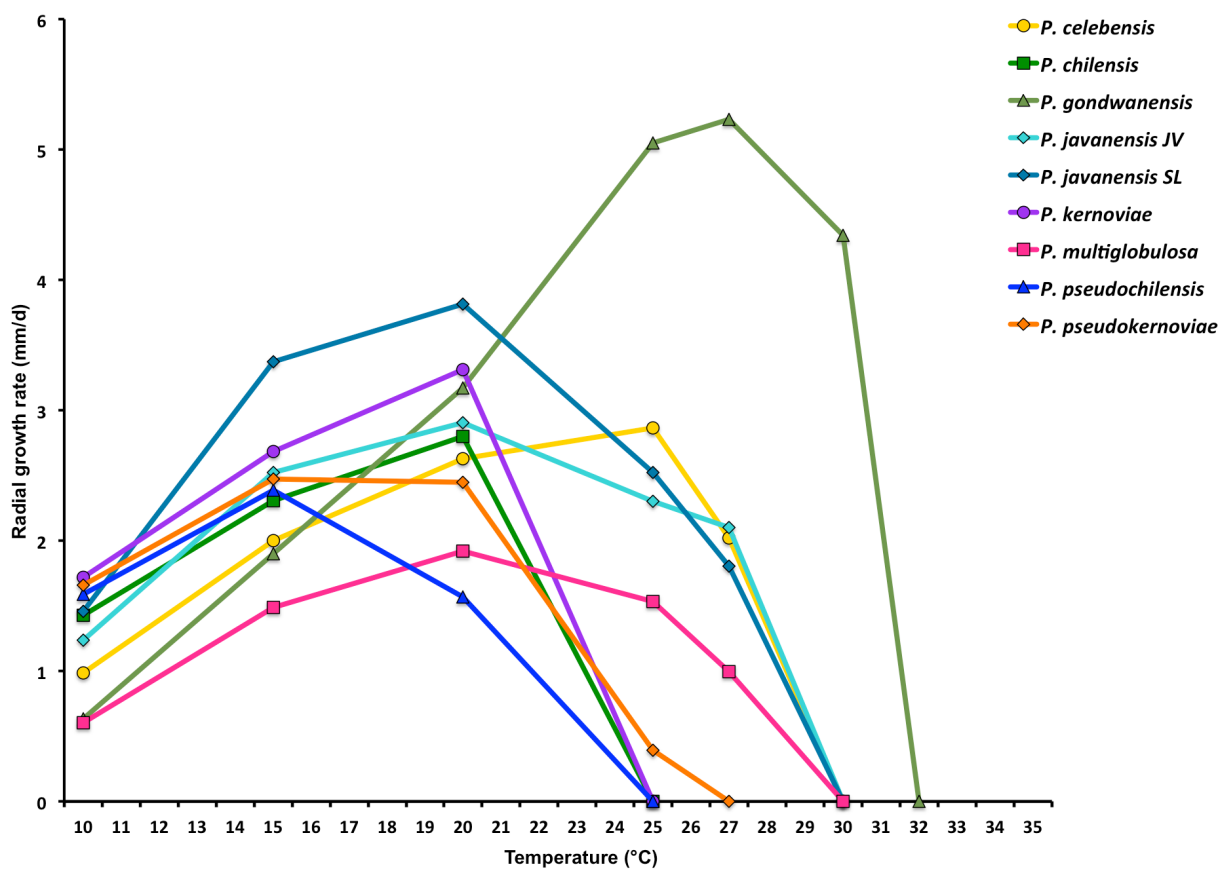

Fig. 24 Mean radial growth rates of two known and six new *Phytophthora* species from Subclade 10c, i.e., *P. celebensis* (5 isolates), *P. chilensis* (6 isolates), *P. gondwanensis* (5 isolates), *P. javanensis* (5 isolates from Java, 5 isolates from Sulawesi), *P. kernoviae* (8 isolates), *P. multiglobulosa* (3 isolates), *P. pseudochilensis* (6 isolates) and *P. pseudokernoviae* (3 isolates), on V8 agar at different temperatures.

P. pseudochilensis and *P. pseudokernoviae* occurring in the Valdivian region (Sanfuentes et al. 2016, Jung et al. 2018a, this study); *P. kernoviae* in New Zealand (Ramsfield et al. 2009, Scott & Williams 2014); *P. morindae* in Hawaii (Nelson & Abad 2010); *P. boehmeriae* in China, India and Taiwan (Tucker 1931, Erwin & Ribeiro 1996, Chowdappa et al. 2014, Burgess et al. 2021); *P.* taxon boehmeriae-like in Argentina (Frezzi 1941, 1950, Yang et al. 2017); *P.* taxon boehmeriae-like 2 in China; *P.* taxon koreanensis in Korea (previously assigned to *P. boehmeriae*; Kim & Kim 2004); *P. gondwanensis* across Australia, in Brazil, South Africa and Papua New Guinea (Shaw 1984, Dos Santos et al. 2006, Maseko et al. 2007, Crous et al. 2015, Burgess et al. 2021) and the Japanese Amami island (this study); *P. celebensis*, *P. javanensis* and *P. multiglobulosa* in Indonesia (this study); and *P.* taxon canthium in the Eastern Cape Province of South Africa (Oh et al. 2013). The only current exception is the introduced *P. kernoviae* in the UK and Ireland (Brasier et al. 2005, O'Hanlon et al. 2016). Since *P. gondwanensis* appears to be native to Australasia it has most likely been introduced to Brazil and South Africa on infested nursery stock of the Australian tree species *Acacia mearnsii* and *Eucalyptus smithii*, respectively.

Regarding the emergence of the three ecologically and phenotypically different Clade 10 subclades we suggest early exposure of a Gondwanan or pre-Gondwanan (> 175 Myr) ancestor to contrasting ecological niches may have resulted in its adaptive sympatric radiation into two largely soil and water inhabiting lineages (Subclades 10a, 10b) and one largely aerial lineage (Subclade 10c). Speciation events within the subclades are likely to reflect many processes during their subsequent range expansions, in particular allopatric, non-adaptive radiations via genetic drift as a result of geographic isolation of populations following migration across geographic barriers, the eruption of new geographic barriers including the separation of islands, and gradual macroclimatic changes (Brasier 1986, Kozak et al. 2006, Rundell & Price 2009); and further adaptive sympatric radiation following exposure to new vegetation types, hosts, microclimates, soil types and microbiomes (Mayr 1942, Brasier 1986, Givnish 1997, 2015, Rundell & Price 2009, Jung et al. 2017a).

Some clues to the possible occurrence of allopatric and sympatric speciation events may be found in the properties of the 25 known Clade 10 taxa, although evidence is patchy due to both extinctions and the limitations of current sampling procedures. For example, the apparent sympatry of the closely related aerial sibling species *P. chilensis*, *P. kernoviae*, *P. pseudochilensis* and *P. pseudokernoviae* in the Valdivian rainforests is consistent with their adaptive radiation from a common ancestor. While the differences between the optimum growth temperatures of *P. chilensis* and *P. kernoviae* (c. 20 °C) and *P. pseudochilensis* and *P. pseudokernoviae* (c. 15 °C) could reflect adaptation to different seasons, or to different layers of the forest ecosystem. Studies of their host ranges, tissue preferences and seasonal and diurnal activities may clarify the selective drivers involved.

Further, the Valdivian rainforests are considered a Gondwana relic, sometimes referred to as a 'tropical rainforest in a non-tropical climate' and a 'biogeographic island' (Hueck 1966, Armesto et al. 1995, Seibert 1996, Tecklin et al. 2011). They are floristically related to temperate rainforests in New Zealand, Tasmania, New Guinea and New Caledonia, but have been isolated by the Pacific Ocean to the west and semi-arid environments to the north and east for many millions of years. This raises the intriguing question whether the ancestor of the *P. kernoviae* sibling cluster was also an endemic Gondwana relic, or whether it migrated from Eurasia. Thus land-bridges existed in Beringia continuously until the early Pliocene c. 5.3 Mya (Gladenkov et al. 2002) and intermittently during the Pleistocene (Vila et al. 2011, Elias & Brigham-Grette 2013); the North Atlantic until the early Oligocene c. 30 Mya (McKenna 1983, Tiffney 1985, Davis et al. 2002); and the Isthmus of Panama, which formed c. 4 Mya. Migrations and interchange between Eurasia and North America are responsible for the striking floristic similarity of East Asia and both western and eastern North America (Wen 1999, Qian 2002, Lang et al. 2007, Wen et al. 2010, 2016, Baskin & Baskin 2016) and the circum-Pacific or Holarctic distributions of numerous animal (Morley 2003, Sharma & Giribet 2012, Van Damme & Sinev 2013, Toussaint et al. 2017, Kim et al. 2018) and plant families and genera including the *Fagaceae* genera *Castanea*, *Fagus* and *Quercus* (Denk & Grimm 2009, Hubert et al. 2014). The possibility that some *Phytophthora* species may have spread over these land-bridges is supported by the endemic and benign occurrence of *P. uniformis* in Alaska and the Pacific Northwest: the only known native record of the otherwise exclusively Eurasian Clade 7a in North America (Adams et al. 2010, Aguayo et al. 2013, Jung et al. 2017b, c). To date, however, no native *Phytophthora* Clade 10c species has yet been found either in North America or in Europe. This despite numerous surveys and despite temperate humid conditions in both the Pacific Northwest rainforests and in the British Isles, comparable to the Valdivian rainforests and ideal for the development of aerial *Phytophthora* tree pathogens (Rizzo et al. 2002, Brasier & Webber 2010, Hansen et al. 2012a, Reeser et al. 2013, O'Hanlon et al. 2016, Scanu & Webber 2016, Pérez-Sierra et al. 2022). Apart from the introduced *P. gondwanensis* in Brazil (Dos Santos et al. 2006), tropical regions across Central and South America also appear to be devoid of Clade 10c species (Legeay et al. 2020, T. Jung, Y. Balci & K. Broders unpubl. data). There are, therefore, strong arguments against immigration of the *P. kernoviae* complex or its ancestor from Eurasia.

More probably the *P. kernoviae* complex evolved from a Gondwanan ancestor in the Valdivian rainforests or in the wider temperate southern region of South America. This is further supported by the widespread, symptomless distribution of *P. kernoviae* in natural *Austrocedrus chilensis* forests in Patagonia, Argentina (Vélez et al. 2020) and the occurrence of the related *P.* taxon boehmeriae-like in orange plantations in Argentina (Frezzi 1941, 1950, Yang et al. 2017). However, *P. kernoviae* is also widespread in natural forests and *Pinus radiata* plantations in New Zealand, where it causes only mild disease symptoms (Ramsfield et al. 2009, Scott & Williams 2014). In a phylogenetic analysis of *P. kernoviae* isolates from New Zealand, Chile and the UK Studholme et al. (2019) concluded that the UK population originated from New Zealand; that the Chilean and New Zealand populations were most likely derived from a pan-Gondwanan population; and that two of the Chilean isolates were an unknown species, shown here to belong to *P. pseudokernoviae*. Since it is highly unlikely that the radiation of the *P. kernoviae* complex pre-dates the break-up of Gondwana 140 Mya, Chile and New Zealand cannot lie within the origin of *P. kernoviae*. Therefore, further phylogenomic analyses of *P. kernoviae* isolates from Chile, New Zealand and Europe and its sibling species are needed to clarify the centre of origin. Similar studies have recently resolved the origins of the panglobal pathogens *P. cinnamomi* and *P. ramorum* (Jung et al. 2021, Shakya et al. 2021).

Other possible examples of sympatric adaptive radiation are the co-occurrence and adaptive differences of

i *P. ludoviciana* (sterile, Topt = 27.5 °C, Tmax = 32.5 °C), *P. procera* (sterile Topt = 25 °C, Tmax = 32.5 °C) and *P. tenuimura* (homothallic, Topt = 27.5 °C, Tmax = 30 °C) in a natural inundated swamp forest in Louisiana;

ii *P. subarctica* (sterile, Topt = 25 °C, slow growth) and *P. ukrainensis* (sterile, Topt = 30 °C, intermediate growth

rate) in the boreal riparian ecosystems of northern Sweden; and

iii *P. pseudogallica* (sterile, chlamydospores, Topt = 15–25 °C, Tmax = 25–27.5 °C) and *P. tonkinensis* (homothallic, no chlamydospores, Topt = 20 °C, Tmax = < 25 °C) in a mountain stream of a remote cloud forest in northern Vietnam.

The closely related *P. celebensis*, *P. javanensis* and *P. multiglobulosa* may have originated via non-adaptive radiation. They exhibit slight differences in cardinal temperatures and growth rates, but an allopatric distribution in ecologically similar tropical hill and lower montane rainforests in Sulawesi, separated only by distances of 20–50 km. Their close genetic relationship indicates they diverged relatively recently in evolutionary terms. The island Sulawesi is of composite geological origin, resulting from the collision of different continental, including Gondwanan, terrains. Belonging to the distinct biogeographic region Wallacea, Sulawesi is a biodiversity hotspot characterised by a high degree of endemism following numerous terrestrial and freshwater radiations (Lohman et al. 2011). During the recurring long Pleistocene glaciations the climate of Southeast Asia was considerably drier than today, resulting in a lowering of altitudinal zones by 300–600 m and a retraction of tropical rainforests into lowland forest refugia separated by mountain ranges and seasonally dry vegetation (Heaney 1991, Laumonier 1997, MacKinnon et al. 1997, Whitten et al. 1997, 2002, Hope 2001). Long-term geographic isolation in Pleistocene refugia of a common ancestor of *P. celebensis*, *P. javanensis* and *P. multiglobulosa*, and genetic drift, may have led to their allopatric speciation. Further studies on their host ranges, tissue preferences and seasonal and diurnal activities are needed to test this hypothesis.

While *P. gallica* has rarely been found in North America, in Europe it is widespread occurring from the UK, Spain, France and Southern Sweden across Central Europe and the Balkan to Ukraine (Jung & Nechwatal 2008, Català et al. 2015, Redondo et al. 2018a, b, Pérez-Sierra et al. 2019, Matsiakh et al. 2020, this study). This suggests a European origin and introduction to North America. Conversely, *P. intercalaris* is most probably native to the Eastern North America, where it is widespread in river systems (Brazee et al. 2016, Yang et al. 2016) but in Europe has been found only once, in the rhizosphere of a nursery seedling (this study). In Subclades 10a and 10b the natural ranges of *P. gallica* (temperate mainland Europe), *P. intercalaris* (Eastern North America), *P. afrocarpa* (South Africa), *P. scandinavica*, *P. subarctica* and *P. ukrainensis* (northern Sweden, plus *P. ukrainensis* in Ukraine), the *P. ludoviciana*-*P. procera*-*P. tenuimura* cluster (Louisiana) and the *P. pseudogallica*-*P. tonkinensis* cluster (northern Vietnam) currently show no geographical overlaps, suggesting that *P. afrocarpa*, *P. gallica*, *P. intercalaris*, *P. scandinavica* and the respective ancestors of the three species clusters diverged allopatrically. In Subclade 10c the same may also apply to *P. boehmeriae* (India, China, Taiwan), *P. gondwanensis* (Australia, Papua New Guinea, Amami island), *P. morindae* (Hawaii), *P.* taxon boehmeriae-like (Argentina), *P.* taxon boehmeriae-like 2 (China), *P.* taxon canthium (South Africa), *P.* taxon koreanensis (Korea) and the ancestors of the *P. celebensis*-*P. javanensis*-*P. multiglobulosa* cluster (Indonesia) and the *P. chilensis*-*P. kernoviae*-*P. pseudochilensis*-*P. pseudokernoviae* cluster (southern Chile), respectively.

Many species in *Phytophthora* major Clades 6 and 9 have largely abandoned sexual reproduction and become functionally sterile, probably during their adaptation to a lifestyle as litter decomposers and opportunistic pathogens in a mainly aquatic environment (Brasier et al. 2003, Jung et al. 2011, Hansen et al. 2012b, 2015, Nechwatal et al. 2013, Yang & Hong 2013, Yang et al. 2014). In Clade 10, a parallel development of sterility has probably occurred in the previously described *P. gallica* and *P. intercalaris* (Jung & Nechwatal 2008, Yang et al. 2016); and in five of the seven new aquatic Clade 10 species described here, *viz*. *P. ludoviciana*, *P. procera*, *P. pseudogallica*, *P. subarctica* and *P. ukrainensis*. It is evident that sexual sterility, as a breeding strategy, has developed via convergent evolution in at least three phylogenetically divergent *Phytophthora* clades.

It has become increasingly clear that interspecific hybridisation has had a significant role in *Phytophthora* evolution, facilitating adaptation to new environments and expansion of host ranges or host jumps (Brasier et al. 1999, Brasier 2000, 2001, Bertier et al. 2013, Burgess 2015, Jung et al. 2017a, c, Van Poucke et al. 2021). To date all known *Phytophthora* hybrids resulted from sexual hybridisation and have allopolyploid genomes (Brasier et al. 1999, Bertier et al. 2013, Burgess 2015, Jung et al. 2017c, Van Poucke et al. 2021). While species from Clades 1, 6b, 7a, 8d and 9 appear particularly prone to interspecific hybridisation (Brasier et al. 2004, Man In' t Veld et al. 2012, Bertier et al. 2013, Nagel et al. 2013, Burgess 2015, Husson et al. 2015, Wang et al. 2016, Jung et al. 2017c, Van Poucke et al. 2021) no Clade 10 hybrids are known yet. *Phytophthora* hybrids are in particular associated with aquatic environments. This may be a consequence of high species diversity and inoculum abundance in these ecosystems leading to multi-species colonisation of leaf litter and, therefore, enhanced opportunities for hybridisation (Brasier et al. 2003, Jung et al. 2011, 2017a). Interestingly, in the present study of Clade 10 species the frequencies of heterozygous positions across the 8 799 characters of the nine nuclear loci varied considerably by lifestyle. While the nine primarily aquatic species had on average 43.7 heterozygous positions, the 11 aerial species were heterozygous at only 5.7 positions. This may reflect the low probability of different aerial *Phytophthora* species co-infecting and colonising the same leaf or fruit in the canopy compared to multi-species colonisation of leaf litter in waterbodies. In the aquatic species *P. gallica*, *P. intercalaris*, *P. ludoviciana* and *P. subarctica* up to 55, 60, 63 and 59 heterozygous positions, respectively, were present, possibly signals of hybrid origin. Many sporangia of *P. subarctica* were unable to differentiate their cytoplasm into individual zoospores, releasing one large multi-nucleate and multi-flagellate zoospore. This could also reflect a hybrid origin, as it is characteristic of several interspecific hybrids in Clades 6 and 7a (Burgess 2015, Jung et al. 2017c). Studies of ploidy levels using flow cytometry and genomic analysis are needed to test this hypothesis (Jung et al. 2017c, Van Poucke et al. 2021).

Whether some of the new *Phytophthora* species from Clade 10 pose a potential threat to agriculture, forestry and natural ecosystems in Europe and North America remains unclear. However, the high aggressiveness of the introduced *P. kernoviae* to the foliage of *Rhododendron*, *Vaccinium*, other European and North American woody species and the bark of *Fagus sylvatica* in the UK (Brasier et al. 2005, Anonymous 2010) indicate that its sibling species *P. chilensis*, *P. pseudochilensis* and *P. pseudokernoviae* might also pose a risk to woody species in Europe and North America. Also, the moderate aggressiveness of *P. gallica* to *Alnus glutinosa* and *F. sylvatica* in zoospore inoculation and underbark inoculation tests (Jung & Nechwatal 2008) suggests that some of the new aquatic Clade 10 species described here might also be potential threats. Proactive host testing of, for example, European and North American tree and crop species is needed to clarify the potential risk that the new Clade 10 species might pose.

In summary, this and previous studies have demonstrated that, while *Phytophthora* major Clade 10 has high species diversity in natural ecosystems of Asia, Europe and the Americas, this often occurs in distinct regional hotspots. Certain biogeographic regions, in particular in Mediterranean climate and in tropical lowland forests, have low Clade 10 diversity or may even be

devoid of Clade 10 species. The evolutionary history of the Clade appears to have involved a pre-Gondwanan divergence into two extant Subclades, 10a and 10b, comprising soil and water inhabiting species and almost exclusively Holarctic distribution; and a third Subclade (10c) comprised of species with an aerial lifestyle and a Gondwanan and circum-pacific distribution. Evidence suggests the current 25 described and informally designated Clade 10 taxa have radiated via both allopatric non-adaptive and sympatric adaptive speciation. Further sampling in as yet unsurveyed natural ecosystems in Asia, Africa and South America is needed to assess the full diversity of the Clade and the factors driving diversity, speciation and adaptation in *Phytophthora*.

Acknowledgements The authors are grateful to the Project Phytophthora Research Centre Reg. No. CZ.02.1.01/0.0/0.0/15_003/0000453 co-financed by the Czech Ministry for Education, Youth and Sports and the European Regional Development Fund, the Portuguese Science and Technology Foundation (FCT) for co-financing the European BiodivERsA project RESIPATH: Responses of European Forests and Society to Invasive Pathogens (BIODIVERSA/0002/2012), the European Union's Horizon 2020 research and innovation programme for financing under grant agreement No. 63564 project POnTE: Pest Organisms Threatening Europe, and the Japanese Society for the promotion of science, KAKEN No. 18H02245. Travel and subsistence support for C.M.B. was provided by Brasier Consultancy. The authors also thank the administration of the company ARAUCO as the owner of Parque Oncol in Chile and the administration of Hoang-Lien National Park in Vietnam for the permission to take samples in their forests. We thank Aneta Bačová, Anna Hýsková, Henrieta Ďatková and Milica Raco (all Mendel University in Brno, Czech Republic), and Mariela González and Sebastian Fajardo (both previously Universidad de Concepción) for much appreciated technical support.

Declaration on conflict of interest The authors declare that there is no conflict of interest.

REFERENCES

Adami M, Bernardes S, Arai E, et al. 2018. Seasonality of vegetation types of South America depicted by moderate resolution imaging spectroradiometer (MODIS) time series. International Journal of Applied Earth Observation and Geoinformation 69: 148–163.

Adams GC, Catal M, Trummer L. 2010. Distribution and severity of alder Phytophthora in Alaska. In: Frankel SJ, Kliejunas T, Palmieri KM (eds), Proceedings of the Sudden Oak Death Fourth Science Symposium, USDA Forest Service, Albany, California, USA. General Technical Report PSW-GTR-229: 29–49.

Aguayo J, Adams GC, Halkett F, et al. 2013. Strong genetic differentiation between North American and European populations of Phytophthora alni subsp. uniformis. Phytopathology 103: 190–199.

Anonymous 2010. Phytophthora kernoviae: A threat to our woodlands, heathlands and historic gardens. Plant Disease Fact Sheet. The Food and Environment Research Agency, Sand Hutton, York, UK.

Armesto J, Villagrán C, Arroyo MTK. 1995. Ecología de los bosques nativos de Chile. Santiago, Editorial Universitaria.

Atchadé YF, Roberts GO, Rosenthal JS. 2011. Towards optimal scaling of metropolis-coupled Markov chain Monte Carlo. Statistics and Computing 21: 555–568.

Balci Y, Balci S, Eggers J, et al. 2007. Phytophthora spp. associated with forest soils in Eastern and North-Central U.S. oak ecosystems. Plant Disease 91: 705–710.

Balci Y, Halmschlager E. 2003. Phytophthora species in oak ecosystems in Turkey and their association with declining oak trees. Plant Pathology 52: 694–702.

Baskin JM, Baskin CC. 2016. Origins and relationships of the mixed mesophytic forest of Oregon–Idaho, China, and Kentucky: Review and synthesis. Annals of the Missouri Botanical Garden 101: 525–552.

Bertier L, Leus L, D'hondt L, et al. 2013. Host adaptation and speciation through hybridization and polyploidy in Phytophthora. PloS ONE 8: e85385.

Blair JE, Coffey MD, Park S-Y, et al. 2008. A multi-locus phylogeny for Phytophthora utilizing markers derived from complete genome sequences. Fungal Genetics and Biology 45: 266–277.

Bose T, Hulbert JM, Burgess TI, et al. 2021. Two novel Phytophthora species from the southern tip of Africa. Mycological Progress 20: 755–767.

Bouckaert R, Drummond A. 2017. bModelTest: Bayesian phylogenetic site model averaging and model comparison. BMC Evolutionary Biology 17: 42.

Bouckaert R, Heled J, Kühnert D, et al. 2014. BEAST 2: A software platform for Bayesian evolutionary analysis. PLoS Computational Biology 10: e1003537.

Bourret TB, Choudhury RA, Mehl HK, et al. 2018. Multiple origins of downy mildews and mito-nuclear discordance within the paraphyletic genus Phytophthora. PLoS ONE 13: e0192502.

Brasier CM. 1986. The dynamics of fungal speciation. In: Rayner ADM, Brasier CM, Moore D (eds), Evolutionary biology of the fungi: 231–260. Cambridge University Press, Cambridge, UK.

Brasier CM. 2000. Rise of the hybrid fungi. Nature 405: 134–135.

Brasier CM. 2001. Rapid evolution of introduced plant pathogens via interspecific hybridization. Bioscience 51: 123–133.

Brasier CM, Beales PA, Kirk SA, et al. 2005. Phytophthora kernoviae sp. nov. an invasive pathogen causing bleeding stem lesions on forest trees and foliar necrosis of ornamentals in Britain. Mycological Research 109: 853–859.

Brasier CM, Cooke DEL, Duncan JM. 1999. Origins of a new Phytophthora pathogen through interspecific hybridisation. Proceedings of the National Academy of Sciences, USA 96: 5878 – 5883.

Brasier CM, Cooke DEL, Duncan JM, et al. 2003. Multiple new phenotypic taxa from trees and riparian ecosystems in Phytophthora gonapodyides–P. megasperma ITS Clade 6, which tend to be high-temperature tolerant and either inbreeding or sterile. Mycological Research 107: 277–290.

Brasier CM, Kirk SA, Delcan J, et al. 2004. Phytophthora alni sp. nov. and its variants: designation of emerging heteroploid hybrid pathogens spreading on Alnus trees. Mycological Research 108: 1172–1184.

Brasier CM, Rayner ADM. 1987. Whither terminology below the species level in the fungi? In: Rayner ADM, Brasier CM, Moore D (eds), Evolutionary biology of the fungi: 379–388. Cambridge University Press, Cambridge, UK.

Brasier CM, Webber J. 2010. Sudden larch death. Nature 466: 824–825.

Brazee NJ, Wick RL, Hulvey JP. 2016. Phytophthora species recovered from the Connecticut River valley in Massachusetts, USA. Mycologia 108: 6–19.

Burgess TI. 2015. Molecular characterization of natural hybrids formed between five related indigenous Clade 6 Phytophthora species. PLoS ONE 10: e0134225.

Burgess TI, Edwards J, Drenth A, et al. 2021. Current status of Phytophthora in Australia. Persoonia 47: 151–177.

Burgess TI, White D, McDougall KM, et al. 2017. Distribution and diversity of Phytophthora across Australia. Pacific Conservation Biology 23: 1–13.

Català S, Pérez-Sierra A, Abad-Campos P. 2015. The use of genus-specific amplicon pyrosequencing to assess Phytophthora species diversity using eDNA from soil and water in Northern Spain. PLoS ONE 10: e0119311.

Chen Q, Bakhshi M, Balci Y, et al. 2022. Genera of phytopathogenic fungi: GOPHY 4. Studies in Mycology 101: 417–564.

Chen Y, Roxby R. 1996. Characterization of a Phytophthora infestans gene involved in vesicle transport. Gene 181: 89–94.

Chowdappa P, Madhura S, Nirmal Kumar BJ, et al. 2014. Phytophthora boehmeriae revealed as the dominant pathogen responsible for severe foliar blight of Capsicum annuum in South India. Plant Disease 98: 90–98.

Cooke DE, Drenth A, Duncan JM, et al. 2000. A molecular phylogeny of Phytophthora and related oomycetes. Fungal Genetics and Biology 30: 17–32.

Corcobado T, Cech TL, Brandstetter M, et al. 2020. Decline of European beech in Austria: Involvement of Phytophthora spp. and contributing biotic and abiotic factors. Forests 11: 895.

Crous PW, Wingfield MJ, Le Roux JJ, et al. 2015. Fungal Planet description sheets: 371–399. Persoonia 35: 264–327.

Ďatková H. 2020. Phytophthora diversity in forest streams of Moravia and Slovakia. Masters Thesis, Mendel University in Brno, Czech Republic.

Davis CC, Bell CD, Mathews S, et al. 2002. Laurasian migration explains Gondwanan disjunctions: Evidence from Malpighiaceae. Proceedings of the National Academy of Sciences USA 99: 6833–6837.

Denk T, Grimm GW. 2009. The biogeographic history of beech trees. Review of Palaeobotany and Palynology 158: 83–100.

Dick MA, Dobbie K, Cooke DEL, et al. 2006. Phytophthora captiosa sp. nov. and P. fallax sp. nov. causing crown dieback of Eucalyptus in New Zealand. Mycological Research 110: 393–404.

Dick MW. 1990. Keys to Pythium. University of Reading Press, Reading, UK.

Dos Santos AF, Luz EDMN, De Souza JT. 2006. First report of Phytophthora boehmeriae on black wattle in Brazil. Plant Pathology 55: 813.

Drummond AJ, Ho SYW, Phillips MJ, et al. 2006. Relaxed phylogenetics and dating with confidence. PLoS Biology 4: 699–710.

Elias S, Brigham-Grette J. 2013. Late Pleistocene glacial events in Beringia. In: Elias S (ed), Encyclopedia of Quaternary Science, 2nd edn: 191–201. Elsevier, Amsterdam, Netherlands.

Erwin DC, Ribeiro OK. 1996. Phytophthora diseases worldwide. APS Press, St. Paul, Minnesota.

Fletcher K, Gil J, Bertier LD, et al. 2019. Genomic signatures of heterokaryosis in the oomycete pathogen Bremia lactucae. Nature Communications 10: 2645.

Fletcher K, Klosterman SJ, Derevnina L, et al. 2018. Comparative genomics of downy mildews reveals potential adaptations to biotrophy. BMC Genomics 19: 851.

Foster ZSL, Albornoz FL, Fieland VJ, et al. 2022. A new oomycete metabarcoding method using the rps10 gene. Phytobiomes Journal: in press. https://doi.org/10.1094/PBIOMES-02-22-0009-R.

Frankel SJ, Conforti C, Hillman J, et al. 2020. Phytophthora introductions in restoration areas: Responding to protect California native flora from human-assisted pathogen spread. Forests 11: 1291.

Frezzi MJ. 1941. Phytophthora boehmeriae, causante de la podredumbre morena de los frutos citricos, en la Republica Argentina (Phytophthora boehmeriae, the agent of brown rot of citrus fruits in the Argentine Republic). Revista Argentina de Agronomía 8: 200–205.

Frezzi MJ. 1950. Las especies de Phytophthora en la Argentina (The species of Phytophthora in Argentina). Revista de Investigaciones Agrícolas 4: 47–133.

Garbelotto MM, Lee HK, Slaughter G, et al. 1997. Heterokaryosis is not required for virulence of Heterobasidion annosum. Mycologia 89: 92–102.

Gardner JF, Dick MA, Bader MK-F. 2015. Susceptibility of New Zealand flora to Phytophthora kernoviae and its seasonal variability in the field. New Zealand Journal of Forestry Science 45: 23.

Givnish TJ. 1997. Adaptive radiation and molecular systematics: aims and conceptual issues. In: Givnish TJ, Systma KJ (eds), Molecular evolution and adaptive radiation: 1–54. Cambridge University Press, New York, USA.

Givnish TJ. 2015. Adaptive radiation versus 'radiation' and 'explosive diversification': why conceptual distinctions are fundamental to understanding evolution. New Phytologist 207: 297–303.

Gladenkov AX, Oleinik AE, Marincovich L, et al. 2002. A refined age for the earliest opening of Bering Strait. Palaeogeography, Palaeoclimatology, Palaeoecology 183: 321–328.

Hansen E[M], Delatour C. 1999. Phytophthora species in oak forests of northeast France. Annales des Sciences Forestière 56: 539–547.

Hansen EM, Reeser PW, Sutton W. 2012a. Phytophthora beyond agriculture. Annual Review of Phytopathology 50: 359–378.

Hansen EM, Reeser PW, Sutton W. 2012b. Phytophthora borealis and Phytophthora riparia, new species in Phytophthora ITS Clade 6. Mycologia 104: 1133–1142.

Hansen EM, Reeser PW, Sutton W, et al. 2015. Redesignation of Phytophthora taxon Pgchlamydo as Phytophthora chlamydospora sp. nov. North American Fungi 10: 1–14.

Heaney LR. 1991. A synopsis of climatic and vegetational change in Southeast Asia. Climatic Change 19: 53–61.

Hope G. 2001. Environmental change in the Late Pleistocene and later Holocene at Wanda Site, Soroako, South Sulawesi, Indonesia. Palaeogeography, Palaeoclimatology, Palaeoecology 171: 129–145.

Hopple JS, Vilgalys R. 1994. Phylogenetic relationships among coprinoid taxa and allies based on data from restriction site mapping of nuclear rDNA. Mycologia 86: 96–107.

Huai WX, Tian G, Hansen EM, et al. 2013. Identification of Phytophthora species baited and isolated from forest soil and streams in northwestern Yunnan province, China. Forest Pathology 43: 87–103.

Hüberli D. 1995. Analysis of variability among isolates of Phytophthora cinnamomi Rands from Eucalyptus marginata Donn ex Sm. and E. calophylla R. Br. based on cultural characteristics, sporangia and gametangia morphology, and pathogenicity. Bachelor thesis, Murdoch University, Murdoch, Western Australia.

Hüberli D, Hardy GEStJ, White D, et al. 2013. Fishing for Phytophthora from Western Australia' s waterways: A distribution and diversity survey. Australasian Plant Pathology 42: 251–260.

Hubert F, Grimm GW, Jousselin E, et al. 2014. Multiple nuclear genes stabilize the phylogenetic backbone of the genus Quercus. Systematics and Biodiversity 12: 405–423.

Hueck K. 1966. Die Wälder Südamerikas ('The forests of South America'). Gustav Fischer, Stuttgart, Germany.

Husson C, Aguayo J, Revellin C, et al. 2015. Evidence for homoploid speciation in Phytophthora alni supports taxonomic reclassification in this species complex. Fungal Genetics and Biology 77: 12–21.

Jones LA, Worobo RW, Smart CD. 2014. Plant-pathogenic oomycetes, Escherichia coli strains, and Salmonella spp. frequently found in surface water used for irrigation of fruit and vegetable crops in New York State. Applied and Environmental Microbiology 80: 4814–4820.

Jönsson U, Lundberg L, Sonesson K, et al. 2003. First records of soilborne Phytophthora species in Swedish oak forests. Forest Pathology 33: 175–179.

Jung T. 2009. Beech decline in Central Europe driven by the interaction between Phytophthora infections and climatic extremes. Forest Pathology 39: 73–94.

Jung T, Blaschke H, Neumann P. 1996. Isolation, identification and pathogenicity of Phytophthora species from declining oak stands. European Journal of Forest Pathology 26: 253–272.

Jung T, Blaschke H, Osswald W. 2000. Involvement of soilborne Phytophthora species in Central European oak decline and the effect of site factors on the disease. Plant Pathology 49: 706–718.

Jung T, Blaschke M. 2004. Phytophthora root and collar rot of alders in Bavaria: distribution, modes of spread and possible management strategies. Plant Pathology 53: 197–208.

Jung T, Chang TT, Bakonyi J, et al. 2017a. Diversity of Phytophthora species in natural ecosystems of Taiwan and association with disease symptoms. Plant Pathology 66: 194–211.

Jung T, Cooke DEL, Blaschke H, et al. 1999. Phytophthora quercina sp. nov., causing root rot of European oaks. Mycological Research 103: 785–798.

Jung T, Durán A, Sanfuentes von Stowasser E, et al. 2018a. Diversity of Phytophthora species in Valdivian rainforests and association with severe dieback symptoms. Forest Pathology 48: e12443.

Jung T, Hansen EM, Winton L, et al. 2002. Three new species of Phytophthora from European oak forests. Mycological Research 106: 397–411.

Jung T, Horta Jung M, Cacciola SO, et al. 2017b. Multiple new cryptic pathogenic Phytophthora species from Fagaceae forests in Austria, Italy and Portugal. IMA Fungus 8: 219–244.

Jung T, Horta Jung M, Scanu B, et al. 2017c. Six new Phytophthora species from ITS clade 7a including two sexually functional heterothallic hybrid species detected in natural ecosystems in Taiwan. Persoonia 38: 100–135.

Jung T, Horta Jung M, Webber JF, et al. 2021. The destructive tree pathogen Phytophthora ramorum originates from the Laurosilva forests of East Asia. Journal of Fungi 7: 226.

Jung T, La Spada F, Pane A, et al. 2019. Diversity and distribution of Phytophthora species in protected natural areas in Sicily. Forests 10: 259.

Jung T, Nechwatal J. 2008. Phytophthora gallica sp. nov., a new species from rhizosphere soil of declining oak and reed stands in France and Germany. Mycological Research 112: 1195–1205.

Jung T, Pérez-Sierra A, Durán A, et al. 2018b. Canker and decline diseases caused by soil- and airborne Phytophthora species in forests and woodlands. Persoonia 40:182–220.

Jung T, Scanu B, Bakonyi, J, et al. 2017d. Nothophytophthora gen. nov., a new sister genus of Phytophthora from natural and semi-natural ecosystems. Persoonia 39: 143–174.

Jung T, Scanu B, Brasier CM, et al. 2020. A survey in natural forest ecosystems of Vietnam reveals high diversity of both new and described Phytophthora taxa including P. ramorum. Forests 11: 93.

Jung T, Stukely MJC, Hardy GEStJ, et al. 2011. Multiple new Phytophthora species from ITS Clade 6 associated with natural ecosystems in Australia: evolutionary and ecological implications. Persoonia 26: 13–39.

Kaliq I, Hardy GEStJ, McDougall KL, et al. 2019. Phytophthora species isolated from alpine and sub-alpine regions of Australia, including the description of two new species; Phytophthora cacuminis sp. nov. and Phytophthora oreophila sp. nov. Fungal Biology 123: 29e41.

Kalyaanamoorthy S, Minh BQ, Wong TKF, et al. 2017. ModelFinder: Fast model selection for accurate phylogenetic estimates. Nature Methods 14: 587–589.

Katoh K, Standley DM. 2013. MAFFT multiple sequence alignment software version 7: improvements in performance and usability. Molecular Biology and Evolution 30: 772–780.

Kim J-S, Kim B-S. 2004. Leaf blight of Ailanthus altissima caused by Phytophthora boehmeriae. The Plant Pathology Journal 20: 106–109.

Kim S, De Medeiros BAS, Byun B-K, et al. 2018. West meets East: How do rainforest beetles become circum-Pacific? Evolutionary origin of Callipogon relictus and allied species (Cerambycidae: Prioninae) in the New and Old Worlds. Molecular Phylogenetics and Evolution 125: 163–176.

Kone A, Kofke DA. 2005. Selection of temperature intervals for parallel-tempering simulations. Journal of Chemical Physics 122: 1–2.

Kozak KH, Weisrock DR, Larson R. 2006. Rapid lineage accumulation in a non-adaptive radiation: phylogenetic analysis of diversification rates in eastern North American woodland salamanders (Plethodontidae: Plethodon). Proceedings of the Royal Society B 273: 539–546.

Kroon LPNM, Bakker FT, Van den Bosch GBM, et al. 2004. Phylogenetic analysis of Phytophthora species based on mitochondrial and nuclear DNA sequences. Fungal Genetics and Biology 41: 766–782.

Lang P, Dane F, Kubisiak TL, et al. 2007. Molecular evidence for an Asian origin and a unique westward migration of species in the genus Castanea via Europe to North America. Molecular Phylogenetics and Evolution 43: 49–59.

Laumonier Y. 1997. The vegetation and physiography of Sumatra. Geobotany 22. Springer Science and Business Media, Dordrecht, Germany.
Legeay J, Husson C, Boudier B, et al. 2020. Surprising low diversity of the plant pathogen Phytophthora in Amazonian forests. Environmental Microbiology 22: 5019–5032.
Lohman DJ, De Bruyn M, Page T, et al. 2011. Biogeography of the Indo-Australian Archipelago. Annual Review of Ecology, Evolution, and Systematics 42: 205–226.
MacKinnon K, Hatta G, Halim H, et al. 1997. The ecology of Kalimantan. Ecology of Indonesia Series Vol. III; Oxford University Press, Oxford, UK.
Man in 't Veld WA, Rosendahl KCHM, Hong C. 2012. Phytophthora × serendipita sp. nov. and P. × pelgrandis, two destructive pathogens generated by natural hybridization. Mycologia 104: 1390–1396.
Martin FN, Tooley PW. 2003. Phylogenetic relationships among Phytophthora species inferred from sequence analysis of mitochondrially encoded cytochrome oxidase I and II genes. Mycologia 95: 269–284.
Maseko B, Burgess TI, Coutinho TA, et al. 2007. Two new Phytophthora species from South African Eucalyptus plantations. Mycological Research 111: 1321–1338.
Matsiakh I, Kramarets V, Cleary M. 2020. Occurrence and diversity of Phytophthora species in declining broadleaf forests in western Ukraine. Forest Pathology 51: e12662.
Mayr E. 1942. Systematics and the origin of species. Columbia University Press, New York.
McCarthy CGP, Fitzpatrick DA. 2017. Phylogenomic reconstruction of the oomycete phylogeny derived from 37 genomes. mSphere 2: e00095–e00017.
McKenna MC. 1983. Cenozoic paleogeography of North Atlantic land bridges. In: Bott MHP, Saxov S, Talwani M, et al. (eds), Structure and development of the Greenland-Scotland Ridge: 351–399. Plenum Press, New York.
Milenković I, Keča N, Karadžić D, et al. 2018. Isolation and pathogenicity of Phytophthora species from poplar plantations in Serbia. Forests 9: 330.
Morley JR. 2003. Interplate dispersal paths for megathermal angiosperms. Perspectives in Plant Ecology, Evolution and Systematics 6: 5–20.
Müller N, Bouckaert R. 2019. Adaptive parallel tempering for BEAST 2. bioRxiv [online]. https://doi.org/10.1101/603514.
Nagel JH, Gryzenhout M, Slippers B, et al. 2013. Characterization of Phytophthora hybrids from ITS clade 6 associated with riparian ecosystems in South Africa and Australia. Fungal Biology 117: 329–347.
Nechwatal J, Bakonyi J, Cacciola SO, et al. 2013. The morphology, behaviour and molecular phylogeny of Phytophthora taxon Salixsoil and its redesignation as Phytophthora lacustris sp. nov. Plant Pathology 62: 355–369.
Nelson SC, Abad ZG. 2010. Phytophthora morindae, a new species causing black flag disease on noni (Morinda citrifolia L) in Hawaii. Mycologia 102: 122–134.
Nguyen LT, Schmidt HA, Von Haeseler A, et al. 2015. IQ-TREE: A fast and effective stochastic algorithm for estimating maximum-likelihood phylogenies. Molecular Biology and Evolution 32: 268–274.
O'Hanlon R, Choiseul J, Corrigan M, et al. 2016. Diversity and detections of Phytophthora species from trade and nontrade environments in Ireland. Bulletin OEPP/EPPO Bulletin 46: 594–602.
Oh E, Gryzenhout M, Wingfield BD, et al. 2013. Surveys of soil and water reveal a goldmine of Phytophthora diversity in South African natural ecosystems. IMA Fungus 4: 123–131.
Pérez-Sierra A, Chitty R, Eacock A, et al. 2022. First report of Phytophthora pluvialis in Europe causing resinous cankers on western hemlock. New Disease Reports 45: e12064.
Pérez-Sierra A, Gorton C, Lewis C, et al. 2019. Phytophthora spp. on trees in Britain through the lens of the Tree Health Diagnostic and Advisory Service. In: Scanu B, Balmas V, Brandano A, et al. (eds), Phytophthoras in forests and natural ecosystems: Ninth meeting of the International Union of Forest Research Organizations (IUFRO) Working Party 7.02.09, La Maddalena, Sardinia, Italy, 17-26 Oct 2019. Book of Abstracts: P24. University of Sassari, Italy.
Qian H. 2002. Floristic relationships between Eastern Asia and North America: Test of Gray's hypothesis. The American Naturalist 160: 317–332.
Rambaut A, Drummond A, Xie D, et al. 2018. Posterior summarization in Bayesian phylogenetics using Tracer 1.7. Systematic Biology 67: 901–904.
Ramsfield TD, Dick MA, Beever RE. 2009. Phytophthora kernoviae in New Zealand. In: Goheen EM, Frankel SJ (eds), Phytophthoras in forests and natural ecosystems. Fourth meeting of the International Union of Forest Research Organizations (IUFRO) Working Party S07.02.09. USDA Forest Service, Pacific Southwest Research Station, Albany, California. General Technical Report PSW-GTR-221: 47–53.
Rea AJ, Burgess TI, Hardy GEStJ, et al. 2011. Two novel and potentially endemic species of Phytophthora associated with episodic dieback of kwongan vegetation in the south-west of Western Australia. Plant Pathology 60: 1055–1068.
Redondo MA, Boberg J, Stenlid J, et al. 2018a. Contrasting distribution patterns between aquatic and terrestrial Phytophthora species along a climatic gradient are linked to functional traits. The ISME Journal 12: 2967–2980.
Redondo MA, Boberg J, Stenlid J, et al. 2018b. Functional traits associated with the establishment of introduced Phytophthora spp. in Swedish forests. Journal of Applied Ecology 55: 1538–1552.
Reeser P, Sutton W, Hansen E. 2013. Phytophthora pluvialis, a new species from mixed tanoak-Douglas-fir forests of western Oregon, U.S.A. North American Fungi 8: 1–8.
Reeser PW, Sutton W, Hansen EM, et al. 2011. Phytophthora species in forest streams in Oregon and Alaska. Mycologia 103: 22–35.
Rizzo DM, Garbelotto M, Davidson JM, et al. 2002. Phytophthora ramorum as the cause of extensive mortality of Quercus spp. and Lithocarpus densiflorus in California. Plant Disease 86: 205–214.
Robideau GP, De Cock AW, Coffey MD, et al. 2011. DNA barcoding of oomycetes with cytochrome c oxidase subunit I and internal transcribed spacer. Molecular Ecology Resources 11:1002–1011.
Rundell RJ, Price TD. 2009. Adaptive radiation, nonadaptive radiation, ecological speciation and nonecological speciation. Trends in Ecology and Evolution 24: 394–399.
Sambles C, Schlenzig S, O'Neill P, et al. 2015. Draft genome sequences of Phytophthora kernoviae and Phytophthora ramorum lineage EU2 from Scotland. Genomics Data 6: 193–194.
Sanfuentes E, Fajardo S, Sabag M, et al. 2016. Phytophthora kernoviae isolated from fallen leaves of Drymis winteri in native forest of southern Chile. Australasian Plant Disease Notes 11: 1–3.
Scanu B, Hunter GC, Linaldeddu BT, et al. 2014. A taxonomic re-evaluation reveals that Phytophthora cinnamomi and P. cinnamomi var. parvispora are separate species. Forest Pathology 44: 1–20.
Scanu B, Jung T, Masigol H, et al. 2021. Phytophthora heterospora sp. nov., a new pseudoconidia-producing sister species of P. palmivora. Journal of Fungi 7: 870.
Scanu B, Linaldeddu BT, Deidda A, et al. 2015. Diversity of Phytophthora species from declining Mediterranean maquis vegetation, including two new species, Phytophthora crassamura and P. ornamentata sp. nov. PLoS ONE 10: e0143234.
Scanu B, Webber JF. 2016. Dieback and mortality of Nothofagus in Britain: ecology, pathogenicity and sporulation potential of the causal agent Phytophthora pseudosyringae. Plant Pathology 65: 26–36.
Scott P, Williams N. 2014. Phytophthora diseases in New Zealand forests. New Zealand Journal of Forestry 59: 14–21.
Seddaiu S, Brandano A, Ruiu PA, et al. 2020. An overview of Phytophthora species inhabiting declining Quercus suber stands in Sardinia (Italy). Forests 11: 971.
Seibert P. 1996. Farbatlas Südamerika – Landschaften und Vegetation ('Colour atlas South America – Landscapes and vegetation'). Eugen Ulmer, Stuttgart, Germany.
Shakya SK, Grünwald NK, Fieland VJ, et al. 2021. Phylogeography of the wide-host range panglobal plant pathogen Phytophthora cinnamomi. Molecular Ecology 30: 5164–5178.
Sharma PP, Giribet G. 2012. Out of the Neotropics: Late Cretaceous colonization of Australasia by American arthropods. Proceedings of the Royal Society 279: 3501–3509.
Shaw DE. 1984. 'Microorganisms in Papua New Guinea.' Department of Primary Industry, Port Moresby, Papua New Guinea. Research Bulletin No. 33.
Shrestha SK, Zhou Y, Lamour K. 2013. Oomycetes baited from streams in Tennessee 2010–2012. Mycologia 105: 1516–1523.
Sims LL, Sutton W, Reeser P, et al. 2015. The Phytophthora species assemblage and diversity in riparian alder ecosystems of western Oregon, USA. Mycologia 107: 889–902.
Stamler RA, Sanogo S, Goldberg NP, et al. 2016. Phytophthora species in rivers and streams of the Southwestern United States. Applied and Environmental Microbiology 82: 4696–4704.
Stöver BC, Müller KF. 2010. TreeGraph 2: Combining and visualizing evidence from different phylogenetic analyses. BMC Bioinformatics 11: 7.
Studholme DJ, McDougal RL, Sambles C, et al. 2016. Genome sequences of six Phytophthora species associated with forests in New Zealand. Genomics Data 7: 54–56.
Studholme DJ, Panda P, Sanfuentes von Stowasser E, et al. 2019. Genome sequencing of oomycete isolates from Chile supports the New Zealand origin of Phytophthora kernoviae and makes available the first Nothophytophthora sp. genome. Molecular Plant Pathology 20: 423–431.

Sukumaran J, Holder MT. 2010. DendroPy: A Python library for phylogenetic computing. Bioinformatics 26: 1569–1571.
Tamura K, Stecher G, Kumar S. 2021. MEGA11: Molecular Evolutionary Genetics Analysis version 11. Molecular Biology and Evolution 38: 3022–3027.
Tecklin D, DellaSala DA, Luebert F, et al. 2011. Valdivian temperate rainforests of Chile and Argentina. In: DellaSala DA (ed), Temperate and boreal rainforests of the world: 132–153. Island Press, Washington, Covelo, London.
Thines M, Choi Y-J. 2016. Evolution, diversity, and taxonomy of the Peronosporaceae, with focus on the genus Peronospora. Phytopathology 106: 6–18.
Thorpe P, Vetukuri RR, Hedley PE, et al. 2021. Draft genome assemblies for tree pathogens Phytophthora pseudosyringae and Phytophthora boehmeriae. G3 11(11): jkab282.
Tiffney BH. 1985. The Eocene North Atlantic land bridge: Its importance in tertiary and modern phytogeography of the northern hemisphere. Journal of the Arnold Arboretum 66: 243–273.
Toussaint EFA, Hendrich L, Hájek J, et al. 2017. Evolution of Pacific Rim diving beetles sheds light on Amphi-Pacific biogeography. Ecography 40: 500–510.
Tucker CM. 1931. Taxonomy of the genus Phytophthora de Bary. University of Missouri. Agricultural Experiment Station Research Bulletin 153.
Van Damme K, Sinev, AY. 2013. Tropical Amphi-Pacific disjunctions in the Cladocera (Crustacea: Branchiopoda). Journal of Limnology 72: 209–244.
Van Poucke K, Haegeman A, Goedefroit T, et al. 2021. Unravelling hybridization in Phytophthora using phylogenomics and genome size estimation. IMA Fungus 12: 16.
Vélez ML, La Manna L, Tarabini N, et al. 2020. Phytophthora austrocedri in Argentina and co-inhabiting Phytophthoras: Roles of anthropogenic and abiotic factors in species distribution and diversity. Forests 11: 1223.
Vettraino AM, Barzanti GP, Bianco MC, et al. 2002: Occurrence of Phytophthora species in oak stands in Italy and their association with declining oak trees. Forest Pathology 32: 19–28.
Vettraino AM, Morel O, Perlerou C, et al. 2005. Occurrence and distribution of Phytophthora species associated with ink disease of chestnut in Europe. European Journal of Plant Pathology 111: 169–180.
Vila R, Bell CD, Macniven R, et al. 2011. Phylogeny and palaeoecology of Polyommatus blue butterflies show Beringia was a climate-regulated gateway to the New World. Proceedings of the Royal Society B 278: 2737–2744.
Wang J, Presser JW, Goss EM. 2016. Nuclear DNA content of the hybrid plant pathogen Phytophthora andina determined by flow cytometry. Mycologia 108: 899–904.
Wen J. 1999. Evolution of Eastern Asian and Eastern North American disjunct distributions in flowering plants. Annual Review of Ecology and Systematics 30: 421–455.
Wen J, Ickert-Bond S, Nie Z-L, et al. 2010. Timing and modes of evolution of eastern Asian-North American biogeographic disjunctions in seed plants. In: Long M, Gu H, Zhou Z (eds), Darwin's heritage today: Proceedings of the Darwin 2010 Beijing International Conference: 252–269. Higher Education Press, Bejing, China.
Wen J, Nie Z-L, Ickert-Bond SM. 2016. Intercontinental disjunctions between eastern Asia and western North America in vascular plants highlight the biogeographic importance of the Bering land bridge from late Cretaceous to Neogene. Journal of Systematics and Evolution 54: 469–490.
White TJ, Bruns T, Lee S, et al. 1990. Amplification and direct sequencing of fungal ribosomal RNA genes for phylogenetics. In: Innes MA, Gelfand DH, Sninsky JJ, et al. (eds), PCR protocols: A guide to methods and applications: 315–322. Academic Press, San Diego, California, USA.
Whitten T, Damanik SJ, Anwar J, et al. 1997. The ecology of Sumatra. Ecology of Indonesia Series Vol. I. Oxford University Press, Oxford, UK.
Whitten T, Mustafa M, Henderson GS. 2002. The ecology of Sulawesi. Ecology of Indonesia Series Vol. IV. Oxford University Press, Oxford, UK.
Winkworth RC, Nelson BCW, Bellgard SE, et al. 2020. A LAMP at the end of the tunnel: A rapid, field deployable assay for the kauri dieback pathogen, Phytophthora agathidicida. PLoS ONE 15: e0224007.
Xu X, Huai W, Hamiti, et al. 2019. Phytophthora species from Xinjiang wild apple forests in China. Forests 10: 927.
Yang X, Balci Y, Brazee NJ, et al. 2016. A unique species in Phytophthora clade 10, Phytophthora intercalaris sp. nov., recovered from stream and irrigation water in the eastern USA. International Journal of Systematic and Evolutionary Microbiology 66: 845–855.
Yang X, Gallegly ME, Hong C. 2014. A high-temperature tolerant species in clade 9 of the genus Phytophthora: P. hydrogena sp. nov. Mycologia 106: 57–65.
Yang X, Hong C. 2013. Phytophthora virginiana sp. nov., a high-temperature tolerant species from irrigation water in Virginia. Mycotaxon 126: 167–176.
Yang X, Hong C. 2018. Differential usefulness of nine commonly used genetic markers for identifying Phytophthora species. Frontiers in Microbiology 9: 2334.
Yang X, Tyler BM, Hong C. 2017. An expanded phylogeny for the genus Phytophthora. IMA Fungus 8: 355–384.
Zeng H-C, Ho H-H, Zheng F-C. 2009. A survey of Phytophthora species on Hainan Island of South China. Journal of Phytopathology 157: 33–39.